Assessment of Climate Change Impact on Surface Water Availability: Gerhu-Sirnay Catchment, Mereb Sub- Basin, Ethiopia

M.Sc. THESIS

ZEGEYE TAMIRU HAMESSO, 2024/2025

HAWASSA UNIVERSITY, ETHIOPIA

October, 2024

Assessment of Climate Change Impact on Surface Water Availability: Gerhu-Sirnay Catchment, Mereb Sub- Basin, Ethiopia

ZEGEYE TAMIRU HAMESSO

A THESIS SUBMITTED TO THE SCHOOL OF BIO SYSTEM AND HYDRAULIC ENGINEERING

INSTITUTE OF TECHNOLOGY, SCHOOL OF GRADUATE STUDIES

HAWASSA UNIVERSITY HAWASSA, ETHIOPIA

IN PARTIAL FULFILLMENT OF THE REQUIREMENTS FOR THE

DEGREE OF MASTER OF SCIENCE

IN HYDRAULIC ENGINEERING

MAIN ADVISOR: Abebe Tadesse (PhD)

October, 2020

HAWASSA UNIVERSITY
SCHOOL OF GRADUATE STUDIES
Advisors Approval Sheet

This is to certify that the thesis entitled "**Assessment of Climate Change Impact on Surface Water Availability: Gerhu-Sirnay Catchment, Mereb Sub- Basin, Ethiopia**" submitted in partial fulfillment of the requirements for the degree of Masters of Science in Civil Engineering with specialization in Hydraulic Engineering, the Graduate Program of the School of Bio System and Hydraulic Engineering, and has been carried out by ZEGEYE TAMIRU HAMESSO Id. No GPHydrW/0019/14, under our supervision. Therefore, we recommend that the student has fulfilled the requirements and hence hereby can submit the thesis to the department.

Name of major advisor	**Signature**	**Date**
Name of co-advisor	**Signature**	**Date**

HAWASSA UNIVERSITY
SCHOOL OF GRADUATE STUDIES
EXAMINERS' APPROVAL SHEET-1
(Submission Sheet-1)

We, the undersigned, members of the board Examiners of the final open defense by ZEGEYE TAMIRU HAMESSO have read and evaluated his thesis entitled with "**Assessment of Climate Change Impact on Surface Water Availability: Gerhu-Sirnay Catchment, Mereb Sub-Basin, Ethiopia**", and examined the candidate. This is therefore, to certify that the thesis has been accepted in the partial fulfillment of the requirements of the degree of Master of Science in Hydraulic Engineering.

Name of the Chairperson	**Signature**	**Date**
Name of Major Advisor	**Signature**	**Date**
Name of Internal Examiner	**Signature**	**Date**
Dr. Sirak Tekleab		30/12/2024
Name of External Examiner	**Signature**	**Date**
SGS Approval	**Signature**	**Date**

Final approval and acceptance of the thesis is contingent upon the submission of the final copy of the thesis to the School of Graduate studies (SGS) through the Department/School PGP of the candidate's department.

Stamp of SGS Date: _____

HAWASSA UNIVERSITY

SCHOOL OF GRADUATE STUDIES

EXAMINERS' APPROVAL SHEET-2

(Submission Sheet-2)

As members of the board Examiners of the final Master's degree open defense, we certify that We have read and evaluated the thesis prepared by ZEGEYE TAMIRU HAMESSO under the title "Assessment of Climate Change Impact Over Surface Water Availability: Gerhu-Sirnay Catchment, Mereb Sub- Basin, Ethiopia", and recommended that it be accepted as fulfilling the thesis requirement for the degree of Master of Science in Hydraulic Engineering.

Name of the Chairperson	**Signature**	**Date**
Name of Internal Examiner	**Signature**	**Date**
Dr. Sirak Tekleab		30/12/2024
Name of External Examiner	**Signature**	**Date**

Final approval and acceptance of the thesis is contingent upon the submission of the final copy of the thesis to the SGS through the PGP of the candidate's department/School.

Thesis approved by:

PGP	Signature	Date

DECLARATION

I, the undersigned person, declare that this thesis is my original work and that all source of materials used for thesis have been duly acknowledged.

Name: ZEGEYE TAMIRU HAMESSO

Signature: _____

Place: Hawassa University

Date of submission:_____

ACKNOWLEDGEMENT

First and foremost, I would like thanks to the Almighty God and his mother Saint Marry for giving me a chance to reach this point of success. God! What you have done for me is really beyond what I was imagined and dreamt.

My truthful thankfulness goes to my advisors; **Abebe Tadesse (PhD.)** and **Mr. Gonse Amelo** for their critical advice, innovative ideas, encouragements and guidance throughout this thesis work. I would like to express my sincere gratitude to all Hawassa University, School of Bio System and Hydraulic Engineering staffs who gave me the postgraduate courses.

LIST OF ABBREVATIONS AND ACRONYMS

CMhyd	Climate Model data for hydrologic modeling
CMIP5	Climate Models Intercomparison Phase-5
CN	Curve Number
CORDEX	Coordinated Regional Climate Downscaling Experiment
GCM	Global Climate Models
GLUE	Generalized Likelihood Uncertainty Estimation
HRU	Hydrologic Response Units
IWMI	International Water Management Institute
MCMC	Markove Chain Monte Carlo
NMA	National Meteorological Agency
NRMSE	Normalized Root Mean Square Error
NSE	Nash-Sutcliffe Efficiency
ParaSol	Parameter Solution
PBIAS	Percent Bias
PSO	Particle Swarm Optimization
RCA4	Rossby Center Regional Climate Model
RCM	Regional Climate Models
RCP	Representative Concentration Pathway
SUFI2	Sequential Uncertainty Fitting version 2
SWAT-CUP	SWAT-Calibration and Uncertainty Program
VCSI	Volumetric Critical Success Index
VFAR	Volumetric False Alarm Ratio
VHI	Volumetric Hit Index
VMI	Volumetric Miss Index
CanESM2	Second Generation Canadian Earth System Model
CNRM-CM5	Center National Research de Meteorology-Version 5
GFDL-ESM2M	Geophysical Fluid Dynamics Laboratory- Second Generation Canadian Earth System Model
ICHEC-EC-EARTH	Irish Centre for High-End Computing- Earth for Climate Center
MIROC-MIROC5	Model for Interdisciplinary Research on Climate Version 5
MPI-ESM-LR	Max Planck Institute for Meteorology- Earth System Model-Low Resolutions
WGEN_CFSR	Weather Generator Database_Climate Forecast System Reanalysis

TABLE OF CONTENTS

Contents Page

LIST OF FIGURES

LIST OF TABLES

ABSTRACT

Investigating surface water availability under climate change impact is vital to ensure water resource sustainability. The general objective of this thesis was to assess the impact of climate change over surface water availability of Gerhu-Sirnay catchment using CORDEX-RCA4 with soil and water assessment tool (SWAT). To achieve this, quality of observed data was accepted for outlier, adequacy and consistency tests, and CORDEX-RCA4 datasets were passed the Power transformation and variance scaling bias correction and square root normalization. The baseline monthly stream flow (1990-2003) was modeled using SWAT, calibrated (1992-1999) and validated (2000-2003) in SWAT-CUP under SUFI2 tool. The CORDEX-RCA4 models were compared their performance at the baseline period (1990 to 2001) using volumetric metrics and Taylor diagram to predict future precipitation and stream flow variability by the best fit RCA4 model under RCP4.5 and 8.5 emission scenarios for 2050s and 2080s periods. The results showed that SWAT was very good at modeling baseline stream flow indicated by R^2, NSE, PBIAS and RSR as 0.93, 0.94, 6.3% and 0.13 for calibration, and 0.82, 0.89, 10.4% and 0.07 for validation respectively. ICHEC-EC-EARTH-RCA4 was best fitted by scoring 0.9838, 0.0000, 0.9838 and 0.0162 for VHI, VFAR, VCSI and VMI respectively for volumetric, and 0.749, little less than 75 and little less than 100 for CC, NRMSE and δ_N respectively and better at annual scale at Taylor diagram. The baseline variability of seasonal rainfall indicated that an increments on the winter and autumn and decrease on the spring season. In the 2050s and 2080s of both emission scenarios significant increase and decrease was projected than the baseline periods at seasonal and annual scales. The mean annual rainfall was decreased by; 7.58% and 9.82% at 2050s and 2080s, and 4.92% and 9.28% during 2050s and 2080s under RCP4.5 and RCP8.5 respectively. The total change of rainfall was; 9.89% for 2050s and 13.52% for 2080s, and 8.79% at 2050s and 13.31% at 2080s for RCP4.5 and RCP8.5 scenarios respectively. Future annual stream flow will be decreased by; 8.84% in 2050s and 10.59% in 2080s, and 6.32% in 2050s and 9.88% at 2080s under RCP4.5 and RCP8.5 respectively. The total annual stream flow change will be; 9.88% during 2050s and 13.67% at 2080s, and 9.96% at 2050s and 13.86% at 2080s for the RCP4.5 and RCP8.5 scenarios respectively. Findings of this study indicated that climate change has significant impact over surface water availability of Gerhu-Sirnay catchment. To conduct policy-oriented climate change impact over surface water availability, future researchers should consider multiple; climate variables, dynamic drivers and uncertainty analysis, and improve CORDEX inputs.

Key words: Surface water availability;CORDEX-RCA4; Baseline; Stream flow; RCP Scenarios

1. INTRODUCTION

1.1. Background

Knowledge of spatio-temporal variability of the available surface water within a catchment is decisive for deciding sustainable and long-lasting water resources management (Negewo and Sarma 2021). Surface water potential variability is the most hazardous event caused from different dynamic drivers (Dwarakish and Ganasri 2015), such as climate change (Bekele and Abate 2020; Khoi et al. 2021) and land use/land cover (LULC) changes (Negewo and Sarma 2021; Aragaw et al. 2021; Lukas et al. 2023). Climate changes were the main anthropogenic driver (Borrelli et al. 2020) that causes the dramatic instability of the catchments, especially over the hydrological regions categorized by high precipitation fluctuation like East Africa, (Gebrechorkos et al. 2019). Surface water availability may be indicated by several climate variable; precipitation, stream flow, evapotranspiration, temperature and surface-runoff (Takele et.al.2022; Ukumo et al. 2022; Khoi et al. 2021; Mollel et al. 2023). However, as reported by Mollel et al. (2023); Gebrechorkos et al. (2019) precipitation is the parameter that mostly controls river discharge in Africa respectively. Therefore, due to the implications of those studies and scope of this study, the impact of climate change on surface water availability of Gerhu-Sirnay catchment was conducted in terms of precipitation and stream flow variability.

Climate change characterizes by varying the intensity and frequency of different hydro-meteorological parameters including precipitation and stream flow (Mollel et al. (2023) leads to instable water availability of a catchment (Tibangayuka et al. 2022). The Intergovernmental panel on climate change(IPCC 2018) reported that the concentrations of atmospheric greenhouse gases, such as carbon dioxide (CO_2), methane (CH_4), nitrous oxide (N_2O) will increase for between 2030 and 2052 likely to reach 1.5°C (Masson-Delmotte et al. 2018) and climate extremes, like precipitation and temperature will be extreme in the future (Pelletier et al. 2015). Greenhouse gases capture heat from the sun, causing global warming and climate change, and are causing weather pattern variability and disrupting nature's natural equilibrium which will accelerate hydrological cycle fluctuations (Makar et al. 2022). This poses several dangers to humans and all other kinds of life on Earth, particularly in the poor world's semi-arid tropical nations (Stella & Deogratias 2017; Wang et al. 2014). As precipitation increases the evaporative loss, surface runoff and stream flow also rise (Liu et al. 2022), and the rising of

temperature lead to increased water consumption by vegetation, significant reductions in river flows and decreased water availability which impacts ecosystems, agriculture, and human water supply (Mollel et al. 2023).

Rainfall was found to be highly variable in space and time, especially in east Africa (Gebrechorkos et al. (2019) and thus there is a need to invest in the early propagation of weather forecasts to reduce vulnerability and prepare for the unfavorable weather (Mugo et al. 2020). Due its dynamic nature (Abbasi et al. 2022), climate impacts, like from lower precipitation led to more frequent droughts resulting hunger and poor nutrition in places where people cannot find sufficient food. Africa is among the most affected continents by climate change over which its socioeconomic development has been hindered (Ayugi et al. 2021; Gebrechorkos et al. 2019). For instance, Kenya and Ethiopia in East Africa have seen more than 3 million cattle deaths, due to water scarcities, considerable vegetation deficits (World Food Programme 2022) and lack of climate change adaptation potentials (Feyisa et al. 2023).

To mitigate this adverse impact, it is essential to get consistent and decision level future climate change information. Climate models are automated mathematical representation of the earth's climate system based on energy budget and various climatic transmission mechanisms on each grid boxes, by conducting the momentum, heat, and moisture equations (Kour et al. 2016; Flato et al. 2006). There are several popular sources of climate data, some of the commonly used are (Panja et al. (2023); National Oceanic and Atmospheric Administration (NOAA), NASA Earth Observing System Data and Information System (EOSDIS), Intergovernmental Panel on Climate Change (IPCC), World Meteorological Organization (WMO), Climate Data Online (CDO) etc. Based on their dimensional scopes, climate models were categorized in to One-Dimensional Energy Balance Models (EBMs), One-Dimensional Radiative-Convective Models (RCOMs), Two-dimensional Statistical-Dynamical Models (SDMs) and Three-Dimensional General Circulation Models (GCMs) (Kour et al. 2016; Flato et al. 2006; Endris et al. 2013), they are easy to use but complex to compare. Therefore, to understand the dynamic human and ecological needs and give the solution against climate variability and impacts, first there must need of conducting systematic studies to select the best site-specific scale climate model to understand the non-linear relationships between the dynamic changes of climate with the hydrological processes of the ecology (Dwarakish and Ganasri 2015).

A coordinated regional climate downscaling experiment (CORDEX) has been planned to simulate the climate of Africa based on a variety of climate regimes and finer resolution allow the simulation of local climate conditions (Geleta et al. 2022). The potential impact of climate change on hydrologic processes is widely studied using the integration of soil and water assessment tool (SWAT) (Arnold et al. 2012) and the dynamical downscaled RCMs data (Kuma et al. 2021; Emiru et al. 2022). In Ethiopian basins, several studies have investigated climate change impacts on precipitation and stream flow (Nigatu et al. 2016; Abraham et al. 2018; Worqlul et al. 2018; Bekele et al. 2021; Chakilu et al. 2022; Takele et al. 2022; Balcha et al. 2022a; Balcha et al. 2023; Alehu et al. 2021). All the mentioned studies were based on different; emission scenarios, downscaling, bias-correction, performance evaluation perspectives (single or multiple) and evaluation metrics to evaluate and rank the ability of RCM models. These methodological differences can have a significant impact on the outcome of an impact study. For example, Chakilu et al. (2022) investigated the impact of climate change on the streamflow in the Upper Nile of Gumera watershed and conclude that streamflow will increase in future scenarios. Mengistu et al. (2021) concluded that there would be a decreasing stream flow up to 22.7% in the same basin and Alehu et al. (2021) over Gidabo Watershed reported that precipitation and stream flow will decrease in the future. This reminds that climate models are specific to local climate and landscape features, spatial resolution, analysis techniques and selection of metrics to simulate the effects of climate change on water resources (Kim et al. 2014). Ghorbanian et al. (2022) noticed that for decision level performance evaluation and ranking of GCM-RCM models, selection of evaluation metrics and ranking skills would mandatory to be based on critical insights.

Therefore, this study has motivated to use noble metric selection frameworks and hybrid perspectives for reliable performance ranking of CORDEX-RCA4 models, and to assess the impact of climate change over surface water availability in terms of baseline precipitation, future precipitation and stream flow variability and overall impact at monthly scale. To conduct this, 7 CORDEX-RCA4 models; CanESM2, CERFACS-CNRM-CM5, GFDL-ESM2M, ICHEC-EC-EARTH, MIROC-MIROC5, MPI-M-MPI-ESM-LR and NorESM1-M were selected from critical literature review and compared their performance using the right metrics included in the hybrid perspectives; volumetric and Taylor diagram.

1.2. Problem statement

Since the period of industrial revolution, human induced practices, like climate change have been activated and subsequently leads to hydrological extremes, which disturbs catchment and causes irreversible environmental hazards (Piao et al., 2010). The anticipated increase of global climate change is expected to increase the rate of evapotranspiration and alter precipitation patterns contributing to changes in drought and flood characteristics (Lindner et al. 2010; IPCC 2007); Bates et al. 2008; Niang et al. 2014). Africa is among the most affected continents by climate change over which its socioeconomic development has been hindered (Ayugi et al. 2021). East Africa is among the most climate change variability, vulnerability and impact faced regions in Africa (Gebrechorkos et al. 2019) and Ethiopia was cited as one of the most extreme examples (Bekele et al. 2021) hence resources including surface water are progressively exposed. For instance, Kenya and Ethiopia have seen more than 3 million cattle deaths due to water scarcities (World Food Programme 2022) and lack of climate change adaptation potentials (Feyisa et al. 2023). As a result, Ethiopian catchment scale land and water security managers, planners and water policy makers are facing uncertainties on the future availability of surface water resources (Kuma et.al. 2021).

Globally and locally, diverse researchers have studied the impact of climate changes on catchment hydrology but none of them were studied in Gerhu-Sirnay catchment. For example, East African future precipitation simulations were performed by Osima et al. (2018) using a 25-member CORDEX-Africa RCM ensemble. They showed that the warming rate of the Greater Horn of Africa is faster than the global mean, and the projected change in precipitation across the region is mostly uncertain. Aragaw et al. (2023); LIU et al. (2022); Ukumo et al.(2022); Kuma et.al. (2021); Alehu et al. (2021) have investigated climate change impacts on hydrologic responses in other Ethiopian basins. Then, they concluded that, temperature and precipitation would face significant fluctuations, especially for catchments having arid weathers (high precipitation fluctuations) (Gebrechorkos et al. 2019) like Gerhu-Sirnay catchment (IPCC 2000) leads to the extreme climate events.

For about 80 % of the Ethiopian population is dependent on rainfed-dominated agricultural economy (Hanjra et al. 2009) hence the economy of the country is greatly influencing by climate variability. As a result, Ethiopia including Gerhu-Sirnay catchment has been under the hardest

hit by climate change and its induced hazards. To adapt and mitigate such impact, the Ethiopian government has designed the green economy program however, there must a need of much more daily climate change impact minimization and adaptation strategies. Furthermore, Gerhu-Sirnay catchment's existing land and water resource management system has been harmed by rapid population growth, continuous war, deforestation, poor agricultural practices and high vulnerability to the adverse effects of climate change. Therefore, to understand the non-linear relationships among the dynamics of climate, hydrological processes and the dynamic human needs, and to give the solution, first there must need of systematic studies to select the best GCM-RCM model (Dwarakish and Ganasri 2015). As a result, this study is an important endeavor to solve the mentioned problems.

1.3. Objective of the study

1.3.1. General objective

The general objective of this thesis is to assess the impact of climate change over the surface water availability in the Gerhu-Sirnay catchment, Mereb basin, Ethiopia.

1.3.2. Specific objectives

- To correct the biases of rainfall and air temperature in the baseline period so as to predict future water availability on annual and seasonal scales.
- To identify better performing RCA4 climate model would best fit to the baseline precipitation data in Gerhu-Sirnay catchment.
- To predict future precipitation variability using the better performed model under RCP4.5 and 8.5 emissions scenarios on annual and seasonal scales.
- To develop calibrated and validated baseline stream flow model for Gerhu-Sirnay catchment using SWAT model at annual and seasonal time steps.
- To predict streamflow variation on annual and seasonal time scales under RCP4.5 and RCP8.5 climate scenarios.

1.4. Research questions

From the result of this study, the systematic points to be clear are bulleted below:

- How can the biases in rainfall and air temperature during baseline period be corrected to predict future water availability on annual and seasonal scales?

- Which RCA4 climate models perform best in fitting the precipitation data for Gerhu-Sirnay catchment?
- How can future rainfall variability be predicted using the better performing RCA4 model under RCP4.5 and 8.5 emissions scenarios?
- To develop calibrated and validated baseline stream flow model for Gerhu-Sirnay catchment using SWAT model at annual and seasonal time steps.
- How can develop the calibrated and validated baseline stream flow model for Gerhu-Sirnay catchment at annual and seasonal time steps?
- How does stream flow variation change on annual and seasonal time scales under RCP4.5 and RCP8.5 climate scenarios?

1.5. Scope of the study

The scope of this study was detailed by its spatial and scientific considerations, which are study regions and number of scientific expected outputs respectively. Therefore, based on these issues this study was limited to Gerhu-Sirnay catchment, 381.34 square kilometers. The planned five scientific outputs were; (1) corrected the biases of rainfall and air temperature in the baseline period so as to predict future water availability on annual and seasonal scales, (2) calibrated and validated baseline stream flow model would be developed using SWAT model, (3) performance evaluation and ranking of 7 CORDEX-RCA4 models in reference to the rain gauge data was performed and future precipitation variabilities was predicted from the better performed RCA4 model under RCP4.5 and 8.5 emissions scenarios, (4) future stream flow variabilities was forecasted and (5) climate change impacts on surface water availability was assessed.

1.6. Significance of the study

In Gerhu-Sirnay catchment, no related studies have been conducted before hence, result of this study was not only modeling aspect, but also has a regional importance of different climate modeling aspects. Therefore, its outputs were implemented on the ground to solve local problems and global scales for knowledge expansion. Government or NGOs who are working with the raised issues in Gerhu-Sirnay catchment may use the result of this research as an input. It was also important to meet the mission of scientific works; contributing knowledge for policy making processes at national and local levels, expand appropriate problem-solving technology,

contributes to the enhancement of teaching-learning process of Hawassa University as per the program.

1.7. Organization of the thesis

The thesis is organized in five chapters as follows:

Chapter one: Introduction- this introductory chapter comprises the background of study, statement of problem, objectives, research questions, significance, scope and organization of the thesis.

Chapter Two: Literature review, it contains previous works of various scientific works related and served as a base to this study.

Chapter Three: Materials and Methods- this chapter presents the location of the study, input materials, corresponding methods and models used towards achieving the research objectives.

Chapter Four: Results and Discussions, which presents the end results of each objective of this thesis work and their corresponding consistent discussions to realize with the existing knowledge.

Chapter Five: Conclusions and Recommendations- which concludes the over all methods, results and reported conclusions, and insights for future researchers.

2. LITERATURE REVIEW

2.1.General

Globally and locally, a number of studies have been carried out by individual researchers, team works and by the respective global and local government organizations for the purpose of understanding climate change; sources, driving parameters, impact severity, modeling aspects, adaptation measures, mitigation strategies, and future climate data sources. All of them have concluded that climate change was the source for irreversible overall environmental hazards, and recommended that respective adaptation and mitigation strategies would be the area of future concern. The impact assessment of climate changes on hydrological system constitutes on the combinations of hydrological and climate models (Kour et al. 2016), up on which hydrological models were used to generate baseline hydrological model and climate models to provide respective weather variable to represent their constants at the developed hydrological model. In the following sub-sections surface water availability as a function of climate change was reviewed to know the existing knowns, to identify the gaps, to compare literatures to select the recent climate data sources, analysis methods and climate impact modeling approaches on surface water availability.

2.2. Climate Data Sources

The source for climate data are climate models, they are automated mathematical representation of the earth's climate system based on energy budget and various climatic transmission mechanisms on each grid boxes, easy for use and complex to compare (Kour et al. 2016; Flato et al. 2006). Climate models are quantitative models used to compute the consequences of greenhouse gas emission concentrations, and to simulate and quantify the climate response to present and future human and natural activities. At each of these grids, the momentum, heat, and moisture equations are designated to solve the remotely large-scale information on the atmosphere, ocean, and land. Based on their dimensional scopes, climate models were categorized in to One-Dimensional Energy Balance Models (EBMs), One-Dimensional Radiative-Convective Models (RCOMs), Two-dimensional Statistical-Dynamical Models (SDMs) and Three-Dimensional General Circulation Models (GCMs) (Kour et al. 2016; Flato et al. 2006; Endris et al. 2013). GCMs are best and multi-dimensional data sources but coarse in resolution and they only conducted for global, and continental studies for more than monthly

and 100km as a temporal and spatial scales respectively. For this reason, the dynamically and statistically downscaled form of GCMs, Regional Climate Models (RCMs) are better for most parts of the world (Aragaw et al., 2023; Tumsa, 2022; Daniel. 2023) in providing better tempo-spatial resolution, its information is physical-models based, its ability to model atmospheric processes and land cover changes explicitly in a better representation of some weather extremes than in GCMs.

RCMs is a high-resolution climate model that covers a limited area of the globe, typically 5,000 km x 5,000 km, with a typical horizontal resolution of 50 km. Hence RCMs are comprehensive physical models, usually including the atmosphere and land surface components of the climate system, and containing representations of the important processes within the climate system (e.g., cloud, radiation, rainfall, soil hydrology)(Flato et al. 2014). However, still the problem of spatial resolution was not solved even within RCMs. Therefore, the Coordinated Regional Climate Downscaling Experiment (CORDEX) was implemented under the sponsorships of the World Climate Research Program (WCRP) in order to providing robust regional climate information globally, including Africa at daily and 25-50km tempo-spatial scales (Lennard and Nikulin 2015).

2.3. CORDEX-Africa Models

The Coordinated Regional Downscaling Experiment1 (CORDEX) was set up by the World Climate Research Programme2 (WCRP) in 2009 to coordinate Regional Climate Downscaling and provide a set of high-resolution regional climate projections for the majority of global land regions (Lennard and Nikulin 2015). CORDEX-Africa consists of a dynamic group of young (and some less young) scientists who are working with data from CORDEX downscalings over the CORDEX African domain. The CORDEX-Africa initiative has been developed to analyze downscaled regional climate data over the CORDEX-African domain, train young climate scientists in climate data analysis techniques and engage users of climate information in both sector specific and region/space-based applications. There are four regional teams (west, central, east and southern Africa) who are addressing region-specific climate questions and one thematic group that is considering applied questions such as health, biodiversity, agriculture and hydrology (https://www.csag.uct.ac.za/cordex-africa/).

CORDEX has many RCMs models, the dynamic downscaled of GCMs by Endris et al. (2013) are among the utilized in East Africa. In Africa, the recent CORDEX-RCMs were derived from the Coupled Model Intercomparison Project Phase-5 (CMIP5) (Al-Hasani et al. 2023). As an assumption of GCMs in CMIP5, the future climate conditions are dependent on the Green House Gas Concentration (GHGCs) trajectory, namely the Representative Concentration Pathway (RCPs) (Petpongpan et al. 2020). The pathways describe different climate futures, all of which are considered possible depending on the volume of greenhouse gases (GHG) emitted in the years to come. The RCPs, originally RCP2.6, RCP4.5, RCP6, and RCP8.5 are labelled after a possible range of radiative forcing values in the year 2100 (2.6, 4.5, 6, and 8.5 W/m^2, respectively). The four RCPs are consistent with certain socio-economic assumptions but are being substituted with the shared socioeconomic pathways which are anticipated to provide flexible descriptions of possible futures within each RCP. RCP 4.5 is described by the IPCC (2014) as an intermediate scenario hence, it is the most probable baseline scenario taking into account the exhaustible character of non-renewable fuels. RCP8.5, generally taken as the basis for worst-case climate change scenarios, and it was based on what proved to be overestimation of projected coal outputs. It is still used for predicting mid-century (and earlier) emissions based on current and stated policies. Therefore, both the intermediate and worst-case climate change scenarios RCP 4.5 and 8.5 will be used in this study to forecast reliable future climate changes.

In addition to the downscaling technique of GCMs to Africa, the POSTDAM Institute for Climate Impact Research under the research team of Liersch et al. (2018), has developed better 7 GCMs-CORDEX-10RCMs datasets for Ethiopia by value addition in bias correction using harmonic based-vector generalized linear model (machine learning algorithms). The dataset provides daily rainfall, daily mean near-surface air temperature (tas), daily maximum near-surface air temperature(tasmax) and daily minimum near-surface air temperature(tasmin) under the Representative Concentration Pathways, RCP4.5 and 8.5 future scenarios. Due to their consideration of regional characteristics, like topography and other physical factors, the performances of RCMs to represent ground data was area specific and uncertainty affected. RCM includes Rossby Center Regional Climate Model (RCA4), Consortium for Small-scale Modeling (COSMO), Climate Limited-Area Model (CCLM) version 4.8, high resolution

limited-area model (HIRHAM5), and Max Planck Institute Regional Model (REMO2009) driven by different GCMs included in the CMIP5 (Aragaw et al. 2023).

RCA4s were used to downscale historical and future simulations of multiple GCMs-CMIP5; CanESM2, CERFACS-CNRM-CM5, GFDL-ESM2M, ICHEC-EC-EARTH, MIROC-MIROC5, MPI-M-MPI-ESM-LR and NorESM1-M than the others in CORDEX project, and it was originated from projections made by ensembles of GCMs in Africa-CORDEX (Nikulin et al. 2012;Tamoffo et al. 2019). Also as stated by Liersch et al. (2018) GCMs-CMIP5; CERFACS-CNRM-CM5, GFDL-ESM2M and NorESM1-M were downscaled to CORDEX project only by RCA4s. Hence, the application of RCA4s provides not only multiple but also an inclusive usage of CORDEX CMIP5-RCM models. Therefore, the outputs of RCA4s were performed better over Africa.

As a result, many investigators, including Aragaw et al. (2023); Tumsa (2022); Alehu et al. (2021) and others were used it under Representative Concentration Pathway (RCP4.5 and 8.5) future scenarios and provided representative and consistent outputs, however they noted that all RCA4s needs careful and skillful bias correction analysis and performance ranking before using their data for any further analysis.

2.4. Modeling Aspects of CORDEX-RCA4 Models

Shanka et al. (2017); Al-Hasani et al. (2023); Liemohn et al. (2021) indicated that decisive modeling of climate change impact on surface water availability was the coupling of selection of appropriate climate model, use of recommended bias correction methods, comprehensive skill of climate models' ranking and selection and skill of hydrological model simulations. Climate models are used to generate weather variables, bias corrections are required to minimize systematic errors, performance evaluation and ranking of climate model are appropriate input generators for hydrological models and hydrological models are used to model the baseline and predicted surface runoff, especially they are important for the un gauged catchment (Tilahun et al. 2023), like Gerhu-Sirnay catchment. This indicates that each modeling aspect has corresponding error reduction capacities, for example, climate models are area specific (Daniel 2023) meaning that not all RCMs can used in every study region (Aragaw et al. 2023); LIU et al. (2022) hence selection of appropriate model for own study area is the pre-request for the application of climate models.

2.4.1. Bias Correction

Moreover, to the spatial resolution problems, CORDEX-RCA4 are still not free of systematic biases (Aragaw et al. 2023; Tumsa 2022) which may come from the imperfect conceptualization, discretization, internal climate variability, regional terrain complexity and spatial averaging of grids (Gunathilake et al. 2020). If this systematic error was not corrected, it causes over or under estimation of ground datasets by the climate models (Legesse et al. 2015). Outputs of RCA4 may not directly be used for impact assessment as the computed variables may differ systematically from the observed ones (Tumsa 2022). Therefore, bias correction will be applied to compensate for any tendency to overestimate or underestimate the mean of downscaled precipitation. Bias correction factors will be computed from the statistics of observed and simulated variables. There are many bias correction methods, including linear scaling (LS), power transformation (PT), local intensity scaling(LIS), distribution mapping (DM), variance scaling (VS), delta change(DC) and quantile mapping(QM) (Daniel. 2023).

Daniel (2023) compared the LS, PT, and DM bias corrections for simulated precipitation in the Gelana Deme watershed, Ethiopia. The result suggested that, the PT method performed better. A parallel study was carried out in the Bilate catchment, Southern Ethiopia by Kuma et al. (2021) and it has supported by Geleta & Gobosho (2018) and Dibaba et al. (2020) in the Finchaa watershed in Ethiopia, and they said PT is best bias elimination method for Ethiopia. Fang et al. (2015) have compared LS, LIS, PT, DM and QM to remove the systematic errors with in the timeseries precipitation in an arid area in China. The result showed that, all bias correction methods effectively improved the simulations with PT and QM methods performed equally best in correcting the frequency-based indices. Daniel and Abate (2022) investigated on LS, PT and DM of precipitation bias reduction methods in the Gelana watershed, Rift valley basin, Ethiopia. They concluded that PT performed better for precipitation correction.

Luo et al. (2018) said that bias correction methods have substantial difference in precipitation than other climate variables hence concluded that careful selection of bias correction method is prior than any climate model application. They compared seven precipitation bias correction methods; Daily Bias Correction (DBC), Daily Translation (DT), Distribution Mapping (DM), Empirical Quantile Mapping (EQM), Local Intensity Scaling (LOCI), LS and PT. Their conclusion showed that all bias correction methods have potential to improve the performance

of reproducing precipitation, although distribution-based DBC and EQM methods performed best.

Teutschbein and Seibert (2012) was compared 6 bias-correction methods; linear-scaling, Local intensity scaling (LOCI), Power transformation (PT), Variance scaling, Distribution mapping and Delta-change correction to adjust the precipitation and temperature of 11 RCMs using statistical evaluation for five catchments in Sweden under current (1961–1990) climate conditions. They insured that all methods were able to correct the daily mean values, with a clear difference to adjust other statistical properties. Hence, their conclusion ensured that PT followed by Variance scaling were performed much better in correcting hydrological extremes in several statistical characteristics.

Daba et al. (2020) indicated that scaling and shifting bias correction of temperature was advisable for Ethiopian watersheds. Abdule et al. (2024) used variance scaling technique in the Yadot watershed, Genale Dawa basin, Ethiopia and concluded that it was advisable for Ethiopian watersheds.

2.4.2. Performance Evaluation and Ranking Perspectives

2.4.2.1.Single Evaluation

Ghorbanian et al. (2022) indicated that no single evaluation perspective or point of view with no all-respective metrics for every hydrologic region (Abiola et al.2013) could provide decision level evaluation of climate model rainfall products. It is understood that, each metric under each evaluation point of view was designed for a specific evaluation task hence, the application of less metrics and single evaluation point of view limits the findings and decision of the study. Evaluation metrics may be subjected to different points of task or measuring points of view, for example, continuous statistical evaluation metrics, like; Mean Absolute Error (MAE), Symmetric Mean Absolute Percentage Error (SMAPE), Root Mean Square error (RMSE), Pearson's correlation coefficient (CC) and Fitness (F) were developed to measure the relation of different continuous variables at a given selected point of the dataset (Abiola et.al. (013). Example, MAE measures only the average difference between the climate and rain gauge values and RMSE measures the average errors by focusing only the extreme values. The most common continuous evaluation metrics were; CC, RMSE and Normalized Standard Deviation (δ_N), which were comprehensively digitized for the purpose of one-way and less vague 2D-

diagrammatic visual plot ranking summary (Xu et al. 2019a; Xu et al. 2019b) which is Taylor diagram (Taylor 2001). CC provides the degree of linear association between the rain-gauge and satellite datasets as a function of time, RMSE represents the overall error level or accuracy and δ_N indicates the scattering of both data sets from their respective mean to represent percent bias (Xu et al. 2016).

In Ethiopia that is outside of the Gerhu-Sirnay catchment several studies have been conducted on valuation and ranking of climate models rainfall products with rain gauges (Daniel 2023; Geleta & Gobosho 2018; Dibaba et al. 2020). In these studies, the widely used methods to measure the performance of grided rainfall products were single evaluation metrics more of continuous. However, as evidenced by Abiola et.al. (2013) continuous statistical metrics were unrealistic for all weather regions of the globe, specifically for the regions where orographic type of rainfall occurs, such as in Ethiopia.

Aghakouchak & Mehran (2013) were developed a new approach on the point of view of measuring the volumetric performance of both gridded and climate datasets in reference with the rain gauge datasets. The parameters of volumetric statistical metrics are Volumetric Hit Index (VHI), Volumetric False Alarm Ratio (VFAR), Volumetric Critical Success Index (VCSI) and Volumetric Miss Index (VMI). VHI is the measure of the volume of correctly detected rainfall by the satellites in reference to the volume of correctly detected satellites and missed rain gauge rainfall observations. VFAR is the volume of false rainfall products by the satellite relative to the sum of rainfall by the satellite. VMI represents the volumetric fraction of missed observations relative to the volume of practically detected simulations and missed observations, and VCSI is defined as the overall measure of volumetric performance (Liemohn et al. 2021); Taylor 2001).

2.4.2.2.Hybrid Evaluation

Tumsa (2022) measured the performance of RCMs using statistical tools and SWAT model-based sediment yield and stream flow at Upper Awash Sub-Basin, Ethiopia. The output of the statistical and SWAT model showed that climate models do not accurately simulate hydro-climatological variables. Finally, the study concluded that climate models were better at simulating the rainy season than the dry season. This integration of statistical tools and the SWAT model to analyze the RCM's performance was a unique method to improve the quality

of the output for its implementation in maintaining water balance and sediment load reduction. Daniel (2023) measured the performance of the three selected RCMs by using four statistical indicators: Pearson correlation coefficient (R), root mean square error, Nash–Sutcliffe efficiency, and percent bias. Moreover, all RCMs performed better in the Deme watershed than in the Gelana watershed, and said that there is no single best performance evaluation technique. Thus, the combined use of many techniques provides a complete overview of model performance.

In the Gidabo catchment of Rift Valley Basin, Ethiopia Gebretsadkan et al. (2023) have studied the performance of multi-satellite rainfall products using hybrid techniques under multiple evaluation metrics. They indicated that the application of hybrid evaluation of satellite or climate model products was evidence to get complementary and decision level results. Therefore, in this study the performance ranking of the 7 RCA4s climate models were performed using the combination of comprehensive statistical metrics in Taylor diagram and volumetric metrics, which is hybrid perspective before proceeded to SWAT model.

2.4.3. Selection of Performance Evaluation Metrics

Regardless of the selected evaluation perspective, selection of each metric with in each evaluation method determines the accuracy of the planned objective to be decisive level (Gebretsadkan et al. 2023). It understood that each metric was designed for a specific evaluation task; hence, the application of less metrics limits the findings and decision of the study. Liemohn et al. (2021) mentioned that metrics can be categorized based on various ways; however, they detailed only groupings and categories that are important to select the number of best metrics. Based on the evaluation perspective of metrics, grouping was clustered into continuous and discrete, which are quantitative and qualitative, respectively. Quantitative metrics are fit performances, and they are based on the exact values of rain gauge-climate model dataset values and qualitative metrics are based on event detections under a given threshold (Liemohn et al. 2021). Quantitative performance of climate model rainfall products in reference to rain-gauge rainfall products can be evaluated using different statistical metrics. However, the issue is in selecting appropriate number of metrics that can build complete and decision level results (Zhou et al. 2021; Liemohn et al.2021).

The application of multiple metrics improves the decision level of climate to rain gauge dataset evaluations (Liemohn et al. 2021). The best way to select an appropriate evaluation metric was the insight consideration of groupings and categories (Liemohn et al. 2021), and evaluation point of view. Groupings of metrics provide specifications for the use of continuous or discrete metrics and/or both of them. Evaluation point of view determines the number of evaluation perspectives; single or hybrid (Gebretsadkan et al. 2023). Categories of metrics are the mechanisms to fix the number of metrics that would be used in each grouping and evaluation point of view based on its multiple criteria: accuracy, bias, precision, association, skill, extremes, discrimination and reliability to evaluate the multi-side performance of climate data.

2.5.Hydrologic Model

To assess climate change impact on surface water availability, hydrologic models are the most common ones (Shanka et al.2017). There exist various hydrologic models while, selecting a suitable model is essential and is an individual task (Al-Hasani et al. 2023). In general hydrologic models can be (1) simple empirical water balance or rainfall-runoff models e.g.; Artificial neural network, unit hydrograph and HEC-HMS are suitable for studying the change of climate variables on the basin hydrology at a regional scale, (2) lumped-parameter conceptual models e.g.; HBV model and TOPMODEL are suitable for quantifying surface flow and (3) physically based distributed models e.g.; SHE or MIKESHE model, and Soil and Water Assessment Tool (SWAT) are suitable for studying spatial patterns of hydrologic properties within watersheds (Al-Hasani et al. 2023). The SWAT model is a physically based, semi-distributed watershed hydrologic model jointly developed by the United States Department of Agriculture (USDA)-Agricultural Research Service (ARS) and Texas A&M AgriLife Research which is part of the Texas A&M University System. SWAT is a small watershed-to-river basin-scale model that simulates the quality and quantity of surface and groundwater, and predicts the environmental impact of land use, land management practices, and climate change (Al-Hasani et al. 2023). In SWAT, hydrologic processes such as surface runoff, infiltration, evapotranspiration, canopy interception and soil water movement are simulated at the Hydrologic Response Units (HRU) level, each one separately, assuming no interaction between HRUs in one subbasin (Al-Hasani et al. 2023).

The SWAT model is computationally effective for assessing the relationships between the climate change and the watershed hydrological process (Daniel and Abate (2022). SWAT has been the most used hydrologic model to assess the impact of climate change on water resources (Hammouri et al.2016). For example, Wang et al. (2012) have assessed the impact of climate change on stream flow in the arid Shiyang River Basin of northwest China using SWAT. Abouabdillah et al. (2010) also used SWAT model to measure the impact of climate change in a Mediterranean catchment (Merguellil, Tunisia). Ashraf et al. (2013) analyzed the impact of climate change on water resource components, drought and wheat yield in a semi-arid region using SWAT, the Karkheh River Basin in Iran. Kishiwa et al. (2018) assessed the impact of climate change on surface water availability using the coupled modeling of SWAT and Water Evaluation and Planning (WEAP) models in the case of upper Pangani River Basin, Tanzania. They concluded that couple modeling approach have more decisive level results on climate impact studies. Saade et al. (2021) have modeled the impact of climate change on surface water availability using SWAT model in a semi-arid basin in Kalb River, Lebanon. SWAT is used to address watershed management questions by predicting the effects of changes in soil, land use, and climate on water quantity and quality. Physically based models are used to help assess current and future problems, which is a prerequisite to planning water management policies and strategies. Rahvareh et al.(2023) indicated that, in addition to the modeling of hydrological parameters, SWAT is good at evaluating runoff management strategies. All these studies indicated that SWAT model was efficient in simulating hydrological process in arid and semi-arid areas. Furthermore, SWAT was applied successfully in these studies to assess the impacts of climate change on water resources. However, to ensure a successful implantation of SWAT, it's results should be verified against measured observation from the field, as for example, simulated stream flow values from stream flow gauges.

3. MATERIALS AND METHODS

3.1.Study Area

3.1.1. Location and Catchment Description

Gerhu-Sirnay catchment is located in the upper-central part of Mereb-basin, Tigray at a total distance of 988 kilometres from Addis Ababa, Ethiopia (Neway and Zewdie 2020). The geographic coordinates of the study area lie between 14º15′0″N and 14º30′0″ N northing and 38º57′0″E and 39º12′0″ E easting (figure 3-1). According to Strahler's (1957) classification depending on the arrangement of drainage with in it, catchment type of this study is Dendric hence is characterized by acute junction of drainages with the main river as displayed in figure 3.1. According to Neway and Zewdie (2020), the catchment was represented by aridity and the hydrological modeling there was influenced by environmental characteristics, like altitude, wind direction and complex topographic. The topography of the catchment is characterized as a steep, according to the 30*30 m DEM, elevation of the area ranges from1441m to 2909m a.m.s.l. The main parameters of the catchment including: average CN, total area, coverage of dominant LULC and soil type were 81.18, 381.34 square kilometres, Pasture/agricultural land generic (294.31 km^2) and Qc2-1bc-176 (285.02 square kilometres) respectively.

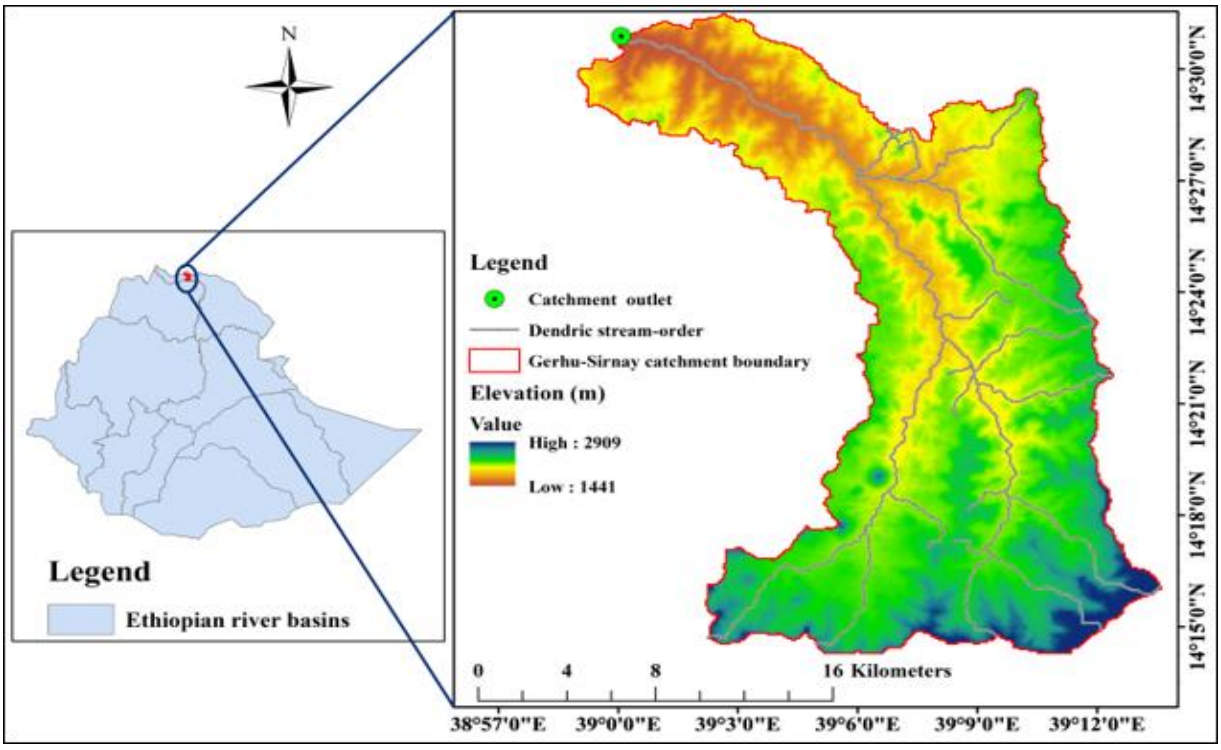

Figure 3-1: Location map of Gerhu-Sirnay catchment

3.1.2. Temporal Data

Gerhu-Sirnay catchment has three meteorological stations; May-dingur (locally Dibdibo), Enticho and Gerhu-Sirnay having 1990 to 2018 commonly recorded data at daily scale. Enticho gauge is class-I station which has all meteorological records however May-dingur has only precipitation, stream flow (1990-2003) and temperature, and Gerhu-Sirnay stations have only precipitation and temperature. Due to the key parameters, they can affect for surface water availability due to climate change impact under SWAT modeling, the only precipitation and river flow were detailed as in below. Especially in the areas receiving orographic type of precipitation, like in Ethiopia of Gerhu-Sirnay catchment, the spatial representation of each rain gauge station should be 41.66 square kilometers (Lopez et al. 2015). From the Theissen polygon's spatial coverage analysis (figure 3-2), the spatial coverage of May-dingur, Enticho and Gerhu-Sirnay stations was 57, 156 and 168 square kilometers respectively. Therefore, the rain gauges of this catchment are distributed sparsely.

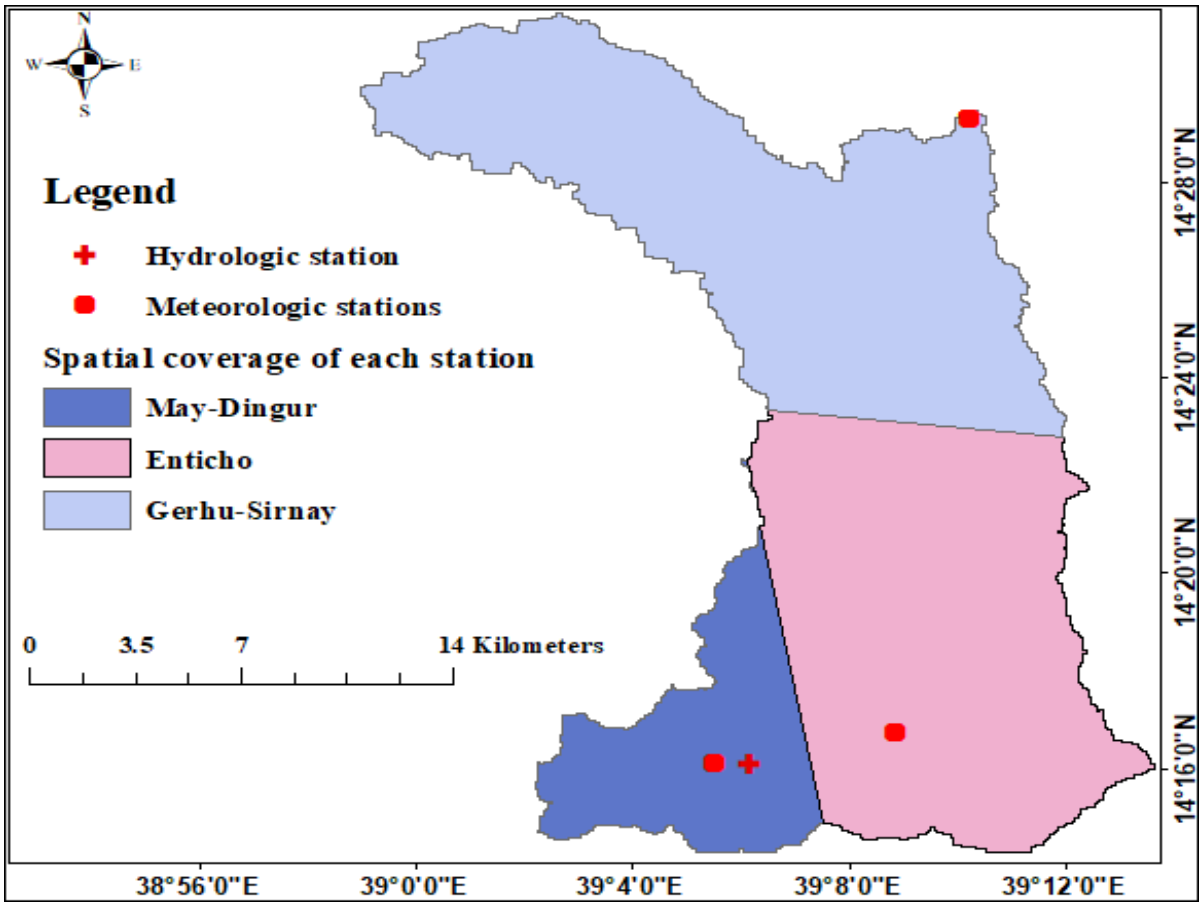

Figure 3-2: Thiesson polygon based spatial coverage (Km^2) of all stations in the catchment

3.1.2.1.Precipitation

According to National Meteorological Agency (NMA 2018), the maximum daily annual rainfall of Gerhu-Sirnay station was 100.74 mm which was observed on the 25th date of august, 2009. The maximum daily annual rainfall of May-dingur and Enticho stations were 150.5 mm and 169 mm recorded at 2001 and 1991 respectively, for more detail it can be looked at Appendix I. Out of the total amount of annual rainfall 60% of the rain is received only in the two months of the year (July and August) (Neway and Zewdie 2020). June and September contribute 26% and the remaining eight months receive 14%, and for quick visualization purpose it was plotted in figure 3-3, below;

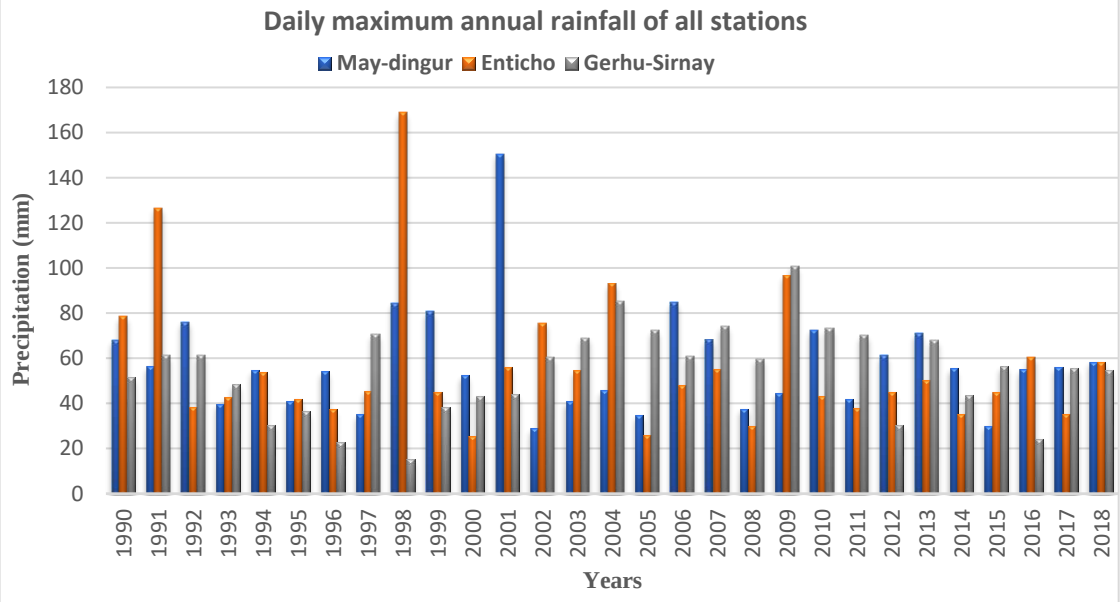

Figure 3-3: Daily maximum annual rainfall of May-dingur, Enticho and Gerhu-Sirnay stations

3.1.3. Spatial Data

3.1.3.1.Land Use Land Cover (LULC)

According to the LULC data of the area obtained from the ministry of water and energy, (MoWE 2018) GIS department, the LULC class of the catchment area is provided in figure 3.3. The largest area is Pasture land which covers for about >75% with good hydrologic condition, and the rest area has covered for about 25% with Agricultural Land-Generic(AGRL*)* in a fair hydrologic condition. More specifically the LULC detail of the catchment was given in figure 3-4;

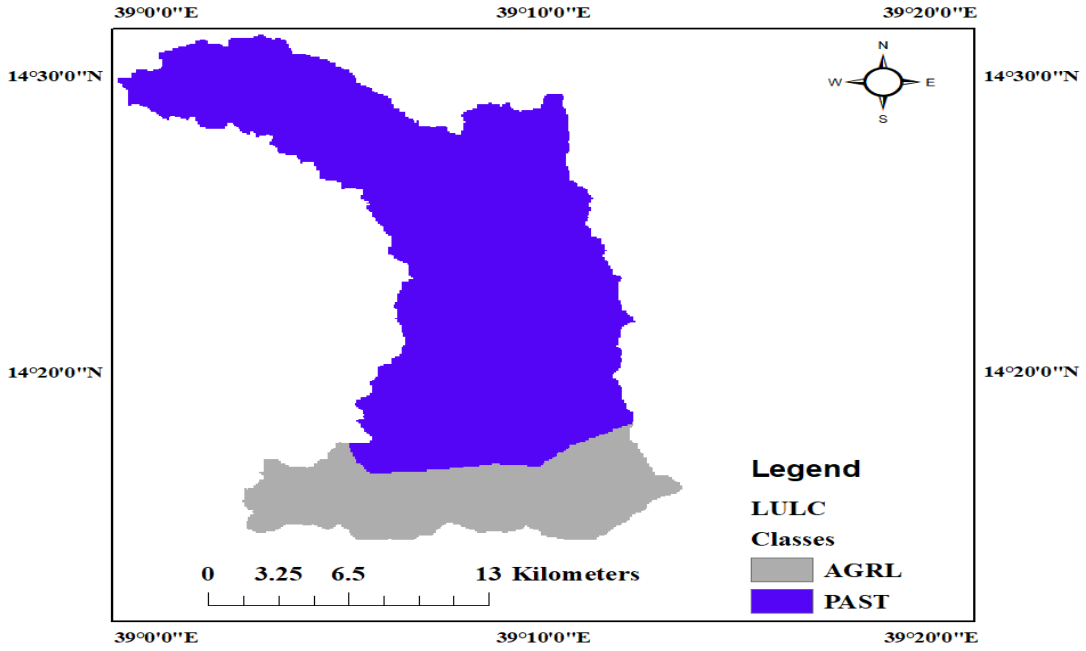

Figure 3-4: LULC map of Gerhu-Sirnay catchment

3.1.3.2.Soil Data

According to FAO (2018) soil class, the soil classification detail of Gerhu-Sirnay catchment was given in figure 3-5. As per the map, the north eastern and southern part of the catchment was dominated with SILT_LOAM and SANDY_LOAM.

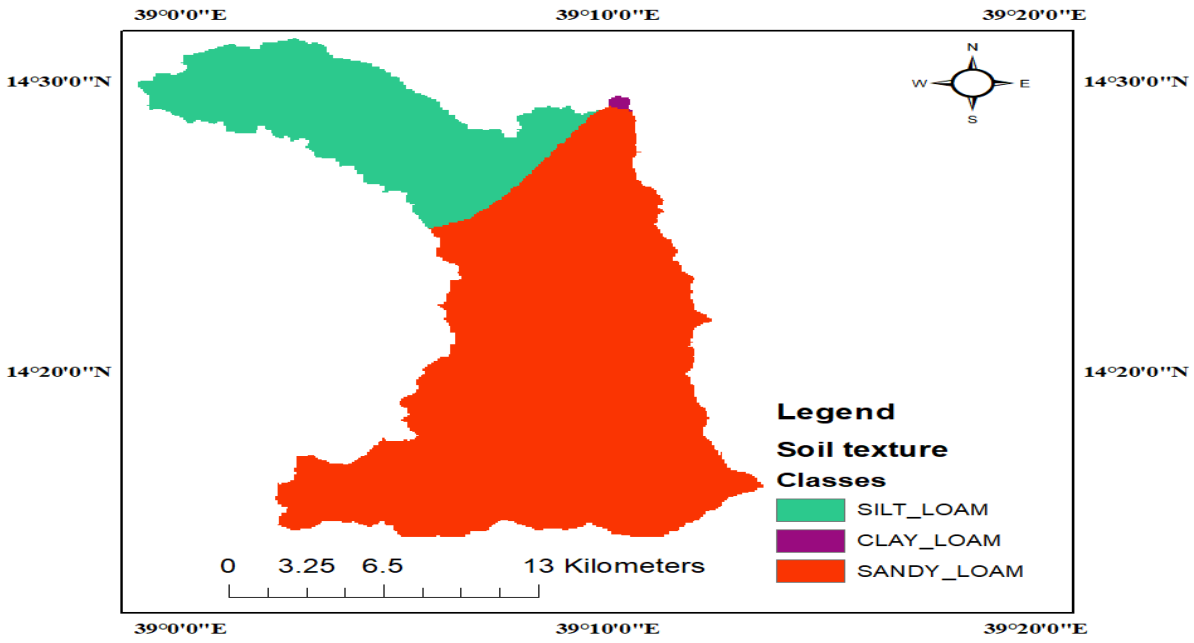

Figure 3-5: Soil map of Gerhu-Sirnay catchment

3.2.Conceptual Framework

The brief theoretical conceptual framework of this study is summarized in figure 3-6:

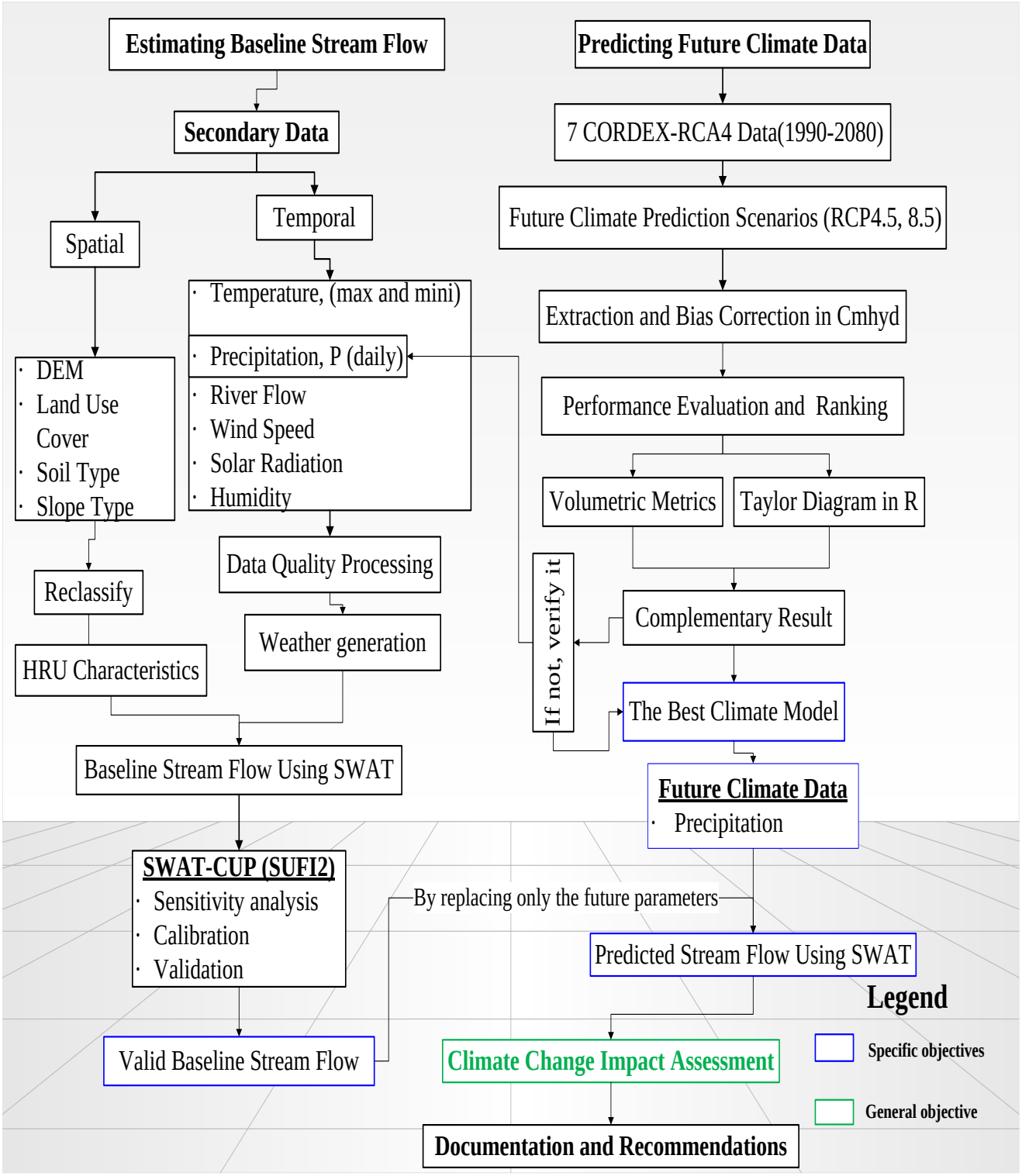

Figure 3-6: Conceptual framework of the study

3.3.Datasets

3.3.1. Observed Data

For this thesis work, the important temporal ground data including daily observed data of rainfall, maximum and minimum temperature, humidity, sunshine hours and wind speed, and flow data for the available hydro-meteorological stations of the catchment were collected from the National Meteorological Agency (NMA 2018), Ethiopia. Spatial data such as DEM and land use land cover and soil data were obtained from GIS department of Ministry of Water and Electricity (MoWE 2018).

Table 3-1: Summary of ground-based data and collection from sources

Data Category	Detail		Time	Data Source
Secondary Data	Temporal	•**Daily meteorological data;** precipitation, max and min temperature, wind speed, solar radiation and relative humidity	1990 to 2018	NMA , Addis Ababa, Ethiopia
		•**Daily hydrological data;** river flow	1990 to 2003	MoWE, Addis Ababa, Ethiopia
	Spatial	•**Catchment detail;** DEM(30m*30m), land use land cover, soil type	2022	

3.3.2. CORDEX-RCA4 Data

For this study RCA4 was selected since it was used to downscale historical and future simulations of multiple GCMs-CMIP5; CanESM2, CERFACS-CNRM-CM5, GFDL-ESM2M, ICHEC-EC-EARTH, MIROC-MIROC5, MPI-M-MPI-ESM-LR and NorESM1-M in CORDEX project, and it was originated from projections made by ensembles of GCMs in Africa-CORDEX. Therefore, the outputs of RCA4 were performed better over Africa (Nikulin et al. 2012;Tamoffo et al. 2019). As a result, many investigators (including Aragaw et al. 2023; Tumsa 2022; and others) were used it under Representative Concentration Pathway (RCP4.5 and 8.5) future scenarios and provided representative and consistent outputs. RCA4s data was accessed from international water management institute (IWMI). The data was derived from

GCMs climate model outputs which were dynamically downscaled by the CORDEX-Africa program, research team (Liersch et al. 2018). Generally, the multi-dimensional description and source for collection of each RCA4 data was summarized in table 3-2.

Table 3-2: Basic description of CORDEX-RCA4s considered in this study

Driving GCMs		RCMs	Tempo/Spatial		Data Collection	
Category	Model Name		Resolution	Coverage	Country, Model Institution	Web Source
CCCma-CanESM2	CanESM2	RCA4	Daily/ 0.44^0 x0.44^0	1969-2099/ Ethiopia	Canadian, Canadian Center for Climate Modelling and Analysis, Victoria	https://dataservices.gfzpotsdam.de/pik/showshort.php?id=escidoc:3124935
CNRMCERFACS-CNRM-CM5	CNRM-CM5	RCA4	Daily/ 0.44^0x0.44^0	1969-2099/ Ethiopia	France, Centre National de Recherches Météorologiques,	
GFDL-ESM2M	ESM2M	RCA4	Daily/ 0.44^0 x0.44^0	1969-2099/ Ethiopia	USA, Geophysical Fluid Dynamics Laboratory	
ICHEC-EC-EARTH	EC-EARTH	RCA4	Daily/ 0.44^0 x0.44^0	1969-2099/ Ethiopia	Irish Centre for High-End Computing	
MIROC-MIROC5	MIROC5	RCA4	Daily/ 0.44^0 x0.44^0	1969-2099/ Ethiopia	Japan, Atmosphere and Ocean Research Institute (The University of Tokyo), National Institute for Environmental	
MPI-M-MPI-ESM-LR	MPI-ESM-LR	RCA4	Daily/ 0.44^0 x0.44^0	1969-2099/ Ethiopia	Germany, Max Planck Institute for Meteorology	
NorESM1-M	ESM1-M	RCA4	Daily/ 0.44^0 x0.44^0	1969-2099/ Ethiopia	Norwegian Climate Center's Earth System Model	

3.4.Used Software Products and Tools

The brief descriptions of tools and their purpose used in this study were provided in table 3.3, below;

Table 3-3: Brief detail of the used Software Products and tools

S no.	Tool Name	Basic description	Purpose
1	**CMhyd v2**	It is Climate Model tool used for hydrologic modeling processing of global and regional climate models data for watershed-based hydrologic impact studies (downloaded from; CMhyd | SWAT | Soil & Water Assessment Tool (tamu.edu).	To extract and bias correct CORDEX-RCA4 data.
2	**ArcGIS 10.3.1**	It is powerful computer software used to create maps using 3D or 2D analytical tools, and conducting geospatial data analyses.	To delineate Gerhu-Sirnay catchment and generate its physical parameters.

3	**Excel**	It is a powerful industry leading spreadsheet software program used for data visualization and analysis.	To process and analyses ground data, normalize CORDEX-RCA4 and perform their volumetric comparison.
4	**SWAT v 10.3.1**	It is a physically-based hydrologic model developed to predict the impact of land management practices on surface water, sediment, and agricultural chemical yields with varying soils, land use, and management conditions over long periods of time.	To conduct baseline and future precipitation-runoff simulation.
5	**SWAT-CUP v 5.1.6**	SWAT Calibration and Uncertainty Program	Used to embed parameter optimization programs including, SUFI2
6	**SUFI2 V 5.4.1**	Sequential Uncertainty Fitting version 2	Used to optimize flow parameters
7	**R-programming**	It is a computer programing free software environment used for statistical computing and graphics (downloaded from; https://mirror.rcg.sfu.ca/mirror/CRAN/).	To generate Taylor diagram and analyses performance and rank CORDEX-RCA4.
8	**WGEN_CFSR_World**	It is SWAT extension new tool weather generator database for the countries which were not included under the installed SWAT weather generator database. It can be downloaded from;https://swat.tamu.edu/media/116061/swat-weatherdatabase-v01803.7z.	To generate the weather data of all gauge stations in this study.

3.5.Data Processing

To evaluate the catchment scale performance of climate prediction models', the availability of tempo-spatially reliable ground reference data is vital (Funk et al. 2015b). However, in developing countries like Ethiopia, the ground data sources, like rain gauges have: tempo-spatial limitations (Bayissa et al. 2017; Ayehu et al. 1921; Funk et al. 2015b), sensitivity to weather disruption and topographic complexity (Cattani et al. 2016); Kimani et al. 2017) which causes difficulties to measure consistently followed by missed information. Therefore, before any performance analysis steps, it is recommended to prepare reliable hydro-meteorologic data using the well-known data quality assessment tests: filling missed observation, outlier, adequacy, consistency and normalization to the rain gauge data, and only normalization and bias correction to the satellite rainfall datasets.

3.5.1. Ground Data

3.5.1.1.Filling of Rainfall Missing Data

The data series which will collect from the stations may contain enormous missing data inside the record. There are enormous missed observation filling techniques hence, selection of appropriate method requires; the percentage amount of missed observation, distribution of

gauges in the catchment, consistency of individual gauge measurements with the nearby gauges and the manner of locations elevation consistencies of the gauge stations (Wijesekera and Perera 2012). Due to the investigation among the methods of filling missing rainfall data and support from many researchers, normal ratio method was accurate for this case study. Its main reason is as per definition of the test: if the normal annual precipitation at the surrounding station differs by more than 10% of the normal annual precipitation at station with missing, then the normal ratio method could be adopted to estimate the missing observations of this study. The formula for this method is:

$$P_x = \frac{1}{m} \sum_{i=1}^{m} [\frac{N_x}{N_i}] P_i \text{ ----------(1)}$$

Where: P_X is estimates for the ungagged stations, Pi represents for rainfall values of the gauged stations, Nx is normal annual precipitation of X stations, M is no. of surrounding stations and Ni is Normal annual precipitations of surrounding.

3.5.1.2.Data Quality Test

Outlier

Outliers are lower and upper values of the data series to show the inclusive lower and upper data boundary limits (Wijesekera and Perera 2012). This happens due to the equipment imperfectness, carelessness of the person who collects data or lack of professionalism, political disorder and other unknown problems. Therefore, according to the concept of outlier test, the values from the series above the highest datum and below the lower datum was removed and again fill according to the missing concept (Chow 1983). The formulas for this datum have provided here:

$$Cs = \frac{N \sum_{n=1}^{n} (Yi - Ym)^3}{(N-1)(N-2)(\delta n)^3} \text{ ---------- (1)}$$

Case 1	If Skewness (Cs) < -0.4 check only for lower outlier
Case 2	If Skewness (Cs) > +0.4 check only for higher outlier
Case 3	If Skewness (Cs), -0.4<CS< +0.4 check for both outlier

Y=log X

$RL = 10^{YL}$

$YL = Yav - Kn * \delta n$---------- (2)

$RH = 10^{YH}$----------

$YH = Yav + Kn * \delta n$---------- (3)

Where:

X=The descending order of daily maximum precipitation of across each stations

Cs=coefficient of Skewness

RL=lowest datum

RH=highest datum

Kn=constant number which is a function of precipitation series size (Chow 1983), Appendix II.

According to outlier test's result, the value of Cs was 0.84; hence as per the rule of the test checking for lower outlier was rejected, and only the test for higher outlier was conducted. Henceforth, the calculated RH value was 175.8, and the maximum observation within the time series data was 169.0. This showed that the maximum precipitation in the time series were within the highest datum of the test, then the collected data were qualified for further processing.

Adequacy

The adequacy of the rain gauge rainfall and temperature data was checked by calculating the Relative Standard Error (δe), which determines either the amount of error with in the data series were acceptable or not (Wijesekera and Perera 2012). Before proceeding to the other analysis, the adequacy of rainfall data series should be checked and realized by calculating the relative standard error, δe and checks it with the rule of consistency as indicated below(Wijesekera and Perera 2012):

$$\delta n = \sqrt{\frac{\sum(X - Xm)^2}{(N - 1)}}$$

$$Se = (\delta n)/\sqrt{N}$$

$$\delta e = \frac{Se}{Xm}\% \text{ ---------- (4)}$$

The data series could be considered as an adequate/reliable if relative standard error, δe <10%.

Where:

N=precipitation series size

X=heaviest precipitation, mm/day of the given N years

Xm=precipitation mean

δe=is the relative standard error.

δn=standard deviation of the precipitation series

Se=standard error

From the test's result the value for Relative standard error, was 6.06 % which was within 10%. Therefore, the sampling error within the 29 years precipitation data series of this study was acceptable and the data was ready or adequate for further analysis.

Consistency test, double mass curve analysis

Consistency refers to the slope proportionality plot of the nearby ground stations during the same period of record to create homogenous and continuous data (Wijesekera and Perera 2012). A data that is consistent is to mean that, the data recorded throughout the time series is not changed with time, and the common method to consistency is double mass curve analysis. Double mass curve analysis based on the assumptions that the mean accumulated precipitation for the group of stations is not significantly affected by the change in the individual stations. If a given station may appear as inconsistent in reference to its nearby stations, it can be adjusted by fixed ratio of; slope of data before departing from the trend and slope of data after departing from the trend with the double mass curve. However, in case of this study all stations with all the needed timeseries data were consistent (figure 3-7). The consistency of rainfall records from all stations was checked by double mass curve analysis (best fit if R^2 is nearest to 1). Double mass curve is a graphical method for identifying and adjusting inconsistency in a station record by comparing its time trend with those of adjacent stations. Hence, the consistency test result of May-dingur (R^2 =0.9992), Enticho (R^2 =0.9991) and Gerhu-Sirnay (R^2 =0.9989) were provided in figure below, as per the result the precipitation with in all stations were consistent.

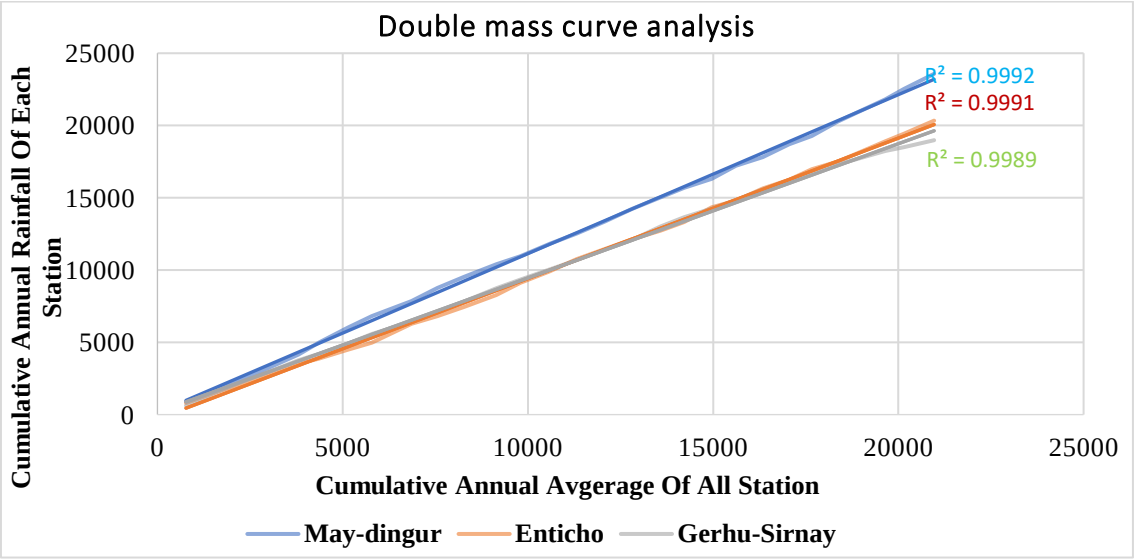

Figure 3-7: Double mass cure analysis for consistency test

3.5.2. Climate Data

3.5.2.1. Extraction of CORDEX-RCA4 Data

CORDEX-RCA4s models are Africa-RCMs models downscaled by RCA4, hence to get pixel or gauge point scale time series data they need to extract. Therefore, the CORDEX-RCA4s data were extracted to the scale of May-dingur, Enticho and Gerhu-Sirnay gauge stations' three-dimensional parameter; longitude, latitude and elevation in the catchment using CMhyd (Climate Model data for hydrologic modeling).

3.5.2.2. Bias Correction

As per the indication by Aragaw et al. (2023); Tumsa (2022) CORDEX-RCA4 are not free of bias hence, to get ground representative future data, they need careful and skill full bias correction analysis on the overlapped observed and simulated historical data. There are many bias correction and performance ranking methods of climate models however, Power transformation (PT) is the best bias correction of RCA4 models' precipitation data for Ethiopian hydrologic regions (Daniel. 2023; Geleta & Gobosho 2018; Dibaba et al. 2020; Daniel and Abate 2022) to specifically adjust the variance statistics of a precipitation and air temperature time series (Teutschbein & Seibert 2012). The PT method utilizes a nonlinear approach in an exponential form to correct the mean and variance of the precipitation and air temperature series (Luo et al. 2018; Zhang et al. 2018). Since the original PT method does not contain frequency correction, the frequency-corrected results from LOCI are also used in PT correction for such a

purpose. In being applied to a given month, the parameter bm is calibrated as below equation to ensure that f(bm) is minimized to zero:

$$f(b_m) = \frac{\sigma(P_{obs,m})}{\mu(P_{obs,m})} - \frac{\sigma(P^{bm}\ LOCI,m)}{\mu(P^{bm}\ LOCI,m)} \text{----------(5)}$$

where bm is the exponent in month m and s represents the standard deviation operator. Subsequently, scaling factors (Sm) are calculated to establish that corrected precipitation amounts are equal to the observations, Sm and corrected precipitation are, respectively, determined in below equations:

$$S_m = \frac{\sigma(P_{obs,m})}{\mu(P^{bm}\ LOCI,hst,m)} \text{----------(6)}$$

$$P^{corr}_{hst,m,d} = S_m\ P^{bm}\ LOCI, hst, m \text{----------(7)}$$

To adjust the systematic biases of CORDEX-RCA4 temperature in Gerhu-Sirnay catchment, variance scaling technique was applied and detailed below:

$$T_C = [T - \mu(T)] * \frac{\sigma(T_o)}{\sigma(T)} + \mu(T_o) \text{----------(8)}$$

Where; T_C corrected temperature, T is the RCA4 model's biased temperature, T_o is the observer's standard deviation, T is biased temperature's standard deviation.

3.5.2.3. Normalization

As per the findings of Taylor (2001), Taylor diagram analysis was the best techniques to validate the quantitative performance of simulated products with reference to the ground data. The frequency distribution of rainfall and temperature in complex terrains, like in Gerhu-Sirnay catchment was skewed tempo-spatially (Abiola et al. 2013). Therefore, to use the mentioned techniques rainfall and temperature of both sources must first normally distributed (Taylor 2001; Abiola et al. 2013). The tempo-spatial skewness within datasets was removed by normalization techniques (Woldemeskel et al. 2013; Botchkarev 2019; Aghakouchak and Mehran 2013). There exists lots of normalization methods. However, in this study the selected performance analysis technique, Taylor diagram and its' corresponding indices were; Pearson Correlation Coefficient (CC), Root Mean Square Error (RMSE) and Normalized Standard Deviation (δN). Therefore, to improve these indices square root normalization was recommended by Woldemeskel et.al. (2013) for the rain gauge rainfall and temperature products. However, due to the need to

minimize the dataset variability across the rain gauge and satellite rainfall products we normalized the satellite rainfall products using the ratio of the standard deviation with the square root normalized/reliable rain gauge data (Botchkarev 2019). The mathematical detail of ratio of the square root normalization was given below;

$$P_{nor(i,n)} = {P^2}_{raw(i,n)} \text{ ----------(8)}$$

Where;

i is the month, n represents the station number, P_{nor} is the monthly normalized rainfall and P_{raw} is the monthly raw rainfall.

3.6.Hydrologic Modeling

3.6.1. The SWAT Model Description

Soil and Water Assessment Tool (SWAT) is a physically-based continuous-event hydrologic model developed to predict the impact of land management practices on surface water, sediment, and agricultural chemical yields in large complex watersheds with varying soils, land use, and management conditions over long periods of time (Bekele and Abate 2020). According to Arnold and Fohrer (2005) SWAT is suitable model to determine watershed scale surface water runoff by subdividing the catchment in to smaller sub watersheds having homogenous land use, soil type and slope which referred as hydrologic response units (HRUs). HRU is a unique combination of land use, slope and soil type in a sub watershed and all calculations in SWAT are performed at the HRU level. As per Neitsch et al. (2005) the climatic variable required by SWAT in modeling the impact of climate change on water resources are; daily precipitation, maximum/minimum air temperature, solar radiation, wind speed and relative humidity. The SWAT model has important applications for assessing the relationships between climate change and the watershed hydrological process (Daniel and Abate 2022). The key processes, which impact stream flow in SWAT model, are discussed below:

i. Water Yield

Water yield is important in the model since it controls the water discharge from the upper soil and it affects the concentration of pollutants being removed from the land area. The leading component of water yield is surface runoff and the quantity of surface runoff also controls the amount of soil erosion that takes place.

B. Hydrologic components

- **Surface Runoff;** SWAT follows two methods for the estimating of surface runoff: SCS curve number method, and Green-Ampt infiltration method. Kannan et al. 2007 observed that SCS curve number generally performed suitably than Green-Ampt method. Besides that, Green-Ampt infiltration method needs hourly precipitation data, and flow routing at hourly time step (rather than daily), and that resulted in the model being computationally demanding for long-term simulations.
- **Percolation;** Soil is categorized into multiple layers in SWAT and water is assumed to permeate through these layers to reach shallow aquifer based on moisture conditions in each layer. Water can permeate to another layer below when soil moisture content in a layer is more than field capacity. Percolation rate is maximum (saturated hydraulic conductivity) at saturation and decreases to zero at field capacity. Temperature also influences the percolation rate, which falls to zero when soil temperature is below zero degree Celsius. Water that percolates through all layers becomes part of groundwater and contribute as part of base flow to a stream.
- **Lateral flow**; Soil water above saturation directly reaches to streams. A kinematic storage model is utilized to model lateral flow through each soil layer. In SWAT volume of lateral flow relies on soil layer properties (saturated hydraulic conductivity and porosity), terrain slope, and flow length.
- **Groundwater flow;** is treated as two aquifer systems including shallow (unconfined) and deep aquifer (confined). Recharge to shallow aquifer from percolation is categorized into two parts: one part that percolates into deep aquifer and never reaches to the stream, while the remaining part in shallow aquifer adds to the stream as base flow and also satisfies a portion of evaporative demand in the root zone. Water table fluctuations are estimated as change in base flow rate from shallow aquifer to the stream using a constant factor defined as base flow recession constant.
- **Evapotranspiration;** SWAT has three alternatives' methods to calculate potential evapotranspiration: Hargreaves et al (1985); Priestley and Taylor (1972); Monteith (1965). Hargreaves method needs only daily air temperature; Priestley Taylor needs solar radiation and air temperature, whereas Penman-Monteith method needs solar radiation, air-temperature, wind-speed, and relative humidity as inputs. Kannan et al. (2007) observed that

performance of Hargreaves method is comparable to complex energy-based Penman-Monteith method. Potential evapotranspiration is the maximum amount of evapotranspiration that can occur in a HRU.

- **Transmission loss;** When a channel runs through a semi-arid region, it releases water when water table is at lower level compared to the channel bottom. SWAT calculates transmission loss using Line's method as a function of channel width, length and flow duration.

ii. Flow Routing

Volume of water to be routed (surface runoff + lateral flow + base flow– transmission loss) are estimated for each HRU and then summed up to find out total volume of water to be routed from a sub watershed. Channel length in each sub watershed is calculated using stream network, and channel dimension are supplied by user (bank full width, depth and side slope). Cross sectional area for flow is estimated by dividing volume of flow to be routed by length of the channel. Manning's equation (manning's n is supplied by user) for uniform flow is deployed to determine flow rate and velocity. In SWAT, water can be routed though channel network by selecting either the variable storage method or Muskingum River routing method using daily time step. Besides transmission loss, channel also loses water through evapotranspiration, which is a function of water surface area in the channel. Evaporation loss in each reach (channel segment) is deducted from total volume before routing the flow through next reach.

3.6.2. Baseline Stream Flow Modeling

3.6.2.1.SWAT Input Data, Project Setup and HRU Analysis

The input data for swat model were temporal and spatial (Abdulea et al. 2024) detailed in table 3-1. The temporal datasets were all meteorologic data, including precipitation, temperature, wind speed, relative humidity and solar radiation collected from the three-gauge stations; may-dingur, Enticho and Gerhu-Sirnay, AND stream flow data collected from May-dingur stations. The spatial datasets were soil, land use and slope class developed from the 30*30 DEM data.

Based on the FAO (2018) soil and land use class and types, three soil types was used, namely SILT_LOAM, CLAY_LOAM and SANDY_LOAM and the corresponding soil code feed for the swat model were detailed in table 3-4. In figure 3-3, two land use classes, AGRL and PAST with spatial-coverage were provided. In this study, the SWAT model setup was done based on the spatial feature of Gerhu-Sirnay catchment, which is divided into seventeen small sub-basins,

and then divided into units of unique soil, land use and slope class characteristics called hydrological response units (HRUs). As per the developed SWAT model, 53 HRUs were created. The summary wised distribution of all HRU components and types with their coverage in the catchment was given in table 3-4;

Table 3-4: Summary of all HRU components and types with their coverage in the catchment

HRU components	**HRU components' detail**	**Spatial coverage**	
		Area, ha	**% coverage**
Land use	Pasture…PAST	29, 434.33	77.19
	Agricultural land generic…AGRL	8, 699.5	22.81
Soils by code	Xh20-2a-314	9568.6638	25.672
	Bh12-3c-31	63.30215	0.162
	Qc2-1bc-176	28501.86195	74.162
Slope class	0 to 5	2417.9491	6.34
	5 to 15	13024.9707	34.16
	15 to 9999	22690.9082	59.50

3.6.2.2.Stream Flow Simulation

In this study, the HRUs of Gerhu-Sirnay catchment was created by overlaying all the meteorologic and spatial data in SWAT model. To estimate stream flow SWAT, have two governing methods; the Soil Conservation System (SCS) curve number and the Green and Ampt infiltration method (Hammouri et al. 2016). Due to data availability constraints, the SCS curve number was used in this study hence, the baseline stream flow (1990-2003) was estimated by the SCS curve number method, and the future surface stream flow under the intermediate future (2020-2049) and distant future (2050-2080) was also calculated by SCS under consideration of the future RCA4 data (Negewo and Sharma 2022). Generally, the mathematical relation for modeling the hydrological processes of the watershed in SWAT was based on the water balance equation given in below equation;

$$\mathrm{SW_t} = \mathrm{SW_0} + \sum_{i=1}^{t} \left(R_{day} - \mathrm{Q}_{surf} - E_a - \mathrm{w}_{seep} - \mathrm{Q_{gw}}\right) \text{----------(9)}$$

Where;SW_t is the final soil water content (mm H_2O), SW_0 is the initial soil water content on day i (mm H_2O), t is the time(days), $R_{day}$is the amount of precipitation on day i (mm H_2O), Q_{surf} is the amount of surface runoff on day i (mm H2O), E_a is the amount of evapotranspiration on day i (mm H2O), w_{seep} is the amount of water entering the vadose zone from the soil profile on day i (mm H_2O) and Q_{gw} is the amount of return flow on day i (mm H_2O) (Arnold et al. 2012).

From eq (9), SWAT calculates the surface runoff of the watershed by USDA conservation service curve number (SCN-CN), the green and amp method (Shigute et al. 2022). However, due to its compatibility, the SCN-CN method was selected for this study.

3.6.3. Flow Parameter Optimization Program

SWAT Calibration and Uncertainty Program (SWAT-CUP) has parameter optimization programs including, SUFI2 (Sequential Uncertainty Fitting version 2), Particle Swarm Optimization (PSO), generalized likelihood uncertainty estimation (GLUE) Parameter Solution (ParaSol) and Markove Chain Monte Carlo (MCMC) (Eawag 2015). However, as per the recommendations from the relevant studies for Ethiopia (Ashine and Bedane 2022; Shigute et al. 2022; Assfaw et al. 2023), SUFI2 is the best flow parameter optimizer for Ethiopian watershed, especially for Abay, Tekeze and Mereb basins. The SUFI2 (Sequential Uncertainty Fitting version 2) embedded in the SWAT Calibration and Uncertainty Program (SWAT-CUP) was used for the sensitivity analysis, calibration and validation of the hydrological model. This algorithm was used for parameter optimization and for time-consuming large-scale models, and it was found to be quite efficient (Daniel and Abate 2022).

3.6.4. Sensitivity Analysis

SWAT model can consider more than 26 parameters while generating stream flow from precipitation however, their sensitivity is variable based on the spatial characteristics of the given watershed, which are LULC type and coverage, soil types and slope (Ashine and Bedane 2022). Therefore, before calibration, the sensitive parameters at generating runoff of the watershed should need to be identified into the most effective with their degree of sensitivity based on low p-Value and a high absolute value of t-Stat using the SUFI-2 algorithm integrated in SWAT-CUP software (Eawag 2015; Dibaba et al. 2020). Then accordingly, from the relevant literatures (Dibaba et al. 2020; Ashine and Bedane 2022; Addis et al.2016; Shigute et al. 2022; Assfaw et al. 2023; Leng et al. 2018; Sahu et al. 2016; Tessema et al. 2020; Al-Hasani et al.

2023; Noreika et al.2021; Anil et al.2024) studied on Ethiopian watersheds and elsewhere in similar study areas with Gerhu-Sirnay catchment, for about twenty flow parameters were initially selected for this study.

In SUFI-2, uncertainty of flow parameters, provided in ranges, accounts for all sources of uncertainties such as uncertainty in driving variables operates by performing several iterations, usually at most <5. At each iteration the parameter ranges get closer, and produced fitted results than the previous iteration (Alim et al. 2018; Ashine and Bedane 2022;). As each iteration zooms into a better region of the parameter space, obtained by the previous iteration, it is going to find a better "best" solution (Eawag 2015). Parameter sensitivity analysis in SUFI2 program can be global and or One-at-a-time, and refers to the sensitivity of a variable to the changes in a multiple regression system of each parameter and a parameter if all other parameters are kept constant against the objective function values (in file goal.txt) respectively (Eawag 2015). Therefore, global sensitivity analysis was time saver and able to consider the changes of all parameters with the selected objective function. Global sensitivity analysis uses the multiple regression analysis, Latin hypercube generated against the objective function to identify the sensitive parameter using the statistics of parameter sensitivity, t-Stat and p-Value. The t-test is used to identify the relative significance of each parameter and p-value indicates the relative sensitivity of the parameters. Hence, the larger absolute value of the t-stat and the smaller the p-value (<0.05) is the more sensitive parameter (Eawag 2015).

In conclusion, in this thesis work, global sensitivity analysis was conducted for the period of twelve years (1992-2003) at an average monthly flow recorded from May-dingur hydrological station as the two years period was used for warm up period of SWAT model. As per the literatures, the selected flow parameters, and their brief description were provided in Table 3-5;

Table 3-5: Initial parameters selected for sensitivity analysis[1]

No.	Parameter	Description
1	r_CN2.mgt	SCS runoff curve number for moisture condition II
2	v_ALPHA_BF.gw	Baseflow alpha factor (dimensionless)
3	a_GW_DELAY.gw	Groundwater delay (days)

[1] Where **r** demonstrates that the existing parameter value is multiplied by (1+ a given value), **a** means a given value is added to the existing parameter value, **v** indicates that the existing parameter value is to be replaced by a given value and the file extensions like, .mgt, .gw and .hru are the SWAT file types.

4	v_GWQMN.gw	Threshold depth of water in the shallow aquifer required for return flow to occur (mm)
5	a_CANMX.hru	Maximum canopy storage (mm H2O)
6	a_CH_K2.rte	Effective hydraulic conductivity in main channel alluvium (mm/h)
7	v_CH_N2.rte	Manning's "n" value for the main channel
8	a_EPCO.hru	Plant uptake compensation factor
9	v_ESCO.hru	Soil evaporation compensation factor
10	v_GW_REVAP.gw	Groundwater "revap" coefficient
11	v_REVAPMN.gw	Threshold water depth in the shallow aquifer for "revap" to occur (mm
12	r_SLSUBBSN.hru	Average slope length
13	r_SOL_ALB().sol	Moist soil albedo
14	r_SOL_AWC().sol	Available water capacity of the soil layer ((mm H2O/mm Soil)
15	r_SOL_K().sol	Saturated hydraulic conductivity (mm/hr)
16	r_SOL_Z().sol	Depth from soil surface to bottom of layer
17	v_SURLAG.bsn	Surface runoff lag coefficient
18	v_TLAPS.sub	Temperature lapse rate
19	r_RCHRG_DP.gw	Deep aquifer percolation fraction
20	v_OV_N.hru	Manning's "n" value for overland flow

3.6.5. Calibration and Validation of SWAT Model

Next to the identified sensitive flow parameters in SUFI2 algorithm, calibration of SWAT model was done by comparing the model's prediction with the observed flow data up to the accepted value of the objective function has been appeared at the best simulation of the corresponding iteration(Arnold et al. 2012). In this study, the used objective function was R^2 for the duration of eight years (1992-1999), and an automated model calibration tool, SWAT-CUP interface was used to provide the link between the input/output of a calibration. The uncertain flow parameters were systematically changed, and the modeled flow outputs (corresponding to measured flow data) have been extracted from the model output files (Leng et al. 2018; Eawag 2015).

In this thesis work, validation was tested for the period of four years (2000-2003) to test the calibrated model without further parameter adjustments with an independent dataset, and the results are compared with the remaining observational data to evaluate the model prediction (Dibaba et al. 2020). It involves running a model using parameters that were determined during the calibration process and comparing the predictions to observed data not used in the calibration (Arnold et al. 2012).

3.6.6. SWAT Model Efficiency Evaluation

In surface water resource management, hydrological models have a vital role nevertheless various sources of uncertainties make it to conduct uncertainty analysis (Zhao et al. 2018). The accuracy of hydrologic model simulation is accomplished by parameter sensitivity and uncertainty analysis. This was done after identifying important parameters through sensitivity analysis for the baseline runoff. The sensitivity algorithm tries to capture most of the measured data within the 95% prediction uncertainty (95PPU) of the model in an iterative process. The 95PPU is calculated at the 2.5 and 97.5% levels of the cumulative distribution of an output variable obtained through Latin hypercube sampling (Abbaspour 2015). The Nash–Sutcliffe efficiency coefficient (NSE), the correlation coefficient (R^2) and PBIAS will be used to test the predictive power of the model (Arnold et al. 2012; Daniel and Abate 2022), and detailed in below equations:

NSE is a normalized statistic that determines the relative magnitude of the residual variance compared to the measured data variance. It indicates how well the plot of observed versus simulated data fits the 1:1 line. The NSE ranges between -∞ and 1 (1 inclusive), with NSE 1 being the optimal value. Values between 0 and 1 are generally viewed as acceptable levels of performance. It is also the most objective function as it is less sensitive to high extreme values due to the squared differences.

$$\mathrm{NSE} = 1 - \frac{\sum_{i=1}^{n}(\mathrm{Q}_{oi}-\mathrm{Q}_{si})^2}{\sum_{i=1}^{n}(\mathrm{Q}_{oi}-\mathrm{Q}_{avg})^2} \text{----------(10)}$$

Correlation coefficient (R^2) is the proportion of the variance in measured data explained by the model. R^2 ranges from 0 to 1, with higher values indicating lower error variance, and typically values greater than 0.5 are considered acceptable.

$$R^2 = \frac{\sum_{i=1}^{n}[(\mathrm{Q}_{oi}-\mathrm{Q}_{avg})(\mathrm{Q}_{si}-\mathrm{Q}'_{avg})]^2}{\sum_{i=1}^{n}(\mathrm{Q}_{oi}-\mathrm{Q}_{avg})^2 \sum_{i=1}^{n}(\mathrm{Q}_{si}-\mathrm{Q}'_{avg})^2} \text{----------(11)}$$

where Q_{oi} and Q_{si}, respectively, are the observed and predicted values at the month i, and Q_{avg} and Q'_{avg}, respectively, are the average observed and predicted values. The R^2 and NSE were used to measure the goodness of fit between the observed and predicted values, and values closer to 1 represent the higher predictive power of the model (Yesuf et al. 2015).

PBIAS measures the average tendency of the simulated data to be larger or smaller than their observed counterparts. The optimal value of PBIAS is 0, with low-magnitude values indicating accurate model simulation. Positive values indicate model underestimation bias and negative values indicate model overestimation. It can indicate poor model performance.

$$\text{PBIAS} = \frac{\sum_{i=1}^{n}(O_i - S_i)}{\sum_{i=1}^{n} O_i} \times 100 \text{----------(12)}$$

where PBIAS is percent bias, O_i is the i^{th} observed parameter, S_i is the i^{th} simulated parameter, and n is the total number of events.

The RMSE-observations standard deviation ratio (RSR) is calculated as the ratio of the RMSE and standard deviation of measured data. RSR varies from the optimal value of 0, to a large positive value. The lower RSR, the lower the RMSE and the better the model simulation performance (Golmohammadi et al. 2014).

$$\text{RSR} = \frac{\sum_{j=1}^{n} (Q_m - Q_S)^2}{\sum_{j=1}^{n} (Q_{m,j} - Q'_m)^2} \text{----------(13)}$$

Where, Q is streamflow, m is observed data, s is simulated data, the symbol quate represents for average and j the j^{th} observed or simulated data.

3.7.Performance Evaluation and Ranking of 7 CORDEX-RCA4 Models

Performance evaluation of CORDEX-RCA4 can be measured quantitatively and or qualitatively at a single and or hybrid statistical evaluation point of view with various metrics and hydrological simulations, or their integration. However, as proved by Tumsa (2022); Gebretsadkan et al. (2023); Daniel (2023), climate models provide decision level results when validated using hybrid statistical, hydrological and/or integrated approaches. In this research, quantitative performance evaluation and ranking of 7 CORDEX-RCA4s was applied using hybrid statistical technique (Taylor diagram and volumetric) to get complementary and high-level future precipitation results at the catchment scale from the three-gauge stations for at about the overlapping 12 years (1990-2001).

3.7.1. Taylor Diagram

Quantitative performance of RCMs products in reference to gauge products can be evaluated using different statistical indices. However, the issue is in selecting appropriate metrics that can build complete and decision level results (Zhou et al. 2021). In most studies, the widely used

methods to measure the performance of climate model products were continuous statistical indices. However, as evidenced by Abiola et al. (2013) continuous statistical indices were unrealistic for all weather regions of the globe, specifically for regions they have orographic type of rainfall which leads to have tempo-spatially skewed data, such as in Ethiopia. Therefore, to fill this methodological gap, the preset study will use the recommended techniques, Taylor diagram analysis to evaluate quantitative performance and rank RCMs products with gauge data. To use Taylor diagram analysis techniques; in addition to the normalization of the observed rainfall and temperature, the simulated rainfall and temperature must also be normalized using the ratio of the standard deviation with the normalized rain gauge data (Botchkarev 2019).

Taylor (2001) is comprehensive statistical-visual plot, quantitative performance evaluation, skill score based one-way and less vague diagrammatic summary which is Taylor diagram to summarize the degree of correspondence between RCMs and observed products in terms of three statistical indices (Xu et al. 2016); Pearson CC, RMSE and δ_N. Correlation coefficient provides the degree of linear correlation between the gauge and RCMs datasets as a function of time however, RMSE represents the overall error level and δN indicates the scattering of both data sets from their respective mean to represent percent bias (Xu et al. 2016).

Taylor diagram can be constructed using normalized input data at different free and commercial software products like GrADS, IDL, and others (Taylor 2001). However, due to its easiness, having active users' community and accessibility, in this paper; it will draw by R-programming software. To accomplish this, Taylor diagram has three geometric components (Xu et al. 2016): the radii sides represents for δN, the isoline curves represents for RMSE and the quartile circle represents for CC. These three statistical metrics are related each other with the concept of error propagation formula derived from the law of cosine, and were detailed in table 3.3:

$$E'^2 = \delta_f^2 + \delta_r^2 - 2\delta_f \, \delta_r \, \mathrm{CC} \ldots\ldots\ldots\ldots\ldots\ldots\ldots\ldots\ldots\ldots\ldots\ldots\ldots\ldots\ldots\ldots\ldots\ldots\ldots\ldots \quad (14)$$

Where E' is the centered pattern of RMSE, δ_f and δ_r are standard deviations of the satellite and observed datasets respectively, and CC is the correlation coefficient of both data sets.

To perform the performance evaluation and ranking, Taylor diagram in R-programming needs R-codes, and temporal data (Appendix-III). In this study the used R-codes to evaluate and rank the 7 CORDEX-RCA4 models were given in

3.7.2. Volumetric Metrics

As stated by Taylor (2001); Aghakouchak & Mehran (2013) quantitative simulation of the RCA4 products needs complementary approach. Therefore, Aghakouchak & Mehran (2013) have developed a new approach by extending categorical metrics to volumetric statistical metrics to examine the volumetric performance of satellite rainfall products which are suitable for gridded dataset, and was used in this study. The parameters of volumetric statistical indices are: Volumetric Hit Index (VHI), Volumetric False Alarm Ratio (VFAR), Volumetric Critical Success Index (VCSI) and Volumetric Miss Index (VMI). VHI is the measure of the volume of correctly detected rainfall by the satellites in reference to volume of correctly detected satellites and missed rain gauge rainfall observations. VFAR is the volume of false rainfall products by the satellite relative to the sum of rainfall by the satellite. VMI represents for the volumetric fraction of missed observation in relative to volume of practically detected simulations and missed observations, and VCSI is defined as the overall measure of volumetric performance. The detail of each metric was provided in table 3.3.

Table 3-6: Summary of volumetric and Tailor Diagram evaluation metrics, [2].

Statistical Metrics		Equation	Value Range	Best Score
Volumetric	VHI	$\frac{\sum_{i=1}^{n}(C_i \mid (C_i > t \,\&\, G_i > t))}{\sum_{i=1}^{n}(C_i \mid (C_i > t \,\&\, G_i > t)) + \sum_{i=1}^{n}(G_i \mid (C_i \leq t \,\&\, G_i > t))}$	[0,1]	1
	VFAR	$\frac{\sum_{i=1}^{n}(C_i \mid (C_i > t \,\&\, G_i \leq t))}{\sum_{i=1}^{n}(C_i \mid (C_i > t \,\&\, G_i > t)) + \sum_{i=1}^{n}(C_i \mid (C_i > t \,\&\, G_i \leq t))}$	[0,1]	0
	VCSI	$\frac{\sum_{i=1}^{n}(\boldsymbol{C_i} \mid (\boldsymbol{C_i} > \boldsymbol{t} \,\&\, \boldsymbol{G_i} \leq \boldsymbol{t}))}{\sum_{i=1}^{n}((\boldsymbol{C_i} \mid (\boldsymbol{C_i} > \boldsymbol{t} \,\&\, \boldsymbol{G_i} > \boldsymbol{t})) + (\boldsymbol{G_i} \mid (\boldsymbol{C_i} \leq \boldsymbol{t} \,\&\, \boldsymbol{G_i} > \boldsymbol{t})) + (\boldsymbol{C_i} \mid (\boldsymbol{C_i} > \boldsymbol{t} \,\&\, \boldsymbol{G_i} \leq \boldsymbol{t})))}$	[0,1]	1
	VMI	$\frac{\sum_{i=1}^{n}(\boldsymbol{G_i} \mid (\boldsymbol{C_i} \leq \boldsymbol{t} \,\&\boldsymbol{G_i} > \boldsymbol{t}))}{\sum_{i=1}^{n}(\boldsymbol{C_i} \mid (\boldsymbol{C_i} > \boldsymbol{t} \,\&\, \boldsymbol{G_i} > \boldsymbol{t})) + \sum_{i=1}^{n}(\boldsymbol{G_i} \mid (\boldsymbol{C_i} \leq \boldsymbol{t} \,\&\, \boldsymbol{G_i} > \boldsymbol{t}))}$	[0,1]	0

[2] *Where C is climate rainfall estimate, G is rain gauge rainfall, n is sample size, t is rainfall threshold, C_i is individual climate rainfall, G_i is individual rain gauge rainfall, N is total number of pairs in both datasets d is the degree of linear freedom, d=2.*

Taylor Diagram	CC	$\frac{\sum((C_i - C_{avg})(G_i - G_{avg})}{\sqrt{\sum ((C_i - C_{avg})^2 \sum (G_i - G_{avg})}}$	[-1,1]	1
	NRMSE	$\sqrt{\frac{1}{N-d}\sum_{t=1}^{N} (C_i - G_i)^2}$	**[0,∞]**	**0**

3.8.Prediction of Future Surface Water Availability and Climate Change Impact Assessment

To evaluate the impact of climate changes over the surface water availability of Gerhu-Sirnay catchment, the first tasks to be accomplished were; simulation of valid baseline stream flow, identification of the best fit RCA4 model and development of future climate scenarios. Since these situations have been completed, only the projected precipitation data from the best RCA4 model was replaced the historical precipitation data at the developed baseline stream flow simulation by SWAT model. By considering the other tempo-spatial inputs for the model as not dynamic, the future stream flow was re-run under RCP 4.5 and 8.5 emission scenarios for the respective future periods, 2050s and 2080s.

Finally, by comparing the baseline and predicted models, the impact of climate change on the surface water availability (precipitation and stream flow) of Gerhu-Sirnay catchment was quantified using equation 14 and 15 respectively;

$$Percentage\ Change = (\frac{P_{pr} - P_{ob}}{P_{ob}}) *100 \quad \text{..... (15)}$$

Where, p represents for monthly precipitation data and the subscripts pr and ob are for the projected precipitation from climate models and observed precipitation respectively.

$$Percentage\ Change = (\frac{Q_{pr} - Q_{ob}}{Q_{ob}}) *100 \quad \text{..... (16)}$$

Where, Q represents for monthly stream flow data and the subscripts pr and ob are for the projected stream flow from climate models and observed stream flow respectively.

4. RESULTS AND DISCUSIONS

4.1.Bias correction of CORDEX-RCA4 models

4.1.1. Precipitation

i. Seasonal timescale

Since CORDEX-RCA4 models are well performed over catchments and coarser time scales (Abdule et al. 2024) hence, seasonal and annual scales at the average of Gerhu-Sirnay catchment than in each station (May-dingur, Enticho and Gerhu-Sirnay) was selected to conduct bias correction of precipitation and temperature (figure 4-1 to figure 4-4).

The seasonal and annual bias corrected rainfall variability of the baseline period (1990-2001) were analyzed using the coefficient of variance (CV), measures the degree of variability. Tessema et al. (2020) mentioned that coefficient of variation **(**CV) is best to explain the degree of variability between the observed and RCA4-based historical rainfall. As of it, the degree of variability is less (CV<20%), moderate (20% <CV <30%), high (CV>30%), very high (CV >40%), and extremely high (CV >70%). In this study's seasonal time scale (figure 4-1), the CV of all RCA4 models over all seasons indicates extremely high variability but comparatively the first three having less variability RCA4 models were ICHEC-EC-EARTH, MIROC-MIROC5 and GFDL-ESM2M orderly.

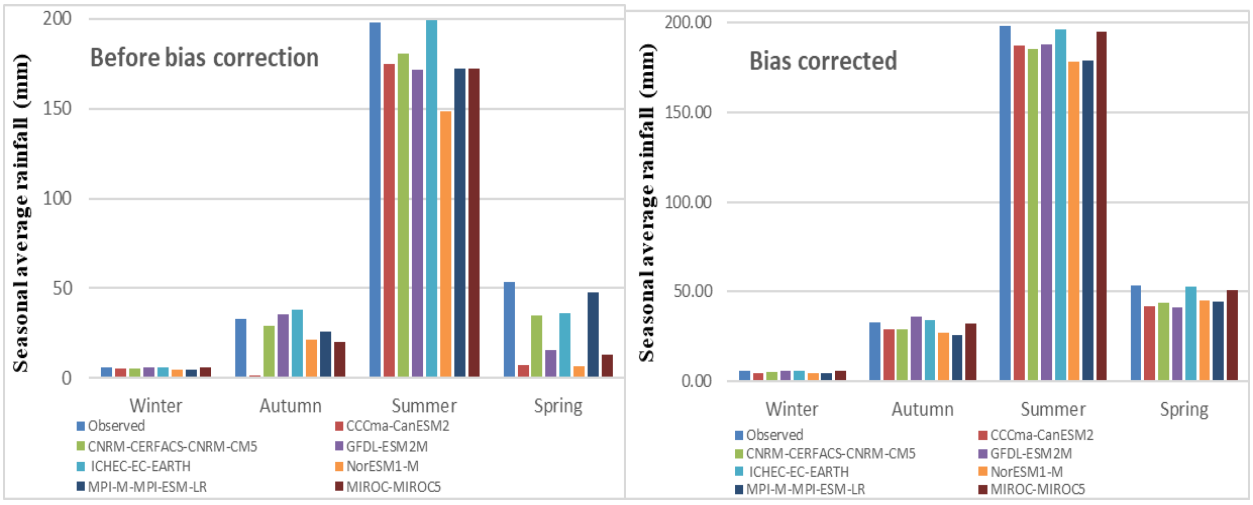

Figure 4-1: Before and after bias correction of average seasonal rainfall at the baseline period (observed and Historical CORDEX-RCA4) (1990–2001) for Gerhu-Sirnay catchment. According to Ethiopian seasons: (1) Winter represents for December, January and February; (2) Autumn represents for march, April and may; (3) Summer represents for Jun, July and august; (4(Spring represents for September, October and November.

In figure 4-1 the variability of total seasonal rainfall at the baseline period for each season was plotted. The result showed that in the winter season GFDL-ESM2M followed by MPI-M-MPI-ESM-LR showed less variability with the areal observed rainfall of the catchment with slight overestimations where as CCCma-CanESM2 and NorESM1-M overestimated principally. MIROC-MIROC5 followed by ICHEC-EC-EARTH and CERFACS-CNRM-CM5 also showed with a high underestimation variability. In the autumn ICHEC-EC-EARTH showed best duplication of the areal observed rainfall with least underestimations while the others with significant underestimation. Regarding in the spring and Summer ICHEC-EC-EARTH estimated the observed rainfall orderly with slight overestimations while the others with substantial overestimation. Generally, ICHEC-EC-EARTH has less variability with the areal observed rainfall of Gerhu-Sirnay catchment at Autumn, Summer and Spring while GFDL-ESM2M has less variability at winter, Ethiopian dry season.

ii. Annual timescale

In this study's annual time scale (figure 4-2), the first three having less variability RCA4 models were ICHEC-EC-EARTH (CV=16.6%), MPI-M-MPI-ESM-LR (CV=31.4%) and MIROC-MIROC5 (CV=33.8 %) while CCCma-CanESM2 (CV=65.6%) observed with very high variability. It concluded that all the used RCA4 models showed less to very high variability of seasonal rainfall at the catchment scale of Gerhu-Sirnay catchment. This indicates that RCA4 models are effective to represent observed precipitation at annual time scale than seasonal.

This result was consistent with studies conducted in Ethiopian basins; Tessema et al. (2020) conducted at Awash River Basin, Ethiopia and Atlas (2015) for the whole Ethiopia. As of Balcha et al. (2022a) on Katar and Meki watersheds, central Rift Valley Lakes Basin, Ethiopia; Balcha et al. (2023) for Katar basin; Bekele et al.(2021) in Argo-Didessa catchment, Upper Blue Nile basin and Chakilu et al. (2022) in Lake Tana sub-basin, Ethiopia ICHEC-EC-EARTH was reported with less variability for Ethiopian basins.

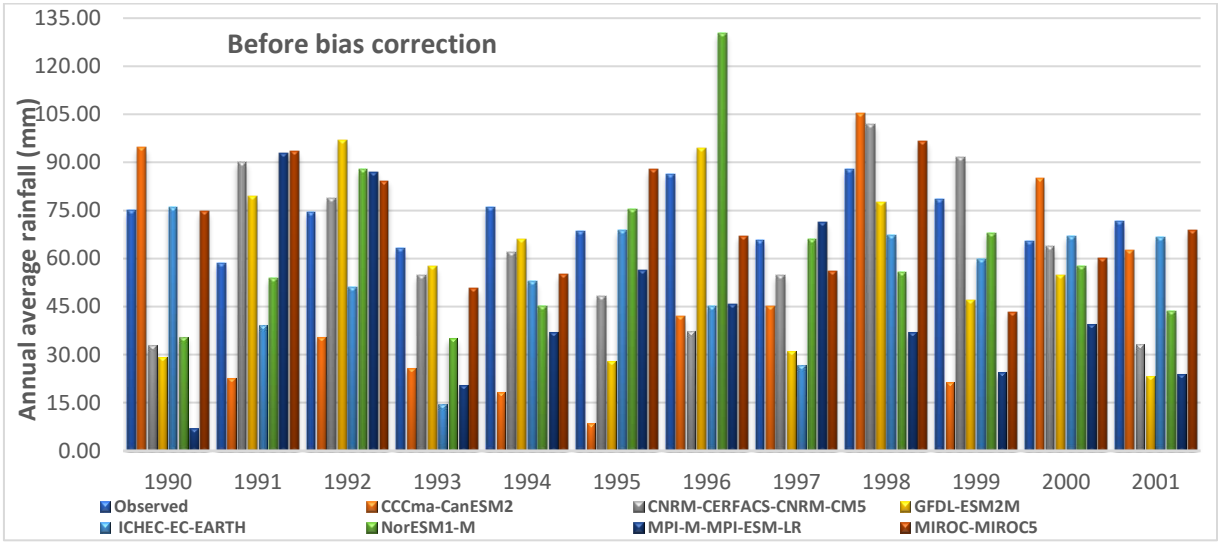

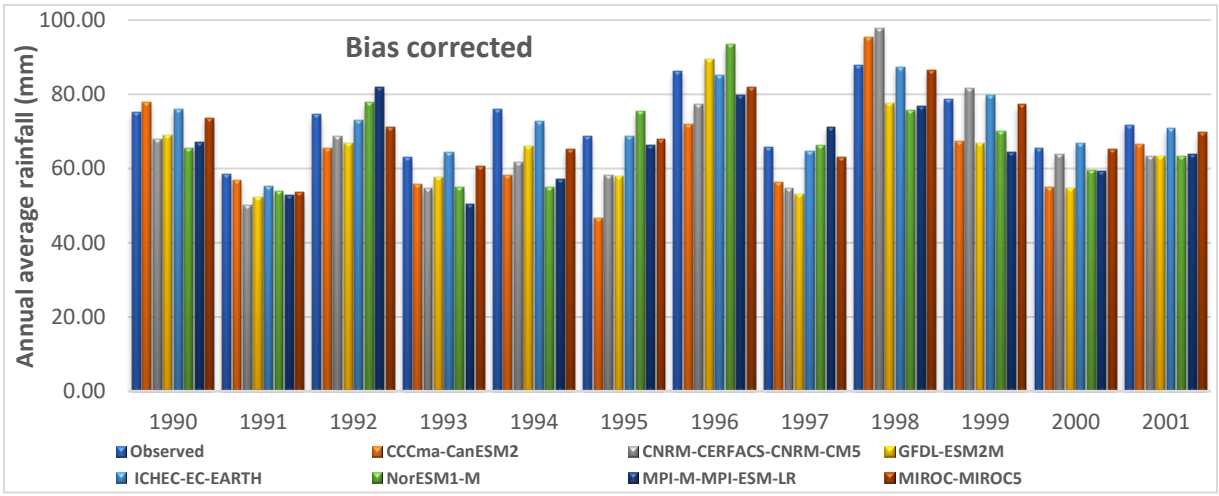

Figure 4-2: Bias corrected annual average rainfall at the baseline period (observed and Historical CORDEX-RCA4) (1990–2001) for Gerhu-Sirnay catchment

4.1.2. Temperature

i. Seasonal timescale

The average seasonal bias corrected temperature variability of the baseline period (1990-2001) was analyzed using the coefficient of variance (CV), measures the degree of variability. As of it, the degree of variability is less (CV<20%), moderate (20% <CV <30%), high (CV>30%), very high (CV >40%), and extremely high (CV >70%). In this study's seasonal time scale (figure 4-1), the CV of all RCA4 models over all seasons indicates extremely high variability but comparatively the first three having less variability RCA4 models were ICHEC-EC-EARTH, MIROC-MIROC5 and GFDL-ESM2M orderly.

In this study's seasonal time scale (figure 4-3), the first three having less variability RCA4 models were ICHEC-EC-EARTH (CV=11.6%), MIROC-MIROC5 (CV=13.01%) and NorESM1-M (CV=13.5%) while CCCma-CanESM2 (CV=51.32%) observed with very high variability. It concluded that all the used RCA4 models showed less to very high variability of seasonal temperature at the catchment scale of Gerhu-Sirnay catchment, that related with rainfall trend. This indicates that the first less sensitive, ICHEC-EC-EARTH model is effective to represent observed average temperature at seasonal time scale.

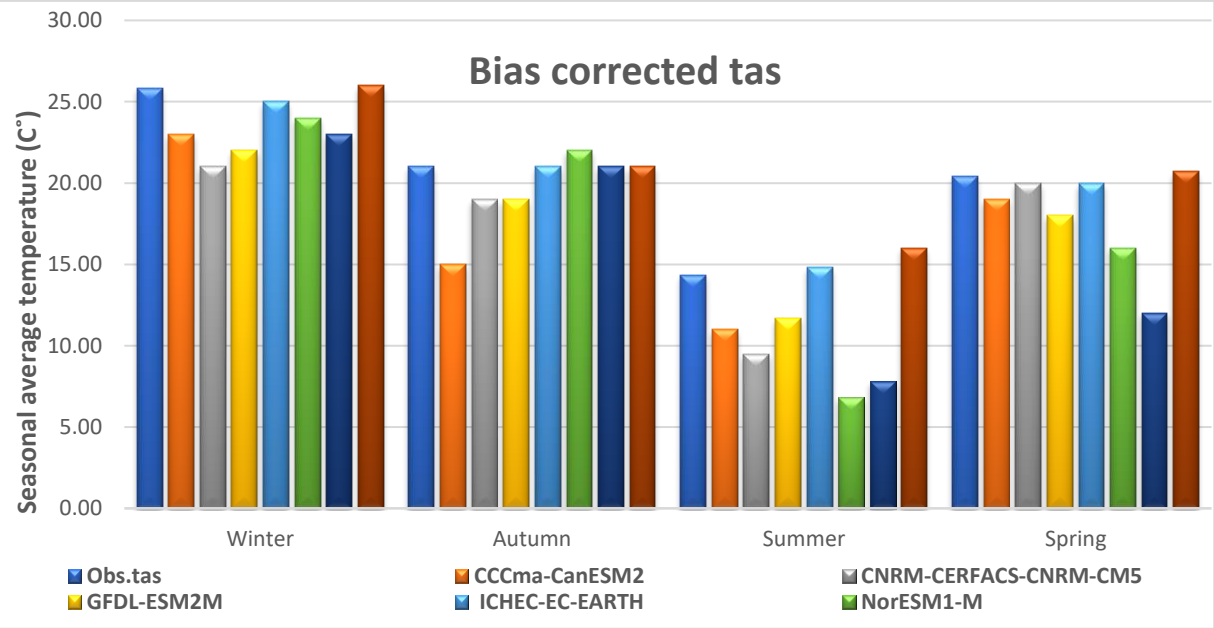

Figure 4-3: Bias corrected seasonal average temperature at the baseline period (observed and Historical CORDEX-RCA4) (1990–2001) for Gerhu-Sirnay catchment

ii. Annual timescale

At an annual time scale (figure 4-4), the first three less variable RCA4 models to represent the observed average temperature were in line with the seasonal scale with a likely less sensitivity at annual scale. Quantitatively ICHEC-EC-EARTH (CV=8.11%), MIROC-MIROC5 (CV=9%) and NorESM1-M (CV=10.21%) while CCCma-CanESM2 (CV=51.32%) observed with very high variability. It concluded that all the used RCA4 models showed less to very high variability of seasonal temperature at the catchment scale of Gerhu-Sirnay catchment, that related with rainfall trend. This indicates that on the comparative wisdom of both analysis time scales, ICHEC-EC-EARTH model is effective to represent observed average temperature at annual time scale than seasonal. This result is in line with that of others studied on other Ethiopian

watersheds including Tessema et al. (2020), Balcha et al.(2023), Takele et.al.(2022), Abdulahi et al. (2022), Kuma et al. (2024) and Gebretsadkan et.al (2023) emphasized that RCA4 models have acceptable ground observation representation at higher temporal scale. Therefore, better representation of observed average temperature at annual than seasonal.

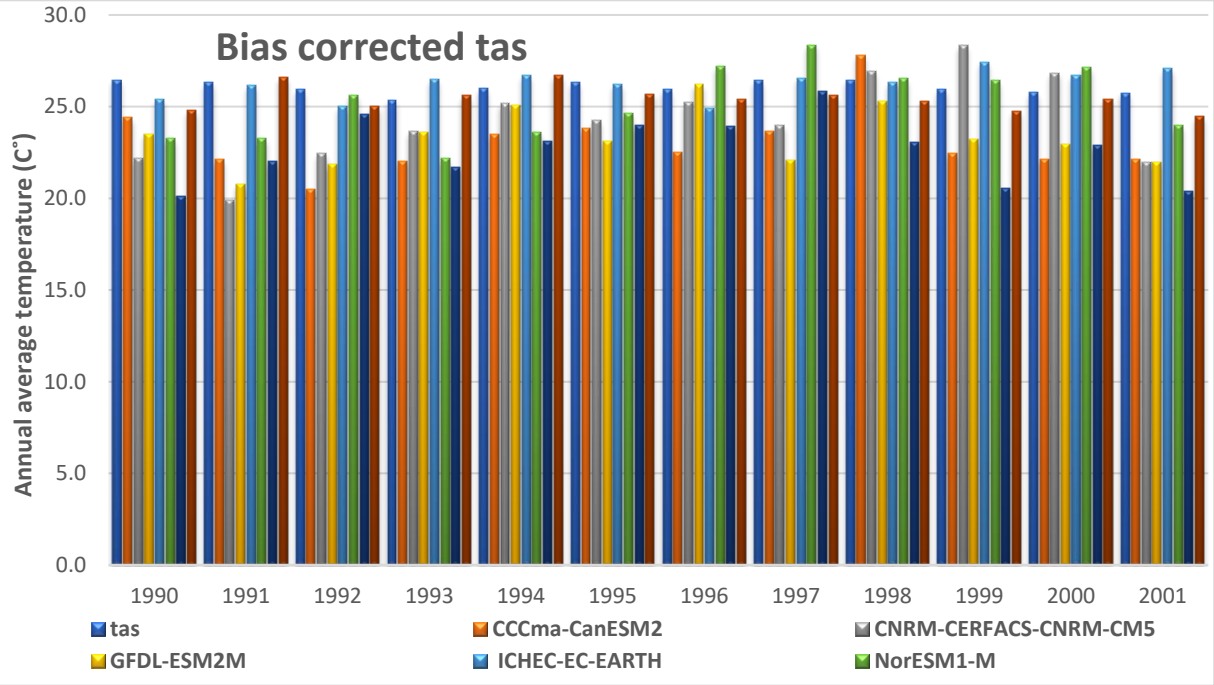

Figure 4-4: Bias corrected annual average temperature at the baseline period (observed and Historical CORDEX-RCA4) (1990–2001) for Gerhu-Sirnay catchment

4.2. Performance ranking of 7 CORDEX-RCA4 Models

To identify better performing RCA4 climate model would best fit to the precipitation data in Gerhu-Sirnay catchment.

4.2.1. Volumetric metrics

i. Seasonal timescale

As per the volumetric principle, the volumetric performance ranking of the seven CORDEX-RCA4 models at seasonal and annual rainfall products were evaluated in 12 years overlapping historical period (1990-2001), and provided in table 4-1 and table 4-2. Ranking of these climate models were conducted by comparing their; VHI and VCSI values at least nearest to 1, and their VFAR and VMI values nearest to 0, to be perfect ground station rainfall volume estimators. The

result evidenced that ICHEC-EC-EARTH exhibited the leading volumetric performance by recording the highest VHI and VCSI, and lowest VFAR and VMI values, denoted by 0.9838 and 0.9838, and 0.000 and 0.0162, respectively. This means ICHEC-EC-EARTH has a 98.38% skill of correctly estimating the observed precipitation volume; however, it still reflected a weakness for about 1.62% false rainfall volume simulations and 1.62% volumetric fraction of missed values in reference to the rain gauge rainfall records. As labeled at the rank column of table 4-4, the rainfall products of MIROC-MIROC5 and CNRM-CERFACS-CNRM-CM5 were the next outperformed products to replace rain gauge stations of the Gerhu-Sirnay catchment at a monthly time scale.

Table 4-1: Volumetric performance summary of CORDEX-RCA4 models at seasonal time scale. Where, ***Volumetric Hit Index (VHI), Volumetric False Alarm Ratio (VFAR), Volumetric Critical Success Index (VCSI) and Volumetric Miss Index (VMI)***

CORDEX-RCA4 models	**Volumetric Metrics**				**Rank**
	VHI	**VFAR**	**VCSI**	**VMI**	
CCCma-CanESM2	0.9762	0.0000	0.9762	0.0238	6
CNRM-CERFACS-CNRM-CM5	0.9819	0.0000	0.9819	0.0181	3
GFDL-ESM2M	0.9803	0.0000	0.9803	0.0197	4
ICHEC-EC-EARTH	0.9839	0.0000	0.9839	0.0162	1
NorESM1-M	0.9754	0.0000	0.9754	0.0246	7
MIROC-MIROC5	0.9822	0.0000	0.9822	0.0178	2
MPI-M-MPI-ESM-LR	0.9787	0.0000	0.9787	0.0213	5

ii. Annual timescale

At annual time scale ICHEC-EC-EARTH revealed best performance by recording the highest VHI and VCSI, and lowest VFAR and VMI values, ass denoted in table 4-2. This means ICHEC-EC-EARTH has a 99.31% skill of correctly estimating the observed areal rainfall volume; however, it still reflected a weakness for about 0.69% false rainfall volume simulations and 0.69% volumetric fraction of missed values in reference to the rain gauge rainfall records. As labeled at the rank column of table 4-2, the rainfall products of MIROC-MIROC5 and CNRM-CERFACS-CNRM-CM5 were the next outperformed products to replace areal rainfall of Gerhu-Sirnay catchment annual time scale.

Table 4-2: Volumetric performance summary of CORDEX- RCA4 models at annual time scale

CORDEX-RCA4 models	Volumetric Metrics				Rank
	VHI	VFAR	VCSI	VMI	
CCCma-CanESM2	0.9782	0.0000	0.9782	0.0218	6
CNRM-CERFACS-CNRM-CM5	0.9913	0.0000	0.9913	0.0087	3
GFDL-ESM2M	0.9878	0.0000	0.9878	0.0122	4
ICHEC-EC-EARTH	0.9931	0.0000	0.9931	0.0069	1
NorESM1-M	0.9758	0.0000	0.9758	0.0242	7
MIROC-MIROC5	0.9921	0.0000	0.9921	0.0079	2
MPI-M-MPI-ESM-LR	0.9799	0.0000	0.9799	0.0201	5

4.2.2. Taylor Diagram

i. Seasonal timescale

Figure 4-5 summarizes the quantitative visual and comprehensive statistical comparison of the CORDEX-Africa RCA4 models in terms of δ_N, CC and NRMSE to define the percent bias, association and accuracy of the seven climate models' rainfall products with the gauges at monthly scale with in a single plot. As indicated by Taylor (2001) and Ghorbanian et al. (2022), the climate model that have closer value of δ_N, CC and NRMSE to the gauged rainfall will have the best accuracy. As per Taylor (2001), CC, NRMSE and δ_N are the most used quantitative measurement of association, accuracy and percent bias in case of dispersion from the mean of the observed values. Based on the CC value as in the result of figure 4-5, the only ICHEC-EC-EARTH has a good linear agreement with the observed rainfall products by scoring the CC=0.749. However, the rest climate models have a poor linear agreement with the observed rainfall products by scoring the CC values less than 0.7 (reference value for good correlation) approximately as 0.699, 0.689, 0.600, 0.596, 0.521 and 0.496 for MIROC-MIROC5, CNRM-CERFACS-CNRM-CM5, GFDL-ESM2M, MPI-M-MPI-ESM-LR, CCCma-CanESM2 and NorESM1-M respectively. Therefore, from the value of the CC, ICHEC-EC-EARTH is the first outclassed CORDEX-RCA4 climate model in the Gerhu-Sirnay catchment.

In case of the NRMSE's concept, the perfect performance of a CORDEX-RCA4 is indicated by its zero value and comparatively to be the best to produce the observed products, its NRMSE score must be the nearest to the gauged products. In figure 4-3, ICHEC-EC-EARTH's value was

little less than 75, which is the nearest to the NRMSE value of the gauged rainfall (NRMSE). The NRMSE scores for MIROC-MIROC5, CNRM-CERFACS-CNRM-CM5, GFDL-ESM2M, MPI-M-MPI-ESM-LR, CCCma-CanESM2 and NorESM1-M were approximately 75, 85, 97, 100, 112 and 116 respectively. Taylor (2001) explained that both CC and NRMSE showed complementary correspondence details; so then to draw complete performance information, a δ_N was an additional parameter. Based on the δ_N result, the value of the gauged products' datasets was lied at a little less than 100, which is represented by the curved solid line extended across the radii. Therefore, based on all CORDEX-RCA4s' δ_N value and alignment with the gauged products in figure 4-3, ICHEC-EC-EARTH's showed the best consistency of mean in reference to the gauged rainfall products. Therefore, the visual plot result in figure 4-3 showed the same agreement with this fact; hence, ICHEC-EC-EARTH the first outclassed CORDEX-RCA4 model in Gerhu-Sirnay catchment to simulate observed precipitation.

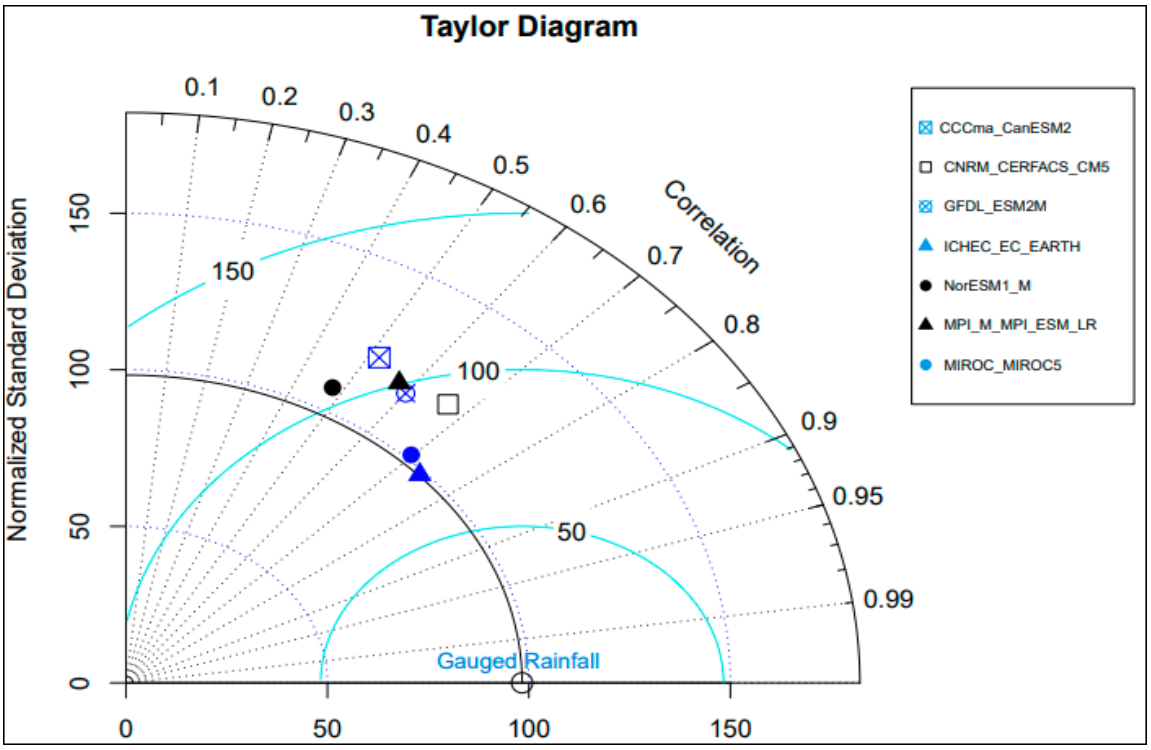

Figure 4-5: Taylor diagram-based performance comparison of 7 CORDEX-RCA4 models at seasonal time scale

ii. Annual timescale

Figure 4-6 summarizes the quantitative visual and comprehensive statistical comparison of the CORDEX-Africa RCA4 models in terms of δ_N, CC and NRMSE to define the percent bias,

association and accuracy of the seven climate models' rainfall products with the gauges at monthly scale with in a single plot. As indicated by Taylor (2001) and Ghorbanian et al. (2022), the climate model that have closer value of δ_N, CC and NRMSE to the gauged rainfall will have the best accuracy. As per Taylor (2001), CC, NRMSE and δ_N are the most used quantitative measurement of association, accuracy and percent bias in case of dispersion from the mean of the observed values. Based on the CC value as in the result of figure 4-6, the only ICHEC-EC-EARTH has a good linear agreement with the observed rainfall products by scoring the CC=0.957, . However, the rest climate models have a poor linear agreement with the observed rainfall products by scoring the CC values less than 0.7 (reference value for good correlation). Therefore, from the value of the CC, ICHEC-EC-EARTH is the first outclassed CORDEX-RCA4 climate model in the Gerhu-Sirnay catchment.

In case of the NRMSE's concept, the perfect performance of a CORDEX-RCA4 is indicated by its zero value and comparatively to be the best to produce the observed products, its NRMSE score must be the nearest to the gauged products. In figure 4-6, ICHEC-EC-EARTH's value was little less than 25, which is the nearest to the NRMSE value of the gauged rainfall. Taylor (2001) explained that both CC and NRMSE showed complementary correspondence details; so then to draw complete performance information, a δ_N was an additional parameter. Based on the δ_N result, the value of the gauged products' datasets was lied at a little more than 100, which is represented by the curved solid line extended across the radii. Therefore, based on all CORDEX-RCA4s' δ_N value and alignment with the gauged products in figure 4-6, ICHEC-EC-EARTH showed the best consistency with the gauged rainfall products. Therefore, the visual plot result in figure 4-6 showed the same agreement with this fact; hence, ICHEC-EC-EARTH was the first outclassed CORDEX-RCA4 model in Gerhu-Sirnay catchment to simulate observed precipitation.

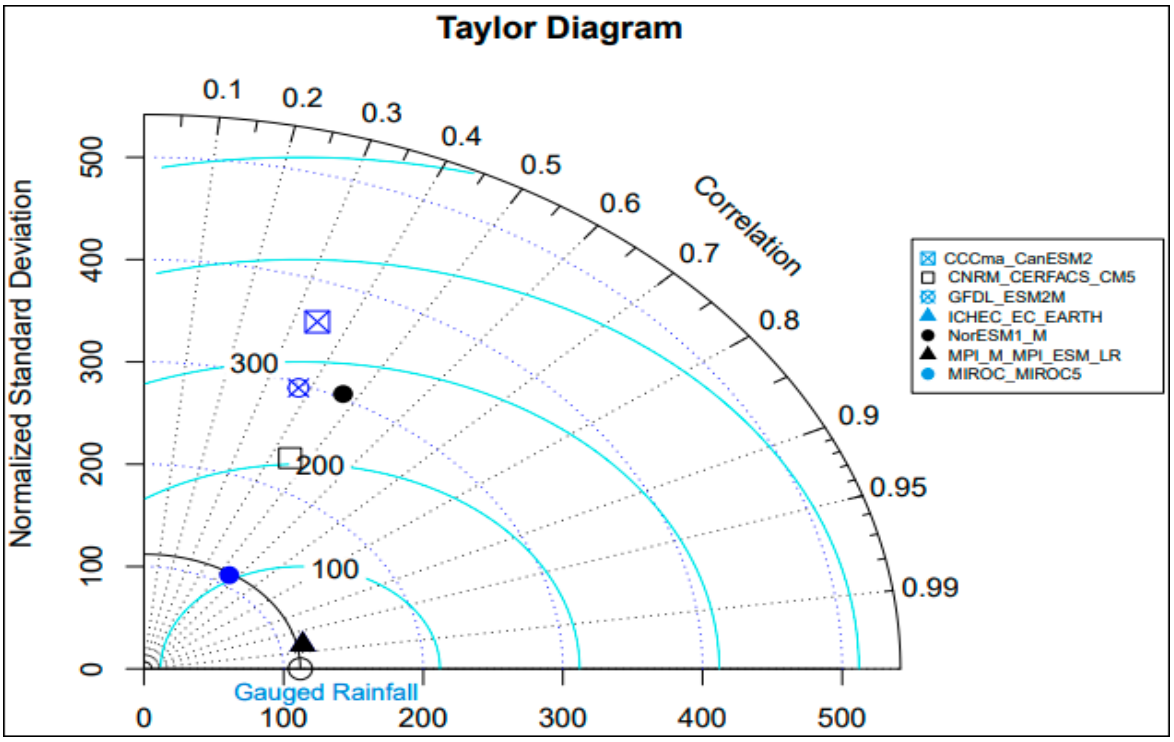

Figure 4-6: Taylor diagram-based performance comparison of 7 CORDEX-RCA4 models at annual time scale

In Ethiopia, several studies with own techniques have been conducted at performance evaluation, ranking and selection of CORDEX-Africa to investigate the impact of climate change on precipitation and surface water resources. However, due to the similarities in catchment characteristics, the selected studies for result validity of this study were; Balcha et al. (2022a) investigated on the performance of 22 CORDEX-Africa CMIP5 by five RCMs (CCLM4-8–17, CRCM5, RACMO22T, RCA4 and REMO2009) on the Katar and Meki watersheds for fifteen gauging stations using Bias, NRMSE, CC and *Lp* metric value to simulate precipitation. ICHEC-EC-EARTH followed by MIROC-MIROC5 were the outperformed RCA4 models in both watersheds. Balcha et al. (2023) was conducted the performance of four CMIP5- RCA4; EC-EARTH, MIROC5, HadGEM2-ES and REMO2009 for Katar basin, and EC-EARTH, MIROC5, HadGEM2-ES and CSIRO-Mk3_6_0 in Meki subbasin for assessing the impact climate change on the surface water resources in seven gauging stations. As per the weighted rank over the gauges, ICHEC-EC-EARTH followed by MIROC-MIROC5 were outclassed in Katar basin, and ICHEC-EC-EARTH followed by CSIRO-Mk3_6_0 was the better RCA4 models in Meki subbasin.

Bekele et al.(2021) studied the impact of climate change on stream flow in Argo-Didessa catchment using four CORDEX-Africa models; HadGM2-ES, MPI-ESM-LR, ICHEC-EC and CM5A-MR downscaled by RCA4, CCLM and RAMO22T under RCP 4.5 and 8.5. The result indicated that all the models have unsatisfactory performance quantified with RMSE, CV and CC however still, ICHEC-EC appeared with better performance. Chakilu et al. (2022) examined climate change and response of stream flow in Lake Tana sub-basin for RCP 8.5 from six CORDEX-Africa models including, CanESM2, EC-EARTH, CNRM-CM5, HadGEM2- ES, NORESM1-M and CSIRO-Mk3–6–0. The study concluded that, the lowest variability was observed from EC-EARTH climate model.

As per the corresponding authors, Katar and Meki watersheds, Argo-Didessa catchment and Lake Tana sub-basin are arid hydrological regions, and influenced by altitude, wind direction and complex topographic characteristics, they are like Gerhu-Sirnay catchment. Therefore, the state of being ICHEC-EC-EARTH-RCA4 was become the best climate model to simulate further hydrological analysis for Gerhu-Sirnay catchment at seasonal and annual time scales is consistent with the mentioned prior studies. Not only result similarities with these literatures but also due to the critical selection of the seven statistical performance indicator metrics included in the hybrid quantitative metrics; volumetric and Taylor diagram performance metrics, the ranking result of the seven CORDEX-RCA4 models of this study tends to be reliable.

4.2.3. Baseline Change of Precipitation

The inter and across monthly rainfall variability of the baseline period (1990-2001) at the catchment were analyzed using mean (Ẋ) and the standard deviation (SD), and the coefficient of variance (CV) respectively. Mean measures the central tendency of the rainfall and SD indicated the degree of dispersion from the mean. As mentioned in Tessema et al. (2020), CV is used to classify the degree of variability between the observed and RCA4-based historical rainfall. As of it, the degree of variability is less (CV<20), moderate (20 <CV <30), high (CV>30), very high (CV >40%), and extremely high (CV >70%).

Based on the CV , 35.05 and 36.73 for the ICHEC-EC-EARTH-RCA4 and observed respectively, this study showed a high monthly rainfall variability. The mean of monthly observed rainfall was 72.63 and that of ICHEC-EC-EARTH-RCA4 was 64.67, this indicates for the same central tendency of both rainfall datasets. From figure 4-4 the SD of both dataset, 98.09

and 104.59 showed that the ICHEC-EC-EARTH-RCA4 rainfall product showed the same trend over the catchments, and in figure 4-4 the whole mean monthly trend was provided. This result was consistent with other studies conducted in Ethiopian catchments (Tessema et al. 2020) at the nearby baseline periods.

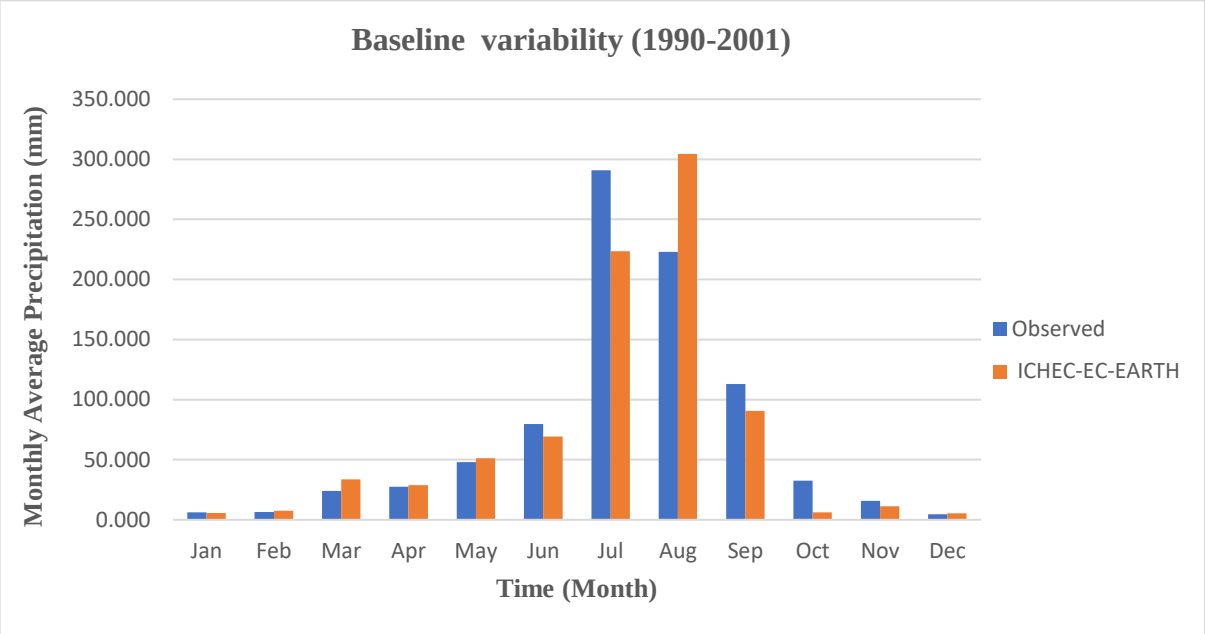

Figure 4-7: Baseline (observed and Historical ICHEC-EC-EARTH-RCA4) trends of the mean monthly precipitation (1990–2001) at the catchment

In figure 4-8 the percentage variability of mean monthly precipitation at the baseline period was plotted. The result showed that from January to May, and at August and December the percentage variability of the precipitation was showed with potential increasement at march and August orderly. On the other hand, the precipitation was observed with a decrease at Jun, July and September to October, with potential decrease at October.

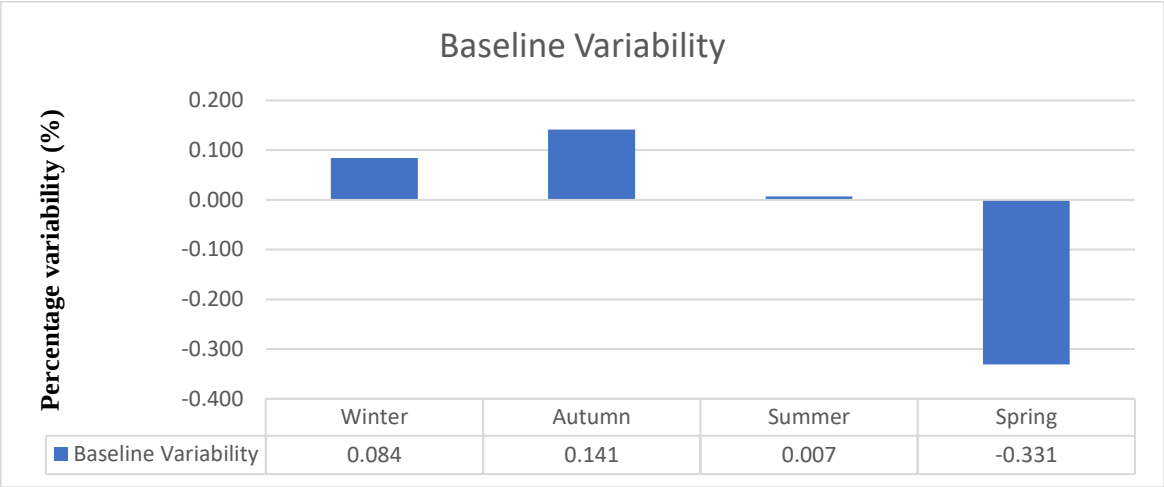

Figure 4-8: Percentage variability of mean seasonal rainfall at the baseline period (1990–2001)

Figure 4-8 showed the bias corrected mean seasonal rainfall variability in percentage of Gerhu-Sirnay catchment at the baseline period (1990–2001). As per it, the winter rainfall was increase by 0.084% , increase by 0.141% (autumn), decrease by negligible percentage in summer and decreased by 0.331% in the spring season. From this it concluded that the average seasonal variability of rainfall in Gerhu-Sirnay catchment was observed by an increasing in the dry and autumn, and the likely constant in the summer and decreased in spring season. This indicates that ICHEC-EC-EARTH-RCA4 model overestimated the observed rainfall at the dry and semi-dry seasons with better accuracy at winter while it underestimated in the semi-wet season. This result was consistent with other studies conducted in Ethiopia. For example, Balcha et al.(2023) studied this issue in 16 stations on the Central Rift Valley Lakes Basin of Ethiopia, and ensured that EC-EARTH and MIROC5 showed 0.24-48% decrease of average rainfall in the spring and the likely in the summer.

4.3. Future Precipitation Variability

The temporal variability of monthly precipitation under RCP4.5 and RCP8.5 emission scenarios of ICHEC-EC-EARTH model was conducted in relation to the observed historical precipitation of the catchment at seasonal and annual time scales. To achieve this the considered future time zones were the 2050s (2020-2049) and 2080s (2050-2080) intermediate and far future respectively. The projected trend and changes of RCP 4.5 and RCP 8.5 emission scenarios are indicated separately in figure 4-9 to 4-12 and table 4-3, and figure 4-13 to 4-16 and table 4-4 respectively.

4.3.1. RCP4.5 Emission Scenario

i. Seasonal

In this study the seasonal classification was done based on winter or dry (December, January and February), Spring or semi-wet (March, April and May), Summer or wet (Jun, July and August) and Autumn or semi-dry (September, October and November).

The projected trend of average seasonal rainfall in the RCP4.5 emission scenarios for 2050s and 2080s future periods was plotted in figure 4-9. In the dry and semi dry seasons, average seasonal rainfall was projected to increase with the progressive increments on the far future period than 2050s. During the wet and semi-wet seasons average seasonal rainfall will progressively decrease with the progressive decrease on the near future period than 2080s. This indicates that on Gerhu-Sirnay catchment higher average seasonal rainfall will appear the far future period in the dry and semi-dry seasons while in the wet and semi-wet seasons higher average seasonal rainfall will appear the near future. This result is consistent with the conclusion of Abdule et al. (2024) conducted Yadot watershed, Genale Dawa basin, Ethiopia, and reported that the semi-dry and dry seasonal rainfall projected to increase in both future periods at RCP4.5 emission scenarios. Kuma et al. (2024) in the Gibe Gojeb catchment Ethiopia investigated that a pronounced decline of rainfall was ensured in the June, July and August which categorized in to summer season under similar future periods and emission scenarios with this study.

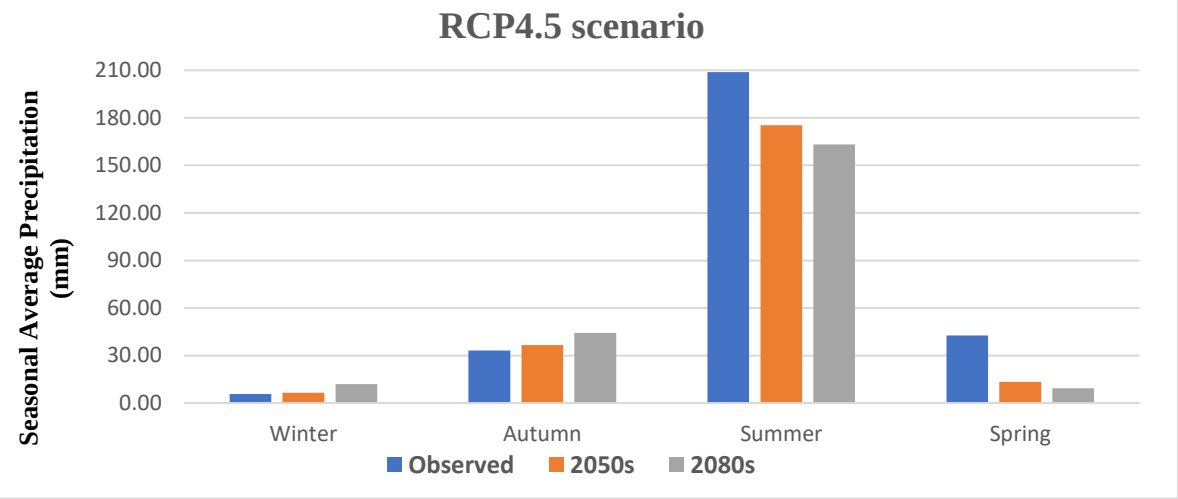

Figure 4-9: The projected trend of average seasonal rainfall in the RCP4.5 emission scenarios for 2050s and 2080s future periods

Figure 4-10 shows the mean seasonal rainfall variability in percentage at RCP4.5 emission scenario for the 2050s and 2080s periods. As a result, it showed that in the winter rainfall will increase by 0.14% , increase by 0.1% (autumn), decrease by 0.16% (summer) and decrease by 0.68% (spring) for the 2050s. In case of 2080s future period rainfall will increase by 1.08% (winter), increase by 0.33% (autumn), decrease by 0.22% (summer) and decrease by 0.78% (spring).

From this it concluded that the average seasonal variability of rainfall in Gerhu-Sirnay catchment was observed by a increasing in the dry and autumn, and decrease in the summer and spring seasons. This indicates that ICHEC-EC-EARTH-RCA4 model overestimates the observed rainfall at the dry and semi-dry seasons with better accuracy at autumn in both 2050s and 2080s periods. While underestimates in the wet and semi-wet season having better accuracy at the wet season in both 2050s and 2080s periods. This result was consistent with other studies conducted in Ethiopia. For example, Balcha et al.(2023) studied related issue in 16 stations on the Central Rift Valley Lakes Basin of Ethiopia, and ensured that EC-EARTH and MIROC5 showed 0.24-48% decrease of average seasonal rainfall.

As per the conclusion of Alehu et al. (2021) at Gidabo catchment up to 20.3mm and 43.7mm decrease detected on summer for 2050s and 2080s respectively, and 56.9mm and 67.5 increase have reported in autumn for 2050s and 2080s respectively. Other studies discussions like, Daba et al. (2020) in the Upstream of Awash Basin, Balcha et. Al (2023), Abdule et al. (2024) and Ukumo et al. (2022) were also in line with the result of this study.

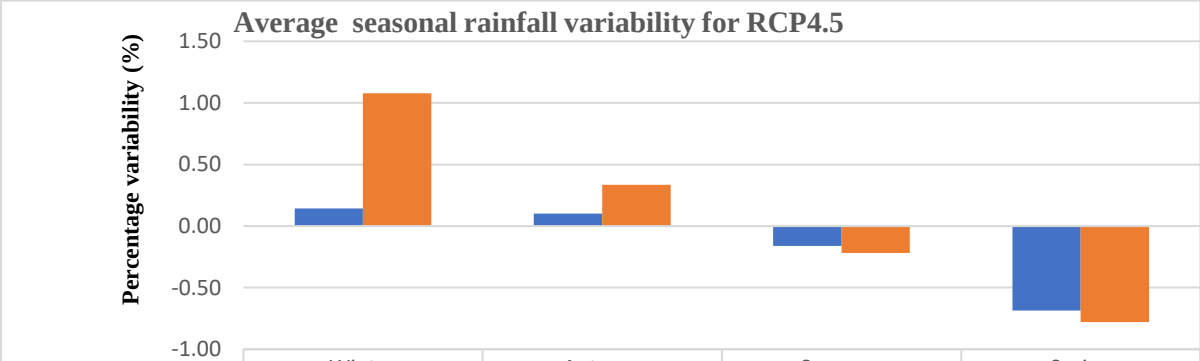

	Winter	Autumn	Summer	Spring
2050s variability	0.14	0.10	-0.16	-0.68
2080s variability	1.08	0.33	-0.22	-0.78

Figure 4-10: Average seasonal rainfall variability at RCP4.5 emission scenario for the 2050s and 2080s

ii. Annual

Since the observed rainfall have no future data availability hence there is no overlapping future period case to compare with the RCP4.5 emission scenarios. Therefore, to harvest overlapping annual case, the observed and ICHEC-EC-EARTH-RCA4 model's RCPs rainfall were converted to average annual at each month of the year. Accordingly, the projected trend of RCP4.5 emission scenarios for both future periods was plotted in figure 4-11. The average annual maximum and minimum rainfall values for the 2050s and 2080s were appeared in the same trend with the observed. The maximum average annual rainfall in the observed case was appeared at July, Augst and Jun as 290.74 mm, 222.83 mm and 111.06 mm respectively. In line with this the maximum mean annual precipitation for the 2050s and 2080s case were also 226,54 mm, 103.2 mm and 196.17 mm. Therefore, the maximum and minimum mean annual precipitation of both emission scenarios were observed at the same month (wet and dry) respectively with the observed mean annual precipitation.

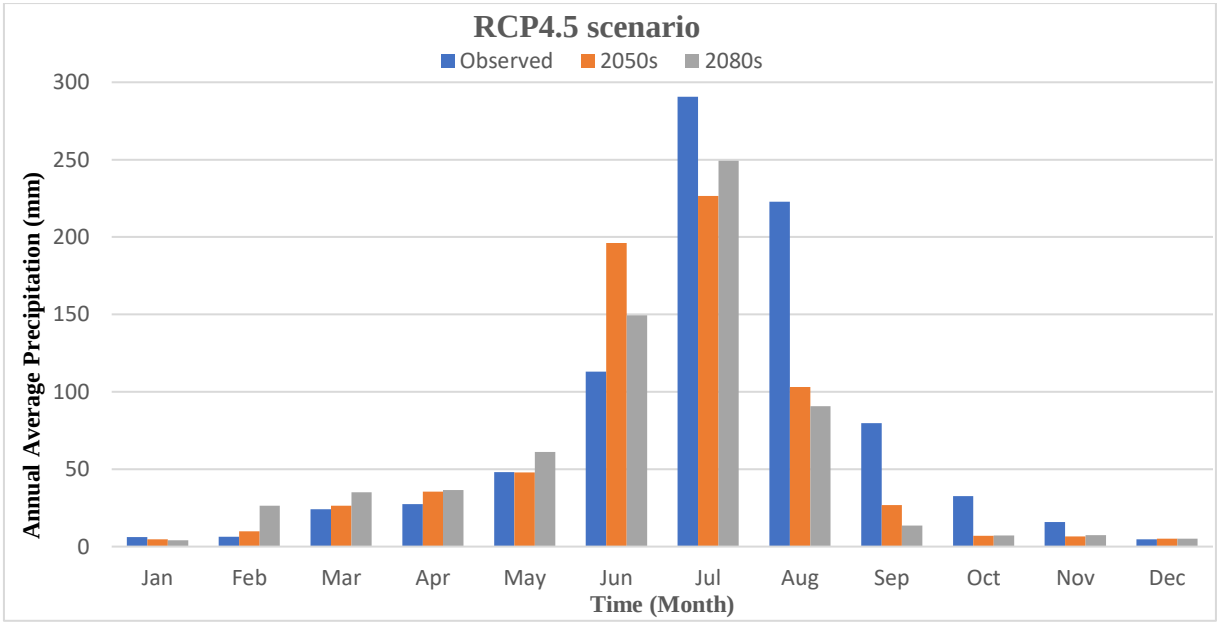

Figure 4-11: Projected average annual precipitation trend for 2050s and 2080s in the RCP4.5 scenario

Figure 4-12 shows the mean annual rainfall percentage variability in each month of the year and table 4-3 shows the total increase and total decrease of the RCP4.5 scenario in the 2050s and 2080s periods. As a result, this study showed 1.16 % and 1.85% increase for the 2050s and 2080s periods respectively. However, for about 8.73% and 11.67% decrease was observed for

the 2050s and 2080s periods respectively. From this it concluded that the total mean annual rainfall variability on each month in Gerhu-Sirnay catchment due to climate change impact has 7.58% and 9.82% decrease in 2050s and 2080s periods respectively (table 4-5). This result was consistent with the study conducted by Daba et al. (2020) in the Upstream of Awash Basin, Ethiopia as decrease by 3.31 % to 9.87% for the 2050s and 2080s periods respectively. Balcha et al.(2023) ensured that for about 0.37-29% decrease of annual rainfall by EC-EARTH in the central rift valley basin of Ethiopia under both 2050s and 2080s on RCP4.5 and emission scenarios.

Generally, the percentage variability of mean monthly precipitation for the RCP4.5 scenario was summarized in table 4-5;

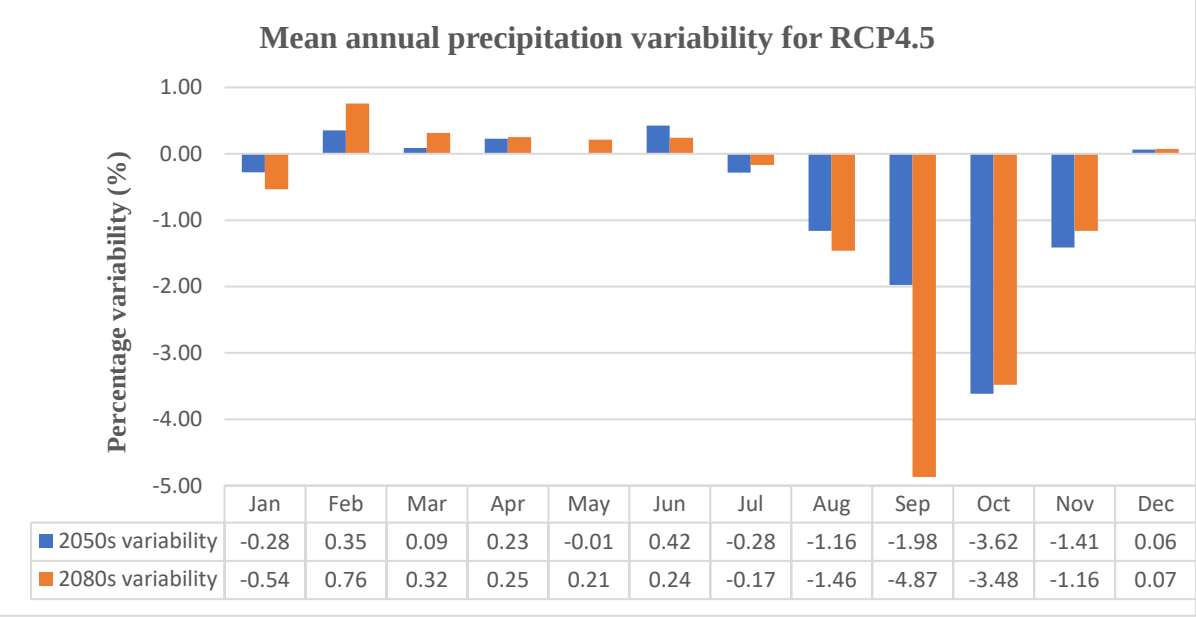

Figure 4-12: Projected mean annual rainfall variability of the RCP4.5 scenario for 2050s and 2080s

Table 4-3: Percentage variability summary of mean annual rainfall in the 2050s and 2080s

Scenario	**Future Period**	**Mean annual precipitation change (%)**		
		Increase	**Decrease**	**Total variability/climate change impact**
RCP 4.5	2050s	1.16	-8.73	-7.58
	2080s	1.85	-11.67	-9.82

4.3.2. RCP8.5 Emission Scenario

iii. Seasonal

The average seasonal rainfall for 2050s and 2080s future periods at RCP8.5 emission scenario was plotted in figure 4-13. The average seasonal rainfall will be higher at the far future period in the dry and semi-dry seasons however in the wet and semi-wet seasons, average seasonal rainfall will be higher 2050s. At winter ICHEC-EC-EARTH-RCA4 model will have related average seasonal rainfall for 2050s (21.3) and 2080s (21.85) future periods than other seasons.

Generally, the quantity of average seasonal rainfall of Gerhu-Sirnay catchment will be higher in the winter and autumn seasons and lower in the wet and semi-wet seasons for both future periods. This result is reliable with Abdule et al. (2024) studied at Yadot watershed, Genale Dawa basin, Ethiopia, and reported that the semi-dry and dry seasonal rainfall will increase in both future periods of the RCP8.5 emission scenario. Alehu et al. (2021) at Gidabo catchment also detected decrease of rainfall in summer and spring for 2050s and 2080s periods RCP8.5 emission scenario. As Kuma et al. (2024) conclusion in the Gibe Gojeb catchment Ethiopia that a noticeable decline of rainfall was ensured in the June, July and August, summer season 2050s and 2080s in RCP8.5 emission scenarios. Therefore, the decreasing of average seasonal rainfall in the wet season for 2050s and 2080s in RCP8.5 emission scenarios was in line with literature.

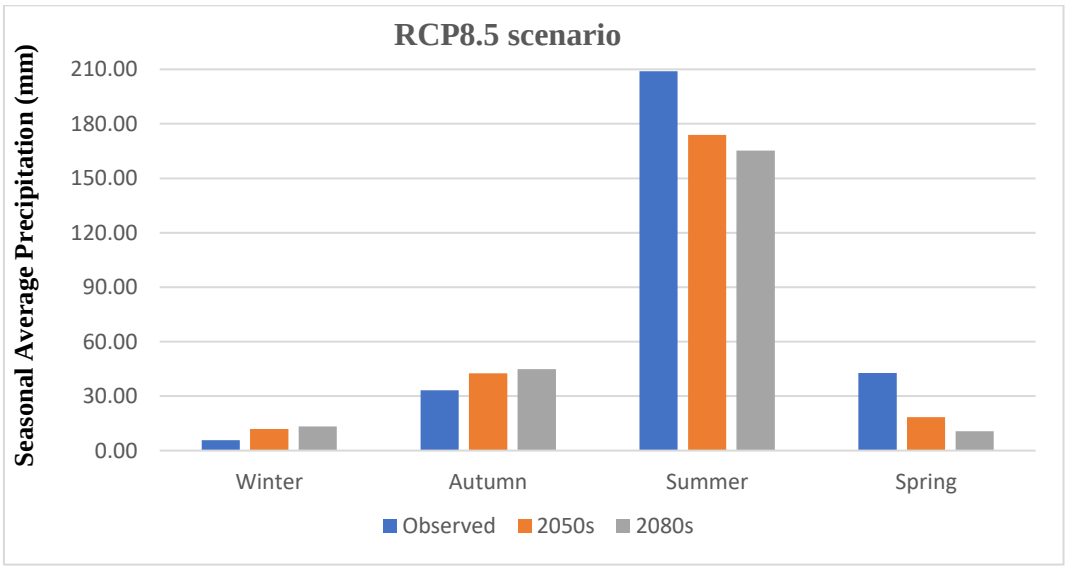

Figure 4-13: Average seasonal rainfall for 2050s and 2080s periods at RCP8.5 scenario

In figure 4-14 the average seasonal rainfall percentage variability at RCP8.5 scenario in the 2050s and 2080s periods was provided. It showed that in the winter rainfall will increase by 1.05% , increase by 0.28 % (autumn), decrease by 0.17% (summer) and decrease by 0.57% (spring) for the 2050s. In case of 2080s future period rainfall will; increase by 1.34% (winter), increase by 0.35% (autumn), decrease by 0.21% (summer) and decrease by 0.75% (spring).

In the RCP8.5 scenario, the average seasonal variability of rainfall in Gerhu-Sirnay catchment was observed by a decrease in the winter and autumn having a potential decrease in the 2080s separately, and increase in the summer and spring seasons having significant increase in the 2080s future period separately. This indicates the ICHEC-EC-EARTH-RCA4 model overestimates the observed rainfall at the winter and autumn seasons with higher increase at winter. In the summer season, average seasonal variability of rainfall will be decreased with significant change at 2080s future period. Other studies conducted in Ethiopia such as, Daba et al. (2020) in the Upstream of Awash Basin, Balcha et. Al (2023), Abdule et al. (2024) and Ukumo et al. (2022) reported reliable conclusion at RCP8.5 scenario. Alehu et al. (2021) on Gidabo catchment conducted for at RCP8.5 scenario that seasonal rainfall reduced by 21.9 and 53.8 mm in summer, and 0. and 4.9 mm in spring for 2050s and 2080s respectively. Therefore, result of this thesis was in line with previous studies conducted in related landscape characteristics and semi-arid climatic zones like Gerhu-Sirnay catchment.

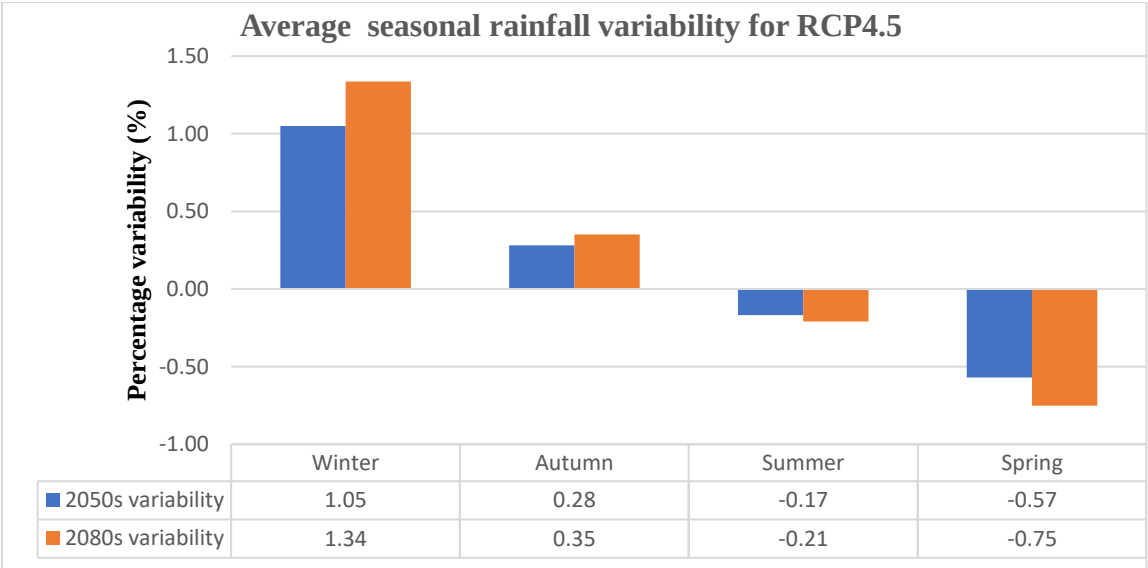

Figure 4-14: Average seasonal rainfall variability at RCP8.5 scenario in the 2050s and 2080s

iv. Annual

The projected trend of mean annual rainfall for the RCP8.5 emission scenarios 2050s and 2080s future periods were plotted in figure 4-15. The maximum and minimum annual rainfall for the 2050s and 2080s were appeared in the same trend with the observed annual rainfall. The maximum mean annual rainfall in the observed case was appeared at July, Augst and Jun as 290.74 mm, 222.83 mm and 111.06 mm respectively. In line with this the maximum mean annual rainfall for the 2050s and 2080s case were also 263.84 mm, 103.36 mm and 79.75 mm. Therefore, the maximum and minimum annual rainfall of both emission scenarios were observed at the same month of the year (considering wet and dry months) respectively with the observed mean annual rainfall.

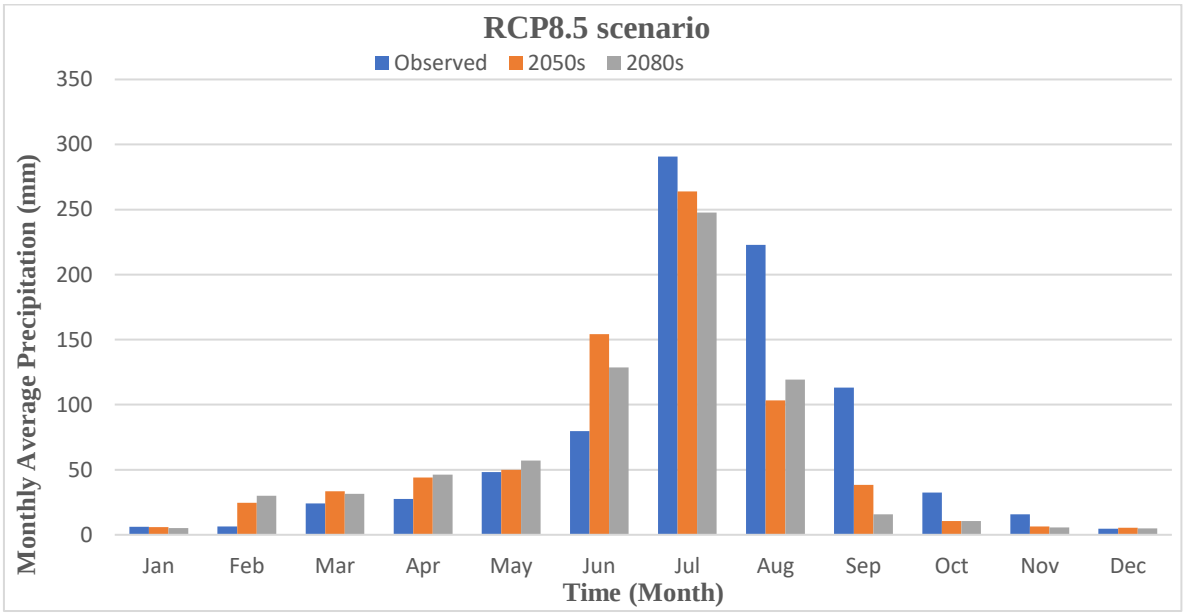

Figure 4-15: Projected mean annual rainfall trend for 2050s and 2080s in the RCP8.5 scenario

Figure 4-16 shows the mean annual rainfall percentage variability in each month of the year and table 4-4 shows the total increase and total decrease of the RCP8.5 scenario in the 2050s and 2080s periods. As a result, it showed 1.94% and 2.02% increase for the 2050s and 2080s periods respectively. However, for about -6.85% and -11.29% decrease was observed for the 2050s and 2080s periods respectively. From this it concluded that the total mean annual rainfall variability in Gerhu-Sirnay catchment was reported by -4.92% and -9.28% decreases in 2050s and 2080s periods respectively (table 4-4). This result was consistent with the study conducted by Daba et

al. (2020) in the Upstream of Awash Basin, Ethiopia as 6.8% to 16.22% for the 2050s and 2080s periods respectively. Balcha et al.(2023) ensured that for about 0.37-29% decrease of annual rainfall by EC-EARTH in the central rift valley basin of Ethiopia under both 2050s and 2080s on RCP8.5 and emission scenarios.

Generally, the percentage variability of mean annual rainfall for the RCP8.5 scenario was summarized in table 4-4;

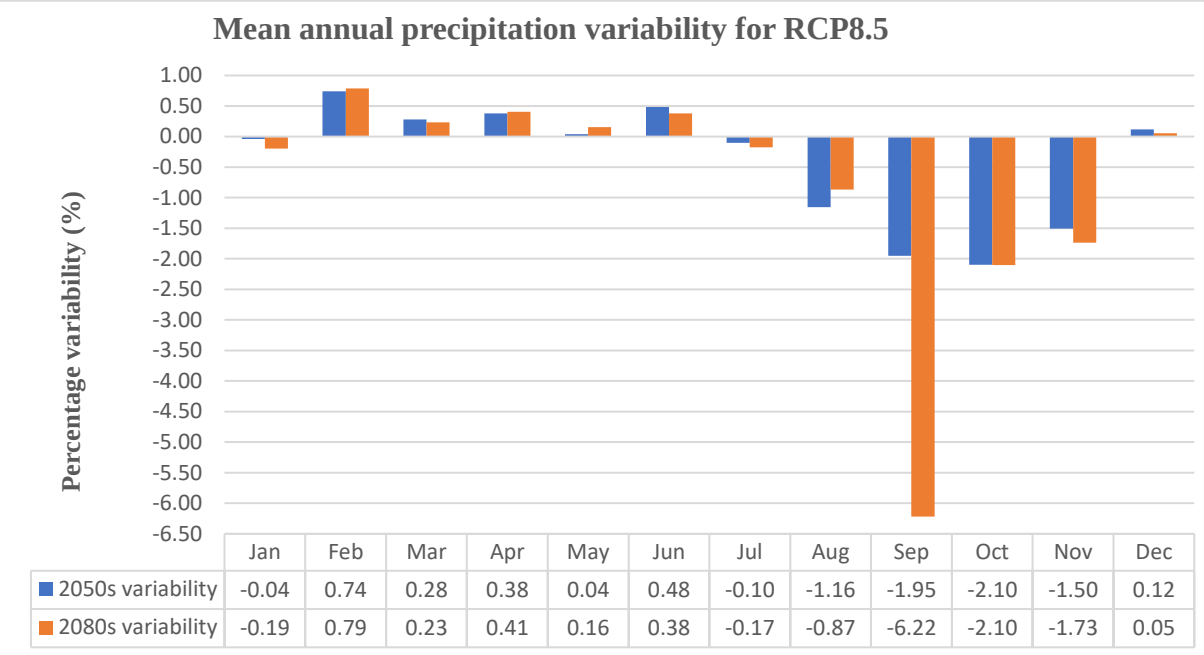

Figure 4-16: Projected mean annual rainfall variability of the RCP8.5 scenario for 2050s and 2080s

Table 4-4: Percentage variability summary of mean annual rainfall in the 2050s and 2080s

Scenario	**Future Period**	**Mean annual precipitation change (%)**		
		Increase	**Decrease**	**Total variability/climate change impact**
RCP8.5	2050s	1.94	-6.85	-4.92
	2080s	2.02	-11.29	-9.28

As a conclusion; in this study the mean annual rainfall for the 2050s and 2080s was observed by potential decrease at the wet months and total percentage decrease at RCP4.5 than RCP8.5. On the comparative sense of the RCP4.5 and RCP8.5 emission scenarios, precipitation showed potential decrease at RCP4.5 emission scenarios on the respective 2050s and 2080s. At RCP4.5 emission scenario, the mean annual precipitation was decreased by 7.58 whereas at rcp8.5 it was decreased by 4.92% for 2050s. In case of 2080s the percentage decrease for rcp4.5 was 9.82% whereas at rcp8.5 the decrease was by 9.28%.

The consistency of this result was supported by Daniela and Abate (2022) in the Gelana watershed, Rift valley basin, Ethiopia; precipitation decline was reported as 15.12% and 7.21% in RCP4.5, and 10.08% and 4.85% in RCP8.5 for the 2050s and 2080s periods respectively. In Dibaba et al. (2020), a large reduction of precipitation was observed in the Finchaa sub-basin, Ethiopia on the CORDEX-RCA4 climate models, and also it was correlated with Dibaba et al. (2019) conducted on the performance evaluation of CORDEX regional climate models in simulating climate conditions of two catchments in Upper Blue Nile Basin, Ethiopia.

4.4.Stream Flow Modeling

4.4.1. Valid Baseline Stream Flow Modeling in SWAT

4.4.1.1. SWAT Model Sensitivity Analysis

As per the relevant literatures, twenty flow parameters (Table 3-5) were tested for their global sensitivity at SUFI2 based of stream flow generation for Gerhu-Sirnay catchment using the Latin hypercube multiple regression. As demonstrated in Table 4-1, the absolute value for t-Stat were between 0.054 and 12.978, and the p-Value were 0.000 to 0.957. According to the sensitivity evaluation of parameters considering the t-Stat and p-Value, parameters having p-Value <0.05 and the corresponding t-Stat value estimates were identified as sensitive for stream flow modeling. Therefore, for this thesis work, only the first seven parameters with p-Value<0.05 and its corresponding t-Stat value (Table 4-1); r_CN2.mgt, r_SOL_K().sol, a_CANMX.hru, v_CH_N2.rte, a_CH_K2.rte, v_ESCO.hru and v_GWQMN.gw were sensitive for Gerhu-Sirnay catchment.

The r_CN2.mgt is hydrological parameter purposed to control the formation of surface runoff, r_SOL_K() is sol soil water parameter which determines the hydraulic conductivity of saturated

soil, a_CANMX.hru is an interception type of precipitation due to plants' leaves, branches and their floors and determines the maximum loss of precipitation doesn't reach the soil (https://en.wikipedia.org/wiki/Interception_(water)). The a_CH_K2.rte is a channel hydraulic conductivity parameter that manages the effective water conductivity with in the channel, v_CH_N2.rte a parameter for channel flow (Leng et al. 2018). v_ESCO.hru a parameter that determines the contribution of soil water for evaporation and v_GWQMN.gw for the management of groundwater (Abeysingha et al.2015; Leng et al. 2018). This indicates surface runoff, channel flow, groundwater, soil water and evapotranspiration were the issued hydrologic components they affect the modeling of stream flow in Gerhu-Sirnay catchment.

As demonstrated in Table 4-1, r_CN2.mgt is the most sensitive parameter for the generation of stream flow to Gerhu-Sirnay catchment at monthly time scale. The consistency of this result was proved in the studies conducted by Tufa and Shime (2020) at Toba watershed, Ethiopia, Shigute et al. (2022) at the Upper Genale River Basin, Ethiopia; Tessema et al. (2020) in the case of Kesem Sub-basin of the Awash, Ethiopia; Addis et al.(2016) in the Ethiopian highlands. Therefore, the sensitivity of r_CN2.mgt against stream flow is the common.

Regardless of their degree of sensitivity to stream flow, the next ranked sensitive parameters of Gerhu-Sirnay catchment; r_SOL_K().sol, a_CANMX.hru, v_CH_N2.rte, v_CH_N2.rte, v_ESCO.hru and v_GWQMN.gw were accepted their sensitivity to Ethiopian river basins, especially in tana, tekeze and mereb areas and consistent with the other studies studied in the same environmental and hydrological characteristics (Shigute et al. 2022; Tessema et al. 2020; Abeysingha et al.2015; Tufa and Shime 2020; Assfaw et al. 2023; Addis et al.2016).

Table 4-5: list of sensitive parameters identified for Gerhu-Sirnay catchment

Name of Parameter	t-Stat	p-Value	Rank
r_CN2.mgt	12.978	0.000	1
r_SOL_K().sol	12.210	0.000	2
a_CANMX.hru	-9.179	0.000	3
a_CH_K2.rte	-8.956	0.000	4
v_CH_N2.rte	-4.412	0.000	5
v_ESCO.hru	-4.378	0.000	6
v_GWQMN.gw	2.305	0.022	7
r_SOL_AWC().sol	1.467	0.144	8

r_RCHRG_DP.gw	-1.465	0.145	9
a_GW_DELAY.gw	1.335	0.184	10
v_GW_REVAP.gw	1.322	0.188	11
v_OV_N.hru	1.174	0.242	12
r_SOL_Z().sol	-1.023	0.308	13
r_SOL_ALB().sol	0.814	0.417	14
r_SLSUBBSN.hru	0.811	0.419	15
v_REVAPMN.gw	-0.604	0.547	16
a_EPCO.hru	-0.445	0.657	17
v_TLAPS.sub	0.346	0.730	18
v_ALPHA_BF.gw	0.283	0.778	19
v_SURLAG.bsn	0.054	0.957	20

The visual trends of the best estimation, observed and 95PPU over the 12 years of sensitivity period at the objective function, R^2 on May-dingur station was provided in figure 4-1. For this matter the used performance measurement parameters for the SWAT model at the labeled flow parameters in figure (4-5) with their score were, R^2 =0.3, NS=0.07, pBIAS=86.6 and RSR=1.04. Since this stage is sensitive parameter investigation and identification for further

model improvement through the most sensitive parameters at the calibration and validation, the performance of the current model was unsatisfactory. In order to be the SWAT model is very good, and may have accepted performance for stream flow simulation in Gerhu-Sirnay catchment, the score of the performance parameters must be, 1, ≥ 0.75, <10%, 0.0 to 0.5, respectively (Tessema et al. 2020; Abeysingha et al.2015).

4.4.1.2. Calibration and Validation

To model the valid baseline stream flow availability, the model was calibrated for eight years (1992-1999) and validated for four years (2000-2003) with the identified sensitive parameters, ranked as the first seven (Table 4-1) at May-dingur hydrological station. To build well performed model for Gerhu-Sirnay catchment, the initial and reasonable range of the sensitive parameters (lower and upper in Table 4-2) were iteratively changed with more than 500 simulations in each iteration in SUFI2 until practical associations between the observed and simulated flow has been appeared for having very good model performance (Eawag 2015; Shigute et al. 2022). The initial values and range of the identified parameters is sensitive and

subjective for each catchment characteristics, SWAT needs the physical information of not only each catchment but also each channel, plains, mountains with in each subbasin (Arnold et al. 2012). Therefore, both values of each sensitive parameters listed in Table 4-2, below was carefully calculated and selected from relevant literatures. For example, the main channel input files were noted as (.rte), for this study only two parameters were sensitive, a_CH_K2.rte and v_CH_N2.rte hence their values were calculated based on Gerhu-Sirnay catchment's main channel characteristics. Considering v_CH_N2.rte both values calculation criteria; in the SWAT input-output documentation (Arnold et al. 2012), the main channel characteristics are (1) excavated or dredged (for Gerhu-Sirnay, not maintained, brushes and weeds with ranges; 0.04 to 0.14), and (2) natural streams (for Gerhu-Sirnay, few trees, stones and brushes with ranges; 0.025 to 0.065). Hence bounding of the range for this variable must inclusive for both properties of Gerhu-Sirnay main channel, which is 0.025 to 0.14. Hence over, the range values for all of the variables selected for Gerhu-Sirnay catchment's streamflow model development were prepared accordingly.

Table 4-6: List of calibrated parameters and their fitted value

No.	Name of Parameter	Lower Value	Upper Value	Fitted Value
1	r_CN2.mgt	-0.2	0.2	0.01573
2	r_SOL_K().sol	0	2000	3.522740
3	a_CANMX.hru	0	50	21.678
4	a_CH_K2.rte	0.01	100	61.394
5	v_CH_N2.rte	0.025	0.14	0.0625
6	v_ESCO.hru	0	1	0.3416
7	v_GWQMN.gw	0	5000	948.612

The performance of the model was measured using the most common statistical parameters, correlation coefficient (R^2), Nash- Sutcliffe Simulation Efficiency (NSE), percent bias (PBIAS) and the Root Means Square Error-Observations Standard Deviation Ratio (RSR) as their visual plot in figure 4-1 a and b respectively. During the calibration period the score with the parameters were, R^2= 0.93, NSE=0.94, RSR=0.16and PBIAS=6.3% (Table 4-3). Based on these parameters' performance measurement criteria; $R^2 \approx 1$, $0.75 \leq NSE \leq 1.00$, $0.00 \leq RSR \leq 0.5$ and $|PBIAS| < 10\%$, this indicates that the model was well calibrated and has very good performance with slight underestimation of simulated streamflow (Abeysingha et al. 2015; Arnold et al. 2012; Daniel and Abate 2022).

In case of validation, the parameters' score was, R^2= 0.82, NSE=0.89, RSR=0.07and PBIAS=10.4% (Table 4-3). This indicates that the model has very good performance with the first three performance indicators however good performance with the last indicator, PBIAS (Abeysingha et al. 2015). When the model's performance was compared during calibration and validation, the variance between the observed and simulated flow was increased, the residual variance trend fitting was reduced, and the percent of underestimating simulated flow was increased by 3.1% during the validation period. This was an expected performance report for SWAT model due to the case that in complex landscape characteristics of catchments like Gerhu-Sirnay catchment, SWAT model needs longer simulation duration to be reported with better simulation performance, and this situation was approved by previous studies in related environmental nature, including Addis et al. (2016) studied in Ethiopian highlands, Tufa and Shime (2020) investigated in Toba sub-watershed, Ethiopia and Shigute et al. (2022) in the upper Genale river basin, Ethiopia.

Table 4-7: Statistical performance indicators for seasonal stream flow, calibration and validation periods

Simulation period	**Statistical performance indicators**			
	R^2	**NSE**	**PBIAS**	**RSR**
Calibration	0.93	0.94	0.063	0.16
Validation	0.82	0.89	0.101	0.07

In Figure 4-17, the hydrograph showing the level of fitting; overestimated and or underestimated trend of the simulated flow for both calibration and validation was provided, and the detailed data was given in Appendix-V;

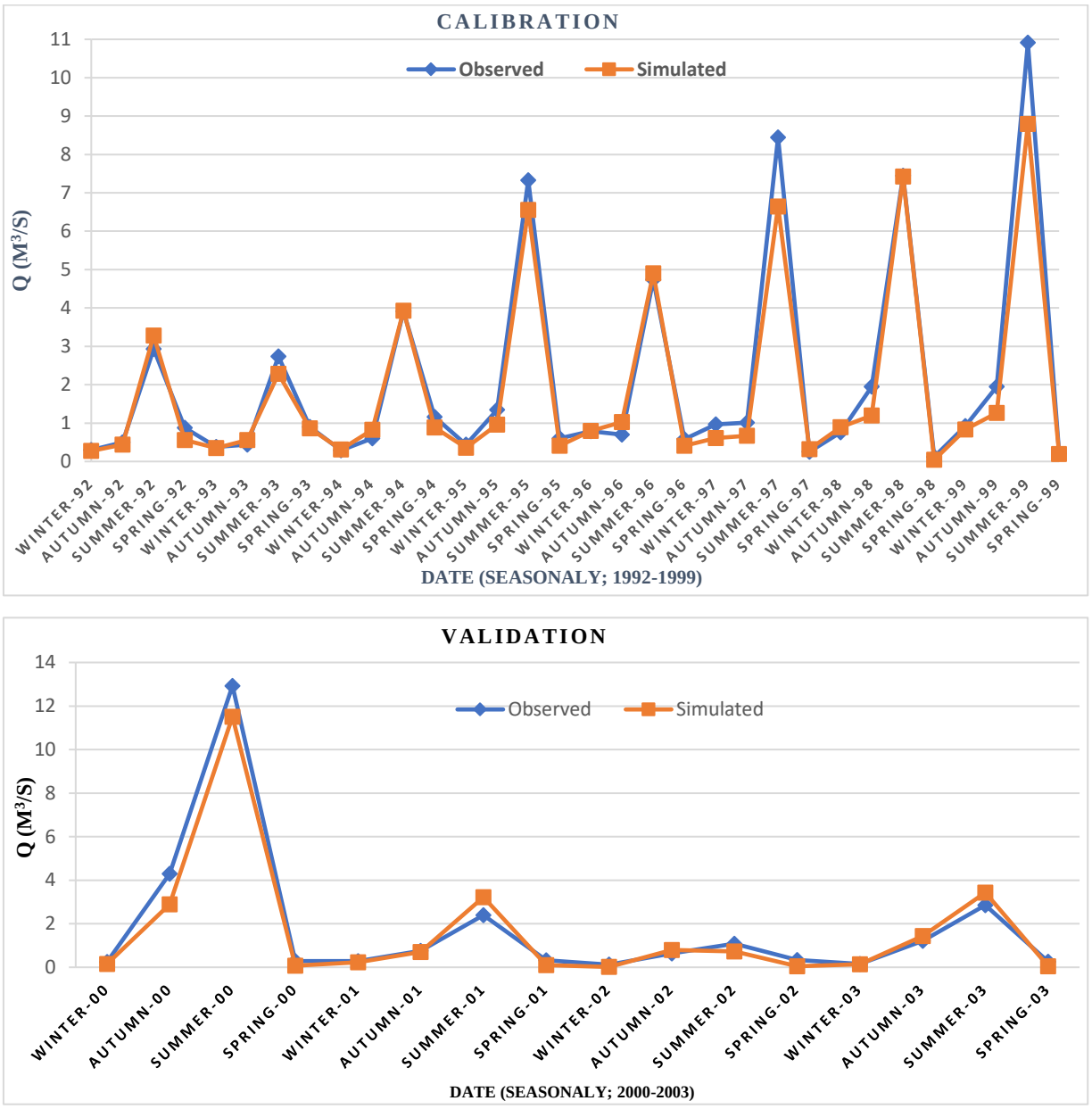

Figure 4-17: Hydrographs of monthly simulated and gauged flows for calibration (a) and validation (b) at the outlet of May-dingur station's catchment

The mean monthly observed and simulated flow at May-dingur station was 0.693 and 0.564 for calibration, and 0.587 and 0.532 for validation. This underestimation result the simulated flow showed consistency with that of Tufa and Shime (2020) as 42.43 and 58.71 and 47.25 and 55.91 m^3/s respectively at Toba, Ethiopia . As labelled in figure 4-2, the maximum mean monthly flow for both calibration and validation were estimated at July, which is the rainiest month in the study area which is northern and most parts of Ethiopia.

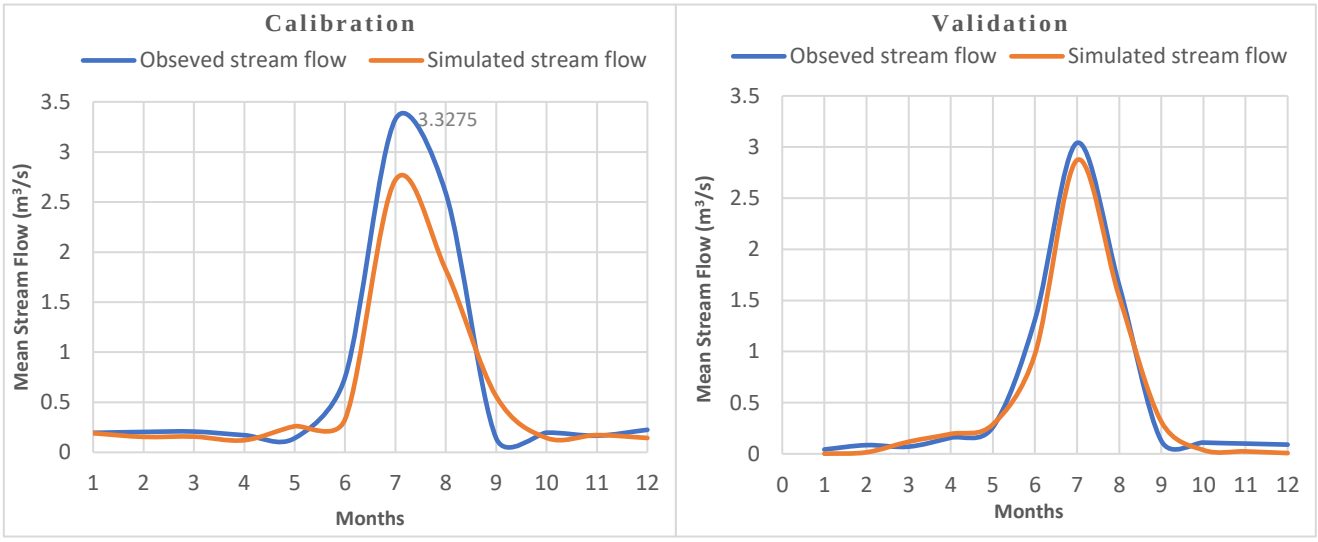

Figure 4-18: Mean monthly observed and simulated stream flow at may-dingur station (Calibration and Validation)

Generally, based on the stated statistical performance indicators, the simulated flow by SWAT model under the SUFI2 parameter optimization program has a very good agreement with the reference flow measured in May-dingur station. Therefore, the SWAT model has the capability to be used for further hydrologic investigations in Gerhu-Sirnay catchment and elsewhere with similar catchment characteristics (Tufa and Shime 2020).

4.4.2. Forecasting Stream Flow

4.4.2.1. RCP 4.5 Emission Scenario

i. Seasonal

The average seasonal stream flow of ICHEC-EC-EARTH-RCA4 model for 2050s and 2080s future periods at RCP4.5 emission scenario was plotted in figure 4-19. The projected average seasonal stream flow will be higher than the observed stream flow in the dry and semi-dry

seasons at 2050s and 2080s. In the wet and semi-wet seasons, the average seasonal stream flow projected to decrease with a slight increment in the 2050s. The average seasonal rainfall trend caused for 2050s and 2080s (figure 4-9) causes corresponding change on the average seasonal flow trend. This result is in line with Gragn et al. (2019) conducted in Awata River Watershed, Genale Dawa Basin: Southern Ethiopia.

Generally, considering the observed average seasonal stream flow, Gerhu-Sirnay catchment will have higher projected flow in the winter and autumn seasons and lower in the wet and semi-wet seasons for both future periods. This is a reliable conclusion with Wodaje et al. (2021) said that flow has been decreased in the high flow seasons in the same future periods and emission scenarios with this study.

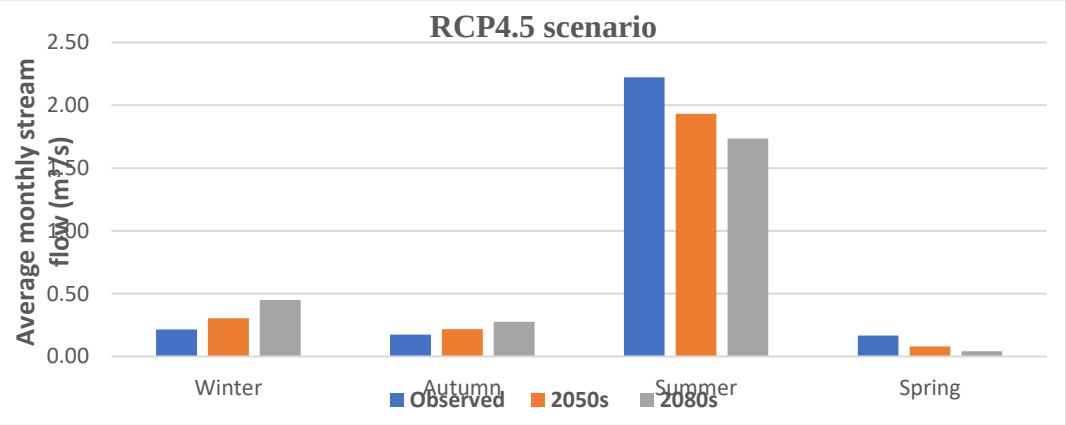

Figure 4-19: Average seasonal stream flow of ICHEC-EC-EARTH-RCA4 model for 2050s and 2080s future periods at RCP4.5 emission scenario

Figure 4-20 showed that the maximum flow increasement was projected in winter and autumn relatively higher flow will occur in the 2080s. In case of summer and spring seasons flow will be projected to decrease relatively higher decrease tends at 2080s. This is in line with Daba et al. (2020) "the maximum increase in flow was labelled in winter for 2050s and 2080s under as RCP4.5 emission scenario while the it decreased by 5.43% and 5.48% in summer". It is also confident with Gragn et al. (2019) conducted on Awata Watershed, Genale Dawa Basin, Southern Ethiopia. The watershed has similar topographic features, soil type and climatic complexities with Gerhu-Sirnay catchment hence realized that 15.3% of average seasonal

rainfall change caused 24.7% average seasonal stream flow change on the 2050s of similar emission scenario.

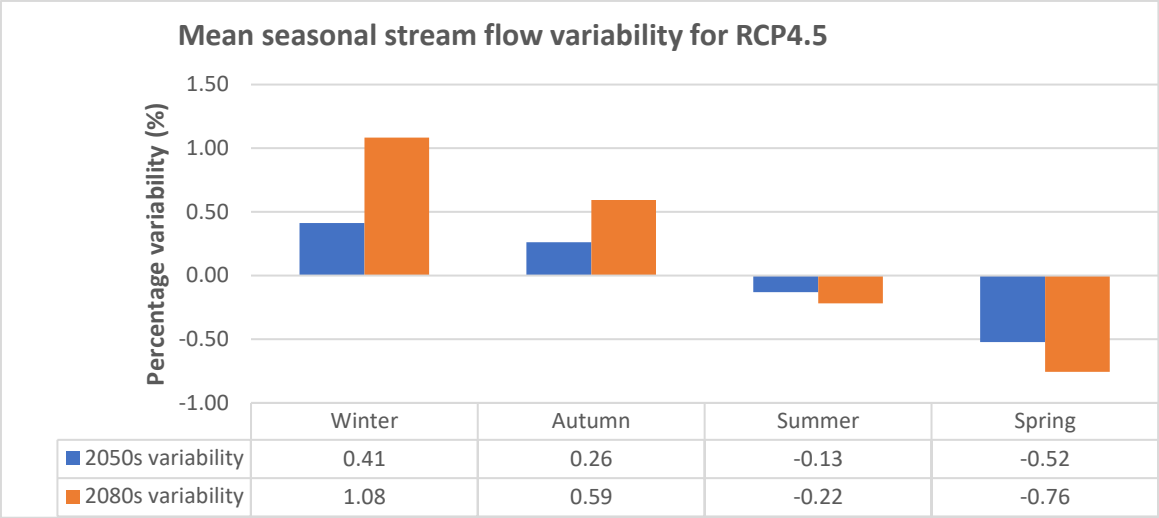

Figure 4-20: Average seasonal stream flow variability for 2050s and 2080s future periods at RCP4.5 emission scenario

ii. Annual

The projected mean annual stream flow for the RCP 4.5 emission scenario of 2050s and 2080s future periods at the outlet of May-dingur station's sub-catchment was plotted in figure 4-21. The maximum and minimum annual stream flow values for the 2050s and 2080s were appeared in the same month with the observed stream flow. For example, the maximum mean stream flow in the observed case was appeared at July, Augst and Jun orderly as 3.33 m^3/s, 2.59 m^3/s and 0.75 m^3/s respectively. In line with this the maximum mean monthly stream flow for the 2050s case were also 1.90 m^3/s, 1.01 m^3/s and 0.78 m^3/s, and also for 2080s were 2.70 m^3/s, 1.54 m^3/s and 0.97 m^3/s respectively for the mentioned months. From this, higher mean monthly stream flow was observed to be occurred at the 2080s future periods with 0.8, 0.53 and 0.19 incremental factors on the July, Augst and Jun respectively.

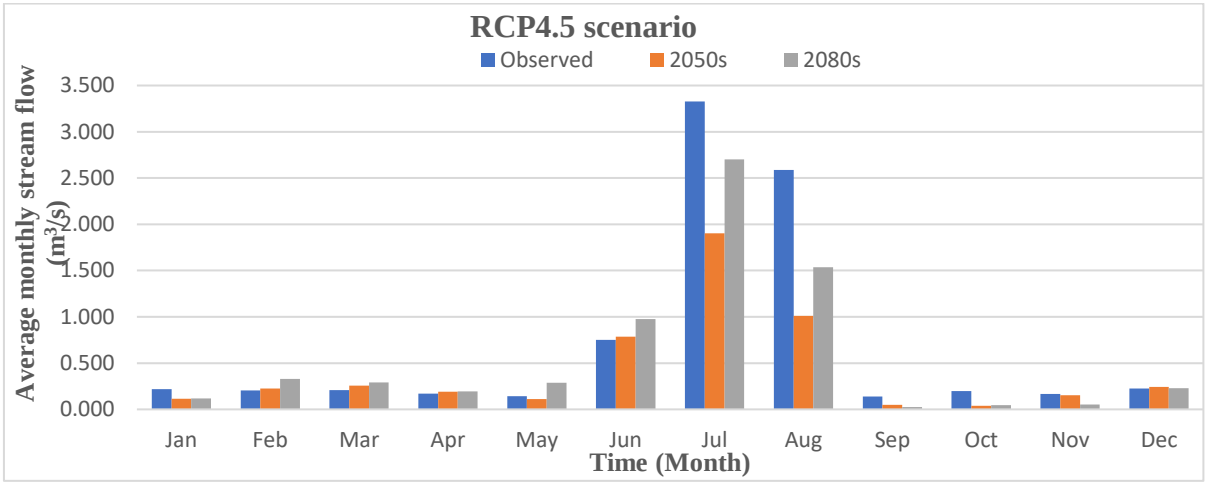

Figure 4-21: Projected mean annual stream flow trend for 2050s and 2080s in the RCP4.5 scenario

Figure 4-22 shows the mean annual stream flow percentage variability in each month due to climate change impact on the RCP4.5 scenario in the 2050s and 2080s periods. Under the 2050s future period, the maximum and minimum stream flow variability were observed on October labeled as 3.91 (decreasing) and June labelled as 0.04 (increasing) respectively. While under 2080s, the maximum and minimum stream flow variability were observed on September labeled as 4.98 (decreasing) and December labelled as 0.02 (increasing) respectively. Generally, the percentage variability of the mean monthly stream flow for each month generated from 2050s and 2080s periods at the RCP 4.5 scenario was summarized in figure 4-11;

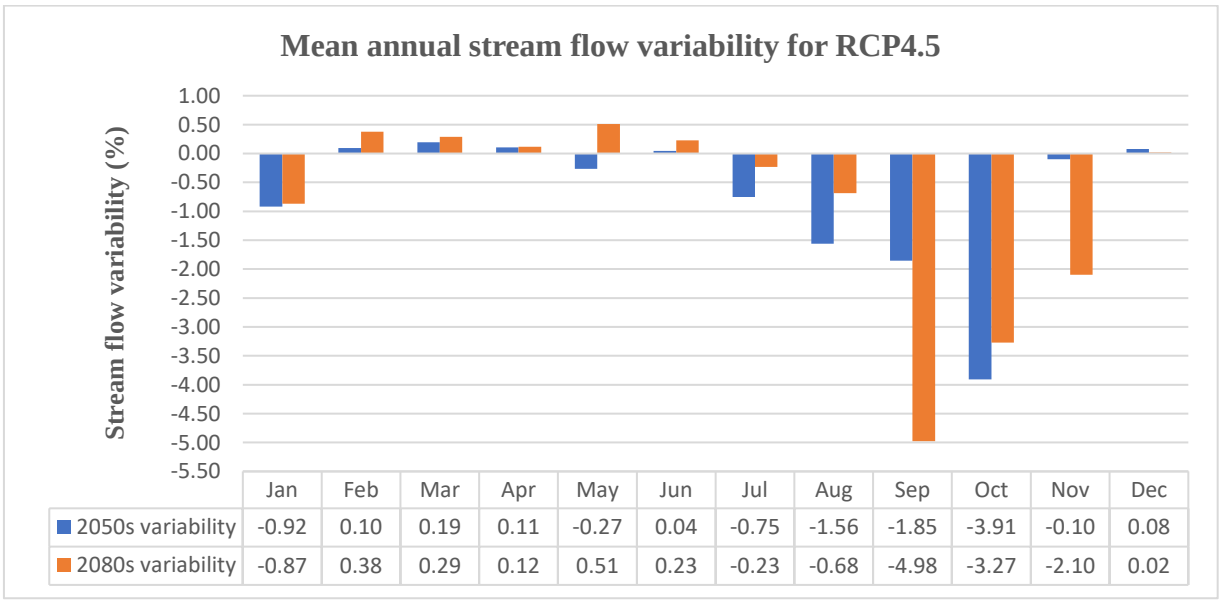

	Jan	Feb	Mar	Apr	May	Jun	Jul	Aug	Sep	Oct	Nov	Dec
2050s variability	-0.92	0.10	0.19	0.11	-0.27	0.04	-0.75	-1.56	-1.85	-3.91	-0.10	0.08
2080s variability	-0.87	0.38	0.29	0.12	0.51	0.23	-0.23	-0.68	-4.98	-3.27	-2.10	0.02

Figure 4-22: Projected mean annual stream flow variability of RCP 4.5 scenario for 2050s and 2080s

4.4.2.2.RCP 8.5 Emission Scenario

i. Seasonal

The average seasonal stream flow of ICHEC-EC-EARTH-RCA4 model for 2050s and 2080s future periods at RCP8.5 emission scenario was plotted in figure 4-23. The projected average seasonal stream flow will be higher than the observed stream flow in the dry and semi-dry seasons at 2050s and 2080s. In the wet and semi-wet seasons, the average seasonal stream flow projected to decrease with a slight increment in the 2050s. The average seasonal rainfall trend caused for 2050s and 2080s (figure4-10) causes corresponding change on the average seasonal flow trend. This result is in line with Gragn et al. (2019) conducted in Awata River Watershed, Genale Dawa Basin: Southern Ethiopia.

Seeing the observed average seasonal stream flow, Gerhu-Sirnay catchment will have higher projected flow in the winter and autumn seasons and lower in the wet and semi-wet seasons for both future periods. This is a reliable conclusion with Daba et al. (2020) and Wodaje et al. (2021) as flow has been decreased in the high flow seasons and decreased in wet and semi-wet season same future periods and emission scenarios with this study.

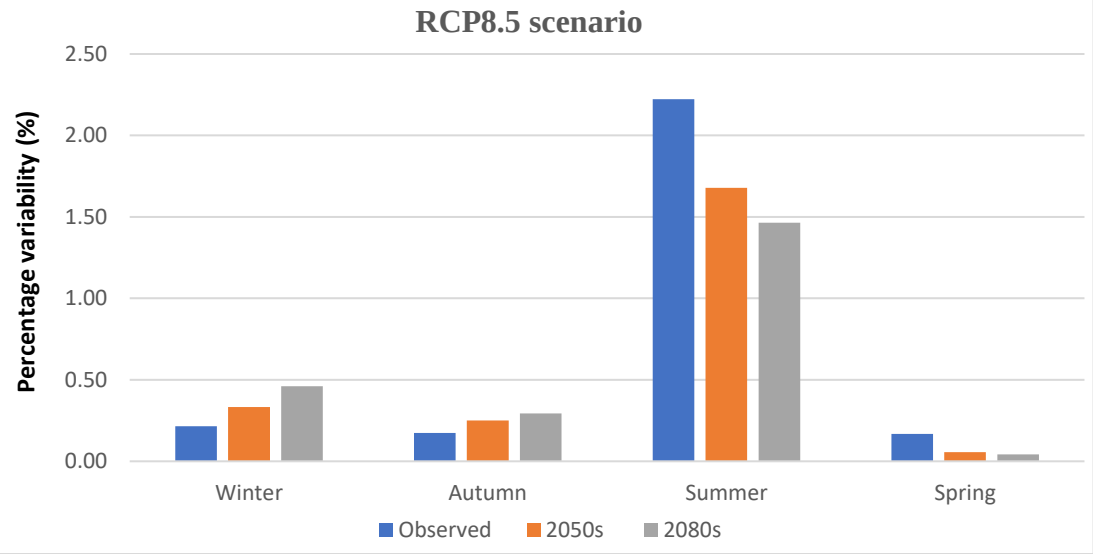

Figure 4-23: Average seasonal stream flow of ICHEC-EC-EARTH-RCA4 model for 2050s and 2080s future periods at RCP8.5 emission scenario

Figure 4-24 showed that the maximum flow increasement was projected in winter and autumn relatively higher flow will occur in the 2080s. In case of summer and spring seasons flow will

be projected to decrease relatively higher decrease tends at 2080s. This is similar with Daba et al. (2020)s' report "the maximum increase in flow was labelled in winter for 2050s and 2080s under as RCP4.5 emission scenario while the it decreased by 5.43% and 5.48% in summer". It is also confident with Gragn et al. (2019) conducted on Awata Watershed, Genale Dawa Basin, Southern Ethiopia. The watershed has similar topographic features, soil type and climatic complexities with Gerhu-Sirnay catchment hence realized that 15.3% of average seasonal rainfall change caused 24.7% average seasonal stream flow change on the 2050s of similar emission scenario.

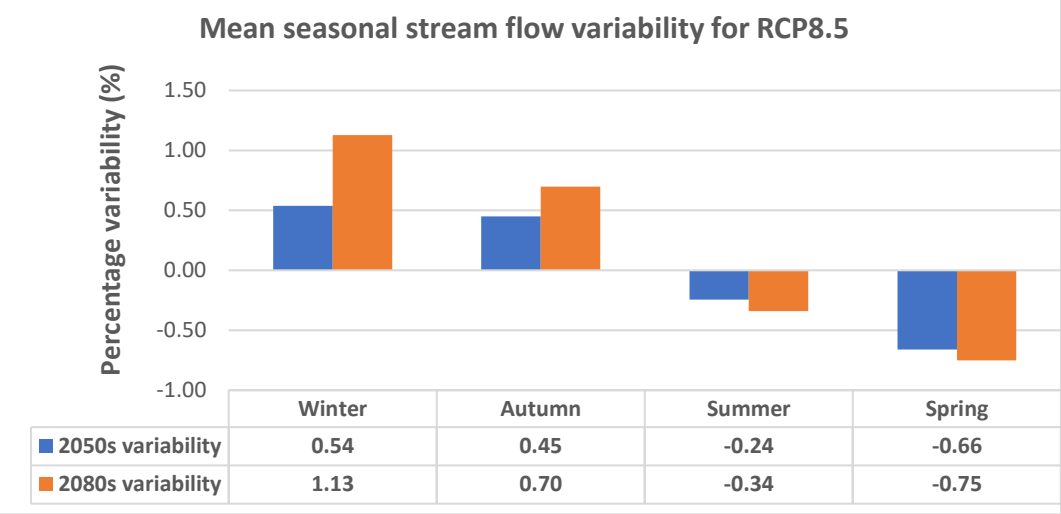

	Winter	Autumn	Summer	Spring
2050s variability	0.54	0.45	-0.24	-0.66
2080s variability	1.13	0.70	-0.34	-0.75

Figure 4-24: Average seasonal stream flow variability for 2050s and 2080s future periods at RCP8.5 emission scenario

ii. **Annual**

In the RCP 4.8 emission scenario, the projected mean annual stream flow for 2050s and 2080s future periods at the outlet of May-dingur station's sub-catchment was plotted in figure 4-25. The maximum and minimum annual stream flow values at monthly case for the 2050s and 2080s were appeared in the same month with the observed stream flow. For example, the maximum mean stream flow in the observed case was appeared at July, Augst and Jun orderly as 3.33 m^3/s, 2.59 m^3/s and 0.75 m^3/s respectively. In line with this the maximum mean monthly stream flow for the 2050s case were 1.92 m^3/s, 1.37 m^3/s and 0.84 m^3/s, and also for 2080s were 2.71 m^3/s, 1.59 m^3/s and 0.99 m^3/s respectively for the mentioned months. From this, higher mean annual

stream flow was observed to be occurred at the 2080s future periods with 0.79, 0.22 and 0.15 incremental factors on the July, Augst and Jun respectively.

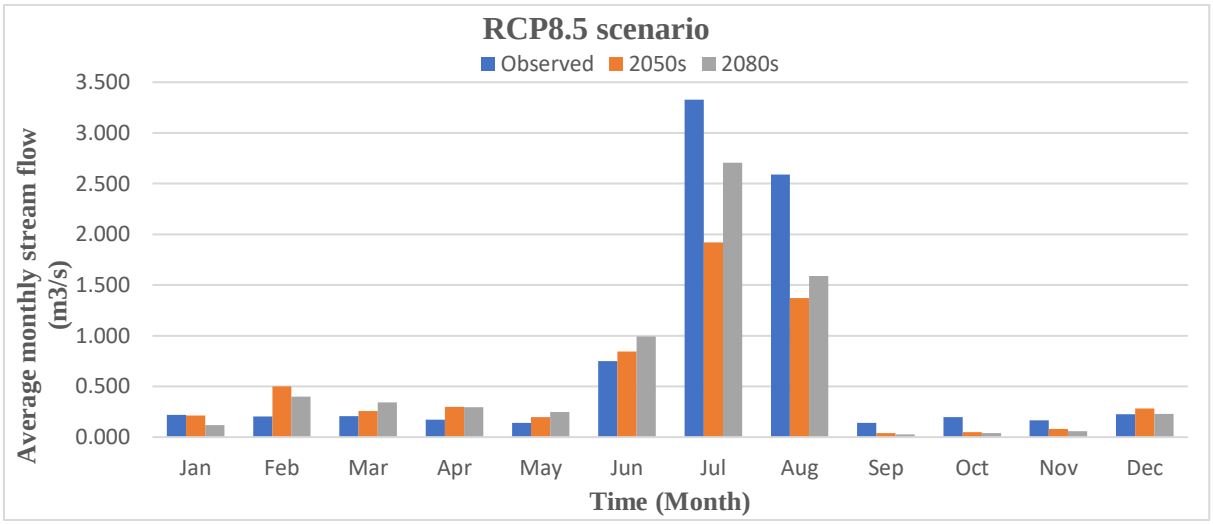

Figure 4-25: Projected mean annual stream flow trend for 2050s and 2080s in the RCP 8.5 scenario

Figure 4-26 shows the mean annual stream flow percentage variability in each month due to climate change impact on the RCP4.5 scenario in the 2050s and 2080s periods. Under the 2050s future period, the maximum and minimum stream flow variability were observed on October labeled as 2.93 (decreasing) and January labelled as 0.02 (decreasing) respectively. While under 2080s, the maximum and minimum stream flow variability were observed on September labeled as 4.34 (decreasing) and December labelled as 0.02 (increasing) respectively. Generally, the percentage variability of the mean monthly stream flow for each month generated from 2050s and 2080s periods at the RCP 8.5 scenario was summarized in figure 4-26;

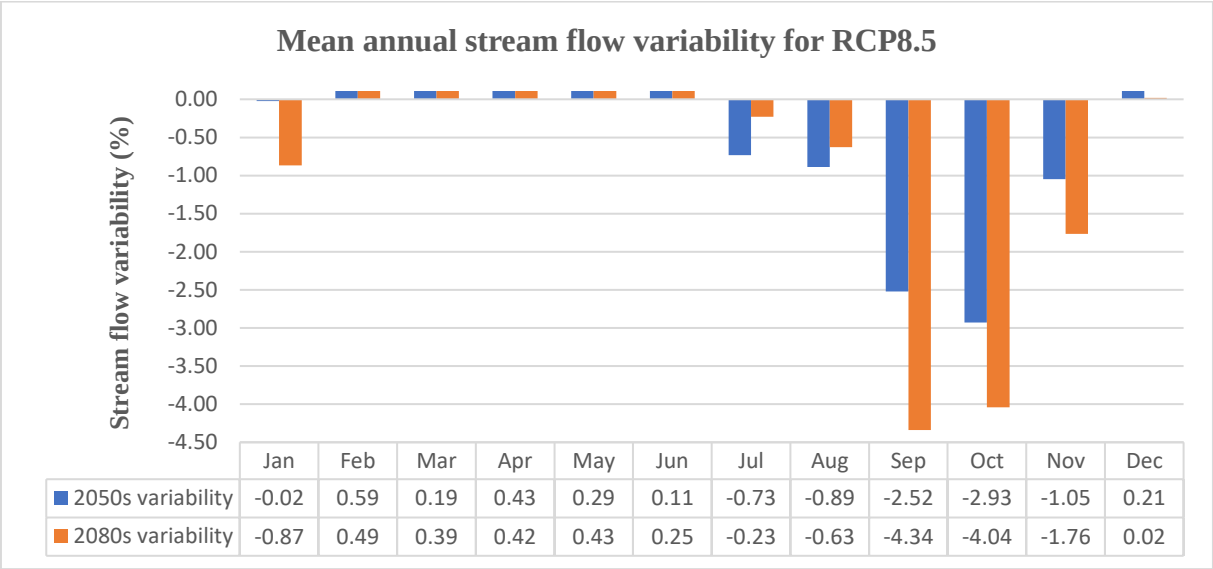

Figure 4-26: Projected mean annual stream flow variability for RCP 8.5 scenario, 2050s and 2080s

4.5.Assessment of Climate Change Impact on Surface Water Availability

In this study the impact of climate change on surface water availability was conducted in terms of mean seasonal rainfall, mean annual rainfall, mean seasonal stream flow, mean annual stream flow, evapotranspiration and water yield changes under RCP 4.5 and RCP 8.5 emission scenarios for the near future and far future periods, 2050s and 2080s respectively at May-dingur station. Therefore, the harvested results were interpreted and discussed in below sub-titles;

4.5.1. Precipitation

The projected trend of average seasonal rainfall in the RCP4.5 and RCP8.5 emission scenarios; n the dry and semi dry seasons, average seasonal rainfall was projected to increase with the progressive increments on the far future period than 2050s. During the wet and semi-wet seasons average seasonal rainfall will progressively decrease with the progressive decrease on the near future period than 2080s. This indicates that on Gerhu-Sirnay catchment higher average seasonal rainfall will appear on the far future period in the dry and semi-dry seasons while in the wet and semi-wet seasons higher average seasonal rainfall will appear the near future. This result is reliably in agreement with studies conducted in other similar hydrological zones of Ethiopia; Abdule et al. (2024), Kuma et al. (2024), Daba et al. (2020), Taye et al. (2018) and Getahun et al. (2014).

Under the RCP 4.5 emission scenario, the mean annual rainfall decreases, increase and total decrease for the 2050s and 2080s detailed in table 4-3. However, the total changes of the mean annual rainfall from climate impact for the 2050s was 9.89% whereas it was 13.52% for 2080s. This showed that with in the RCP 4.5 emission scenario, the impact of climate change over the mean annual rainfall would be 3.63% higher in 2080s. This result was consistent and relevant with the Fifth Assessment Report (AR5) representative concentration pathways (RCPs) adopted by the IPCC (2014). RCPs are climate change scenarios developed to project future greenhouse gas concentrations for global warming in degree Celsius. Hence, the average global warming will be projected to increase 1.4 to 1.8 degrees for the durations of 2046-2065 and 2081-20100 respectively for RCP 4.5 emission scenario, and causes significant impact (https://en.wikipedia.org/wiki/Representative_Concentration_Pathway).

Under the RCP 8.5 scenario, the mean v variability was summarized in Table (4-4). As a conclusion, the total changes of the mean annual rainfall due to climate change impact for 2050s was 8.79% whereas 13.31% for 2080s. This showed that with in the RCP 8.5 scenario, the impact of climate change over the mean annual rainfall would be 4.52% higher in 2080s. As per in the AR5 of IPCC (2014), the average global warming will be 2 to 3.7 degrees for the durations of 2046-2065 and 2081-20100 respectively for RCP 8.5 emission scenario, and causes significant impact (https://en.wikipedia.org/wiki/Representative_Concentration_Pathway). Therefore, the result of this study was consistent and relevant with the RCPs's implications.

On the comparative sense of the RCP4.5 and RCP8.5 emission scenarios, annual rainfall showed potential change or impact from climate change at RCP 8.5 emission scenario, as by comparing the respective over all changes, 3.63% and 4.52%. The consistency of this result was supported by Daniela and Abate (2022) and Dibaba et al. (2020); as precipitation decline with significant impact from climate change was reported at RCP4.5 than from RCP8.5 for the 2050s and 2080s periods respectively.

4.5.2. Stream Flow

The trend and variability of average seasonal stream flow of ICHEC-EC-EARTH-RCA4 model for 2050s and 2080s future periods at RCP4.5 (figure c) and RCP4.5 (figure d) emission scenario was projected from the corresponding changes of average seasonal rainfall. This result

is in line with Gragn et al. (2019) conducted in Awata River Watershed, Genale Dawa Basin: Southern Ethiopia. Under RCP4.5 emission scenario 0.6% decrease and 0.41% increasing variability causes 0.02 and 0.7% increase respectively for the 2050s and 2080s respectively. Whereas for the RCP8.5 emission scenario 0.59% and 0.73% increasing variability causes an about 0.08% and 0.76% increasing change was projected for the 2050s and 2080s respectively. Hence result of this study had proofed the state of corresponding changes among the corresponding emission scenarios and future periods.

Under the RCP 4.5 emission scenario, the decreasing and or increasing, total decrease and total changes of the mean annual stream flow due to climate impact for 2050s and 2080s periods was summarized in Table (4-7). As a result, this study showed 0.52 % and 1.54% increase for the 2050s and 2080s periods respectively. Whereas, for about 9.36% and 12.13% decrease was observed for the 2050s and 2080s periods respectively. From this it concluded that the total mean annual stream flow decrease due to climate change impact in Gerhu-Sirnay catchment was reported by 8.84% and 10.59% decreasing change in 2050s and 2080s periods respectively (table 4-7). This climate change impact result on annual stream flow was consistent with the study conducted by Daba et al. (2020) as 12.03 % and 4.12% % reduction for the 2050s and 2080s periods respectively under RCP 4.5 scenario. The total changes (without considering the signs of decease and increase) due to climate impact for 2050s was 9.88% and was 13.67% for 2080s (table 4-7). This showed that with in RCP 4.5 emission scenario, the impact of climate change over the mean annual stream flow would be 3.79% higher in in the intermediate future, 2080s.

In case of RCP 8.5 emission scenario, the decreasing and or increasing, total decrease and total changes of the mean annual stream flow due to climate impact for 2050s and 2080s periods was labelled in Table (4-8;below). As a result, this study showed 1.82 % and 1.99% increase for the 2050s and 2080s periods respectively. However, for about 8.14% and 11.87% decrease was observed for the 2050s and 2080s periods respectively. From this it concluded that the total mean annual stream flow variability due to climate change impact in Gerhu-Sirnay catchment was reported by 6.32% and 9.88% decreasing change in 2050s and 2080s periods respectively (table 4-8). This result was consistent with other studies in Ethiopia; Daba et al. (2020) as 12.65% to 5.31% for the 2050s and 2080s periods respectively for RCP 8.5 scenarios. The total

changes for 2050s were 9.96% and for 2080s was 13.86%. In this scenario also, the impact of climate change over the mean annual stream flow would be higher 3.9% in 2080s.

Generally, the findings of this study revealed that, climate change impact over mean monthly precipitation and stream flow was higher in 2080s than 2050s in both RCP 4.5 & 8.5 emission scenarios, separately. This result showed consistency with the principles of RCPs (IPCC 2014), and states that from the near to intermediate future, the projected average global warming will increase up to 1.8 degrees for RCP 4.5 scenario, and climate change impact will improve linearly (https://en.wikipedia.org/wiki/Representative_Concentration_Pathway).

In Ethiopia many studies including Daniela and Abate (2022); Wagesho et al. (2013); Koch & Cherie (2013); Haile et al. (2017); Mengistu et al. (2021); Takele et.al.(2022) were conducted the impact of climate change on average seasonal and annual stream flow. Hence, the result of this study was consistent with the conclusion of these studies at the confluence future periods, emission scenarios and prediction parameters; seasonal and annual precipitation and stream flow.

When we consider the comparative sense of both emission scenarios, the potential impact of mean annual rainfall and mean annual stream flow due to climate change was observed at RCP 8.5 emission scenario, which are 0.89% (4.52-3.63) and 0.11% (3.9-3.79) more respectively. The consistency of this result was supported by studies in Ethiopia; Daniela and Abate (2022) and Dibaba et al. (2020); concluded that significant impact from climate change was reported at RCP8.5 than from RCP4.5. Also, it was supported by the principles of RCPs, IPCC (2014), and states that RCP 8.5 has higher radiative forcing values than RCP 4.5 (8.5 and 4.5 W/m^2) respectively. Therefore, the higher greenhouse gas emission was pronounced to cause higher climate change impact (https://en.wikipedia.org/wiki/Representative_Concentration_Pathway).

Table 4-8: Percentage climate change impact summary of mean monthly stream flow Gerhu-Sirnay catchment for the 2050s and 2080s under RCP 4.5 and 8.5 emission scenarios

Scenario	Future Period	Mean annual stream flow change (%)			
		Increase	Decrease	Total Decrease	Total Change
RCP 4.5	2050s	0.52	-9.36	-8.84	9. 88
	2080s	1.54	-12.13	-10.59	13.67
RCP 8.5	2050s	1.82	-8.14	-6.32	9.96
	2080s	1.99	-11.87	-9.88	13.86

4.5.3. Water Yield

In seasonal time scale analysis, the water yield variability of Gerhu-Sirnay catchment was projected by in line with the variability of its corresponding seasonal rainfall. This analysis result was in a strong agreement with Kuma et al.(2024) conducted in Gibe Gojeb catchment, Ethiopia. Quantitatively 0.17 and 0.13% water yield increments on the winter and autumn were sourced from 0.14 and 0.10% increments respectively for 2050s and 1.17 and 0.67% water yield increments also trended from 1.08 and 0.33% increase for the 2080s period under RCP 4.5 emission scenario. For the case of RCP 8.5 emission scenario, 1.37 and 0.33% water yield increments on the winter and autumn were sourced from 1.05 and 0.28% increments respectively for 2050s and 1.35 and 0.37% water yield increments also trended from 1.34 and 0.35% increase for the 2080s period.

At annual water yield analysis, the same trending with seasonal scale was projected. Under RCP 4.5 emission scenario, water yield will decrease by 6.13 % from 7.58% average annual rainfall decrease in the 2050s period. In the far future, 7.65% decrease was projected from 9.82% decrease of average annual rainfall. Under RCP 8.5 emission scenario, water yield will decrease by 3.03 % from 4.92% average annual rainfall decrease in the 2050s period. In the far future, 5.41% decrease was projected from 9.28% decrease of average annual rainfall.

5. CONCLUSIONS AND RECOMMENDATIONS

5.1. CONCLUSIONS

This thesis assessed the impacts of climate change over the surface water availability of Gerhu-Sirnay catchment using the best fit model from 7CORDEX-RCA4 models under RCP4.5 and 8.5 emission scenarios for 2050s and 2080s future periods.

According to the volumetric and Taylor diagram performance perspectives, ICHEC-EC-EARTH-RCA4 model best fitted to observed precipitation at the seasonal baseline period by scoring 0.9838, 0.0000, 0.9838 and 0.0162, and 0.749, little less than 75 and little less than 100 respectively for VHI, VFAR, VCSI and VMI, and CC, NRMSE and δ_N respectively. Hence the mean seasonal rainfall variability in reference to the observed precipitation at the overlapped historical simulation of ICHEC-EC-EARTH model was increased by 1% and decreased by 5.42%, and showed 4.42% decreasing as an overall variability. In case of annual time scale ICHEC-EC-EARTH model showed the leading rank by scoring better CC=0.957, NRMSE<=25 and δ_N<=110 values than seasonal scale.

The baseline hydrological model for monthly stream flow was modeled by soil and water assessment tool (SWAT), and calibrated and validated in SWAT-CUP under SUFI2 parameter optimizer tool considering the baseline period (1990-2003) with 2 years period is model warm up time. As a result of this, SWAT model showed a very good performance at modeling baseline stream flow quantified by R^2, NSE, PBIAS and RSR as 0.91, 0.93, 7.3% and 0.14 for calibration and 0.80, 0.89, 0.104 and 0.05 for validation respectively. Therefore, SWAT model has the capability to conduct further hydrologic investigations in the catchment.

The climate change impact over the surface water availability of Gerhu-Sirnay catchment was indicated as; (1) the average seasonal rainfall was projected to change by 1.02% in both future periods of RCP4.5 emission scenario. RCP8.5 emission scenario by 0.59 and 0.73% will be changed for the 2050s and 2080s respectively. (2) the mean annual rainfall was potentially decreased by 7.58% and 9.82% at 2050s and 2080s under RCP4.5, and 4.92% and 9.28% during 2050s and 2080s under RCP8.5 respectively. (3) the total impacts due to climate change annualy were; 9.89% and 13.52% during 2050s and 2080s respectively in the RCP 4.5 emission scenario; with 3.63% times higher impact during 2080s, and 8.79% and 13.31% at 2050s and 2080s

respectively for the RCP 8.5 scenario; having 4.52% higher in 2080s. (4) The corresponding future annual stream flow was decreased by 8.84% and 10.59% for the 2050s and 2080s under RCP4.5, and 6.32% and 9.88% for the 2050s and 2080s respectively under RCP8.5. (4) the total impacts at annual scale were; 9. 88% and 13.67% during 2050s and 2080s respectively in the RCP 4.5 emission scenario; with 3.79% times higher during 2080s, and 9.96% and 13.86% at 2050s and 2080s respectively for the RCP 8.5 emission scenario; 3.9% higher in 2080s. In case of the comparative sense of both emission scenarios, the potential impact of climate change on mean monthly precipitation and stream flow was observed at RCP 8.5 scenario of 2080s future period, which are 0.89% (4.52-3.63) and 0.11% (3.9-3.79) respectively. (6) the average seasonal stream flow will changed by 0.72% at both future periods of RCP4.5 emission scenario and 0.82% change also projected for both future periods of RCP8.5 emission scenario.

Generally, the findings of this study indicated that climate change has significant impact over surface water resources of Gerhu-Sirnay catchment. Hence, it provides indication on how the seasonal and annual rainfall and stream flow variability and change will be occurred in the 2050s and 2080s periods for RCP 4.5 and RCP 8.5 emission scenarios in the catchment. This could help to plan sustainable water resources and climate resilience frameworks in the stated futures. Moreover, the result highlights the need for the concerned bodies to develop strong climate-resilient management strategies and counteract the climate changes in the catchment.

5.2. RECOMMENDATIONS

As per result of this thesis, the following recommendations have been raised to improve future researches;

- In this study, the used meteorological stations are distributed scarcely, henceforward their datasets including, precipitation are unrecommendable to measure the performance of multiple CORDEX-RCA4 models. Therefore, there is a need of improving theses datasets either (1) future researchers should use additional multiple datasets such as satellite models (like, CHIRPS v2, Re-analysis,) to prepare spatially inclusive gauge datasets or (1) installing additional gauges by the responsible organizations.
- In this thesis work, only precipitation, stream flow, water yield and evapotranspiration variability were considered to assess the impact of climate change on surface water availability. However, due to the limited number of parameters, this can't be reported with real result hence which can't serve for climate change impact policy generation. Therefore, to get accurate climate change impact with full capacity of SWAT model, future researchers must consider multiple future water variability parameters', such as soil moisture, surface runoff, temperature and evapotranspiration.
- According to the performance evaluation of the seven CORDEX-RCA4 climate models of this thesis, ICHEC-EC-EARTH-RCA4 observed with the leading performance however, still it was with lots of errors. Hence before using its datasets for further hydrological analysis, future researchers need to conduct performance improvement techniques like, comparison of different bias-correction methods and blending of their corrected values, and integration of different climate models' data.
- This study considers only one dynamic driver, which was climate change impact however, in the real ground lots of drivers, including land use land cover changes and socio-economic issues were applied their dynamic impacts over the surface water availability. Therefore, future studies should consider the combined effects of these environmentally dynamic drivers to model decision-to-policy level surface water availability.
- This study's hydrological modeling was conducted only uncertainty analysis of flow parameters however, for capacity level result of SWAT model, future researchers should employ multi-uncertainty analysis, like input parameters and model structures.

REFERENCES

Abbasi, A., Amirabadizadeh, M., Afshar, A. A., & Yaghoobzadeh, M. (2022). Potential influence of climate and land-use changes on green water security in a semi-arid catchment. Journal of Water and Climate Change, 13(1), 287-303.

Abbaspour, K. 2015 SWAT Calibration and Uncertainty Programs – A User Manual. Swiss Federal Institute of Aquatic Science and Technology, Eawag, Switzerland.

Abdulea, A. M., Muluneh, A., & Woldemichael, A. (2024). Modeling climate change projection and its impact on the streamflow in the Yadot watershed, Genale Dawa basin, Ethiopia. Journal of Water and Climate Change, jwc2024404.

Abeysingha, N. S., Singh, M., Sehgal, V. K., Khanna, M., Pathak, H., Jayakody, P., & Srinivasan, R. (2015). Assessment of water yield and evapotranspiration over 1985 to 2010 in the Gomti River basin in India using the SWAT model. Current science, 2202-2212.

Abiola, S., Mohd-Mokhtar, R., Ismail, W., Mohamad, N., & Mandeep, J. S. 2013 Categorical statistical approach to satellite retrieved rainfall data analysis in Nigeria. 8(43), 2123–2137. https://doi.org/10.5897/SRE2013.5512.

Abouabdillah A, Oueslati O, De Girolamo AM, Lo Porto A (2010) Modelin the impact of climate change in a Mediterranean catchment (Merguellil, Tunisia). Fresenius Environ Bull 19(10a):2334–2347.

Abraham, T., Abate, B., Woldemicheal, A. & Muluneh, A. 2018. Impacts of climate change under CMIP5 RCP scenarios on the hydrology of Lake Ziway catchment, central rift valley of Ethiopia. Journal of Environment and Earth Science 8 (7), 2224–3216. Available from: www.iiste.org. ISSN ISSN 2225-0948.

Addis, H. K., Strohmeier, S., Ziadat, F., Melaku, N. D., & Klik, A. (2016). Modeling streamflow and sediment using SWAT in Ethiopian Highlands. International Journal of Agricultural and Biological Engineering, 9(5), 51-66.

Aghakouchak, A., & Mehran, A. 2013 Extended contingency table: Performance metrics for satellite observations and climate model simulations. Water Resources Research, 49(10), 7144–7149. https://doi.org/10.1002/wrcr.20498.

Alehu, B. A., Desta, H. B., & Daba, B. I. (2022). Assessment of climate change impact on hydro-climatic variables and its trends over Gidabo Watershed. Modeling Earth Systems and Environment, 8(3), 3769-3791.

Al-Hasani, I.; Al-Qinna, M.; Hammouri, N.A. Potential Impacts of Climate Change on Surface Water Resources in Arid Regions Using Downscaled Regional Circulation Model and Soil Water Assessment Tool, a Case Study of Amman-Zerqa Basin, Jordan. Climate 2023, 11, 51. https://doi.org/10.3390/cli11030051.

Alim, N., Tarigan, S. D., Baskoro, D. P. T., & Wahjunie, E. D. (2018). Parameter sensitivity test of SWAT hydrological model on two different resolutions (a case study of upper Cisadane subbasin, West Java). Journal of Tropical Soils, 23(1), 47-53.

Anil, S., P, A. R., & Vema, V. K. (2024). Catchment response to climate change under CMIP6 scenarios: a case study of the Krishna River Basin. Journal of Water and Climate Change, 15(2), 476-498.

Aragaw , H. M, Manmohan Kumar Goel & Surendra Kumar Mishra (2021). Hydrological responses to human induced land use/land cover changes in the Gidabo River basin, Ethiopia, Hydrological Sciences Journal, 66:4, 640-655, DOI: 10.1080/02626667.2021.1890328.

Aragaw , H. M, Surendra Kumar Mishra and Manmohan Kumar Goel (2023). Assessing the impact of climate change on the hydrology of Gidabo river sub-basin, Ethiopian Rift Valley Lakes Basin, Sustainable Water Resources Management, 9:65, https://doi.org/10.1007/s40899-023-00858-7.

Arnold, J. G., Moriasi, D. N., Gassman, P. W., Abbaspour, K. C., White, M. J., Srinivasan, R., Santhi, C.,

Harmel, R., Van Griensven, A. & Van Liew, M. W. 2005 SWAT: Model use, calibration, and validation. Transactions of the ASABE 55 (4), 1491–1508.

Arnold, J.G.; Kiniry, J.R.; Srinivasan, R.; Williams, J.R.; Haney, E.B.; Neitsch, S.L. Soil and Water Assessment Tool,Input/Output Documentation Version 2012. Texas Water Resources Institute TR-439. sn. 2012. Available online: https://swat.tamu.edu/media/ 69296/swat-io-documentation-2012. (accessed on 1 January 2018).

Ashine, E.T , & Bedane, M.T. (2022). Most Sensitive Parameters of Soil and Water Assessment Tool (SWAT) Hydrological Model: A Review. Advances in Oceanography & Marine Biology ISSN: 2687-8089, http://dx.doi.org/10.33552/AOMB.2022.02.000558.

Ashraf Vaghefil S, Mousavil SJ, Abbaspour KC, Srinivasan R, Yang H (2013) Analyses of the impact of climate change on water resources components, drought and wheat yield in semiarid regions: Karkheh River Basin in Iran. Hydrol Proces (Online pre-publication) doi: 10.1002/hyp.9747.

Assfaw, M. T., Neka, B. G., & Ayele, E. G. (2023). Modeling the impact of climate change on streamflow responses in the Kessem watershed, Middle Awash sub-basin, Ethiopia. Journal of Water and Climate Change, 14(12), 4837-4859.

Atlas (Climate Change Adaptation, Thought Leadership and Assessments)., 2015. Climate Variability and Change in Ethiopia; Technical Report; Ask Order No. AID-OAA-I-14-00013, under the Restoring the Environment through Prosperity, Livelihoods, and Conserving Ecosystems (REPLACE) IDIQ; United States Agency for International Development: Washington, DC, USA.

Ayehu, G. T., Tadesse, T., Awoke, B. G., Dinku, T., & Gessesse, B. 1921. Validation of new satellite rainfall products over the Upper Blue Nile Basin, Ethiopia Satellite Images for Drought Monitoring View project Climate informed malaria prevention, control and elimination View project Validation of new satellite rainfall products over the Upper Blue Nile Basin, Ethiopia. Atmos. Meas. Tech, 11. https://doi.org/10.5194/amt-2017-294

Ayugi, B.; Zhihong, J.; Zhu, H.; Ngoma, H.; Babaousmail, H.; Rizwan, K.; Dike, V. Comparison of CMIP6 and CMIP5 Models in Simulating Mean and Extreme Precipitation over East Africa. Int. J. Climatol. 2021, 41, 6474–6496.

Ayyad, S. and Khalifa, M. (2021) Will the Eastern Nile Countries Be Able to Sustain Their Crop Production by 2050? An Outlook from Water and Land Perspectives. Science of the Total Environment, 775, Article ID: 145769. https://doi.org/10.1016/j.scitotenv.2021.145769. ***not cited***

Balcha, S. K., Hulluka, T. A., Awass, A. A., & Bantider, A. (2022a). Performance evaluation of multiple regional climate models to simulate rainfall in the Central Rift Valley lakes basin of Ethiopia and their selection criteria for the best climate model. Environmental Monitoring and Assessment, 195(7), 888.

Balcha, S. K., Awass, A. A., Hulluka, T. A., Bantider, A., & Ayele, G. T. (2023). Assessment of future climate change impact on water balance components in Central Rift Valley Lakes Basin, Ethiopia. Journal of Water and Climate Change, 14(1), 175-199.

Bates, B., Kundzewicz, Z., & Wu, S. (2008). Climate change and water. Intergovernmental Panel on Climate Change Secretariat.

Bayissa, Y., Tadesse, T., Demisse, G., & Shiferaw, A. 2017 Evaluation of satellite-based rainfall estimates and application to monitor meteorological drought for the Upper Blue Nile Basin, Ethiopia. Remote Sensing, 9(7). https://doi.org/10.3390/rs9070669.

Bekele, W. T., Abate, A. T. & Rientjes, T. 2021 Impact of climate change on the streamflow of the Arjo Didessa catchment under RCP scenarios. J. Water Clim. Change. 12, 1–13. doi:10.2166/wcc.2021.307.

Bekele, S., & Brook, A. (2021). Estimation of sediment yield using swat model: A case of soke River watershed, Ethiopia. International Journal of Engineering Research and Technology, 20, 2291-2300.

Borrelli, P., Robinson, D. A., Panagos, P., Lugato, E., Yang, J. E., Alewell, C., ... & Ballabio, C. (2020).

Land use and climate change impacts on global soil erosion by water (2015-2070). Proceedings of the National Academy of Sciences, 117(36), 21994-22001.

Botchkarev, A. 2019 Performance Metrics (Error Measures) in Machine Learning Regression, Forecasting and Prognostics: Properties and Typology. 2018, 1–37. http://arxiv.org/abs/1809.03006.

Cattani, E., Merino, A., & Levizzani, V. (2016). Evaluation of monthly satellite-derived precipitation products over East Africa. Journal of Hydrometeorology, 17(10), 2555–2573. https://doi.org/10.1175/JHM-D-15- 0042.1.

Chakilu, G. G., Sándor, S., Zoltán, T., & Phinzi, K. (2022). Climate change and the response of streamflow of watersheds under the high emission scenario in Lake Tana sub-basin, upper Blue Nile basin, Ethiopia. Journal of Hydrology: Regional Studies, 42, 101175.

Chow V. T., Maidment D. R. and Mays L. W.(1988). Applied hydrology. New York: McGraw College of Tropical and Human Resources, University of Hawaii-Manoa, Honolulu, HI,USA.

Daba, M. H., & You, S. (2020). Assessment of climate change impacts on river flow regimes in the upstream of Awash Basin, Ethiopia: based on IPCC fifth assessment report (AR5) climate change scenarios. Hydrology, 7(4), 98.

Daniel, H. (2023). Performance assessment of bias correction methods using observed and regional climate model data in different watersheds, Ethiopia. Journal of Water and Climate Change.

Daniel, H., & Abate, B. (2022). Effect of climate change on streamflow in the Gelana watershed, Rift valley basin, Ethiopia. Journal of Water and Climate Change, 13(5), 2205-2232.

Dibaba, W. T., Miegel, K. & Demissie, T. A. 2019 Evaluation of the CORDEX regional climate models performance in simulating climate conditions of two catchments in Upper Blue Nile Basin. Dynamics of Atmospheres and Oceans.

Dibaba, W. T., Demissie, T. A. & Miegel, K. 2020 Watershed hydrological response to combined land use/land cover and climate change in highland Ethiopia: Finchaa catchment. Water (Switzerland) 12 (6). https://doi.org/10.3390/w12061801.

Dwarakish, G.S. & B.P. Ganasri | (2015) Impact of land use change on hydrological systems: A review of current modeling approaches, Cogent Geoscience, 1:1, 1115691, DOI: 10.1080/23312041.2015.1115691.

Eawag, Dübendorf. (2015). SWAT-CUP: SWAT calibration and uncertainty programs—A User Manual, Switzerland, 16-70.Emiru et al. 2022).

Emiru, N. C., Ayal, D. Y., Kebede, H. Y., Belay, A., & Mekuyie, M. (2022). Climate variability and indigenous adaptation strategies by Somali pastoralists in Ethiopia.

Endris H. S., P. Omondi, S. Jain et al., "Assessment of the performance of CORDEX regional climate models in simulating east African rainfall," Journal of Climate, vol. 26, no. 21, pp. 8453–8475, 2013.

Fang, G. H., Yang, J., Chen, Y. N., & Zammit, C. (2015). Comparing bias correction methods in downscaling meteorological variables for a hydrologic impact study in an arid area in China. Hydrology and Earth System Sciences, 19(6), 2547-2559.

Fao, F. A. O. S. T. A. T. (2018). Food and agriculture organization of the United Nations. Rome, URL: http://faostat. fao. org, 403-403.

Feyissa, T.A.; Demissie, T.A.; Saathoff, F.; Gebissa, A. Evaluation of General Circulation Models CMIP6 Performance and Future Climate Change over the Omo River Basin, Ethiopia. Sustainability 2023, 15, 6507. https://doi.org/ 10.3390/su15086507.

Flato, G.; Marotzke, J.; Abiodun, B.; Braconnot, P.; Chou, S.C.; Collins, W.; Cox, P.; Driouech, F.; Emori, S.; Eyring, V.; et al. Climate change 2006: The physical science basis. In Contribution of Working Group I to the Fifth Assessment Report of the Intergovernmental Panel on Climate Change; Cambridge University Press: Cambridge,UK,2014.

Flato, G., Marotzke, J., Abiodun, B., Braconnot, P., Chou, S. C., Collins, W., ... & Rummukainen, M.

(2014). Evaluation of climate models. In Climate change 2013: the physical science basis. Contribution of Working Group I to the Fifth Assessment Report of the Intergovernmental Panel on Climate Change (pp. 741-866). Cambridge University Press.

Funk, C., Peterson, P., Landsfeld, M., Pedreros, D., Verdin, J., Shukla, S., Husak, G., Rowland, J., Harrison, L., Hoell, A., & Michaelsen, J. 2015b The climate hazards infrared precipitation with stations - A new environmental record for monitoring extremes. Scientific Data, 2. https://doi.org/10.1038/sdata.2015.66.

Gebrechorkos, S. H., Hülsmann, S., & Bernhofer, C. (2019). Regional climate projections for impact assessment studies in East Africa. Environmental Research Letters, 14(4), 044031.

Gebretsadkan, K. N., Tamrie, M. B., & Desta, H. B. (2023). Performance evaluation of multi-satellite rainfall products in the Gidabo catchment, Rift Valley Basin, Ethiopia. Journal of Water and Climate Change, 14(11), 3950-3966.

Geleta, C. D. & Gobosho, L. 2018 Climate change induced temperature prediction and bias correction in Finchaa watershed. AmericanEurasian Journal of Agricultural & Environmental Sciences 18 (6), 324–337. https://doi.org/10.5829/idosi.aejaes.2018.324.337.

Geleta, T. D., Dadi, D. K., Funk, C., Garedew, W., Eyelade, D., & Worku, A. (2022). Downscaled climate change projections in urban centers of Southwest Ethiopia using CORDEX Africa simulations. Climate, 10(10), 158.

Getahun, Y.S.; van Lanen, I.H.; Torfs, P.P. Impact of Climate Change on Hydrology of the Upper Awash River Basin (Ethiopia): Inter-comparison of Old SRES and New RCP Scenarios. Ph.D. Thesis, Wageningen University, Wageningen, The Netherlands, 2014.

Ghorbanian, A., Mohammadzadeh, A., Jamali, S., & Duan, Z. 2022 Performance Evaluation of Six Gridded Precipitation Products throughout Iran Using Ground Observations over the Last Two Decades (2000–2020). Remote Sensing, 14(15). https://doi.org/10.3390/rs14153783.

Golmohammadi, G., Prasher, S., Madani, A., & Rudra, R. (2014). Evaluating three hydrological distributed watershed models: MIKE-SHE, APEX, SWAT. Hydrology, 1(1), 20-39.

Gunathilake, M. B., Amaratunga, Y. V., Perera, A., Chathuranika, I. M., Gunathilake, A. S. & Rathnayake, U. 2020 Evaluation of future climate and potential impact on streamflow in the Upper Nan River Basin of Northern Thailand. Advances in Meteorology 2020. https:// doi.org/10.1155/2020/8881118.

Haile, A. T., Akawka, A. L., Berhanu, B. & Rientjes, T. 2017 Changes in water availability in the Upper Blue Nile basin under the representative concentration pathways scenario. Hydrological Sciences Journal 62 (13), 2139–2149. doi:10.1080/02626667.2017. 1365149.

Hammouri, N., Adamowski, J., Freiwan, M., & Prasher, S. (2017). Climate change impacts on surface water resources in arid and semi-arid regions: a case study in northern Jordan. Acta Geodaetica et Geophysica, 52, 141-156.

Hanjra, M.A., Ferede, T., Gutta, D.G., 2009. Pathways to breaking the poverty trap in Ethiopia: investments in agricultural water, education, and markets. Agric. Water Manag. 96, 1596–1604.

Hargreaves, G. H., & Samani, Z. A. (1985). Reference crop evapotranspiration from temperature. Applied engineering in agriculture, 1(2), 96-99.

IPCC, 2014: Climate Change 2014: Synthesis Report. Contribution of Working Groups I, II and III to the Fifth Assessment Report of the Intergovernmental Panel on Climate Change [Core Writing Team, R.K. Pachauri and L.A. Meyer (eds.)]. IPCC, Geneva, Switzerland, 151 pp.

IPCC, 2007: Climate Change 2007: Impacts, Adaptation and Vulnerability. Contribution of Working Group II to the Fourth Assessment Report of the Intergovernmental Panel on Climate Change, M.L. Parry, O.F. Canziani, J.P. Palutikof, P.J. van der Linden and C.E. Hanson, Eds., Cambridge University Press, Cambridge, UK, 976pp.

IPCC, 2018: Global warming of 1.5°C. An IPCC Special Report on the impacts of global warming,

sustainable development,[V. Masson-Delmotte, P. Zhai, H. O. Pörtner, D. Roberts, J. Skea, P.R. Shukla, A. Pirani, W. Moufouma-Okia, C. Péan, R. Pidcock, S. Connors, J. B. R. Matthews, Y. Chen, X. Zhou, M. I. Gomis, E. Lonnoy, T. Maycock, M. Tignor, T. Waterfield (eds.)]. In Press.

IPCC, 2000 – Nebojsa Nakicenovic and Rob Swart (Eds.) Cambridge University Press, UK. pp 570 Available from Cambridge University Press, The Edinburgh Building Shaftesbury Road, Cambridge CB2 2RU ENGLAND.

Kannan, N., White, S. M., Worrall, F., & Whelan, M. J. (2007). Hydrological modelling of a small catchment using SWAT-2000–Ensuring correct flow partitioning for contaminant modelling. Journal of Hydrology, 334(1-2), 64-72.

Khoi, K.D., Nguyen, V. T., Thao Sam, T., & Thao Nhi, P. T. (2019). Evaluation on effects of climate and land-use changes on streamflow and water quality in the La Buong River Basin, Southern Vietnam. Sustainability, 11(24), 7221.

Kim, J., Waliser, D. E., Mattmann, C. A., Goodale, C. E., Hart, A. F., Zimdars, P. A., Crichton, D. J., Jones, C., Nikulin, G., Hewitson, B., Jack, C., Lennard, C. & Favre, A. 2014 Evaluation of the CORDEX-Africa multi-RCM hindcast: systematic model errors. Climate Dynamics 42 (5–6), 1189–1202. https://doi.org/10.1007/s00382-013-1751-7.

Kimani, M. W., Hoedjes, J. C. B., & Su, Z. 2017 An assessment of satellite-derived rainfall products relative to ground observations over East Africa. Remote Sensing, 9(5). https://doi.org/10.3390/rs9050430.

Kishiwa, P., Nobert, J., Kongo, V., & Ndomba, P. (2018). Assessment of impacts of climate change on surface water availability using coupled SWAT and WEAP models: case of upper Pangani River Basin, Tanzania. Proceedings of the International Association of Hydrological Sciences,378,23-27.

Koch, M., & Cherie, N. (2013, June). SWAT-modeling of the impact of future climate change on the hydrology and the water resources in the upper blue Nile river basin, Ethiopia. In Proceedings of the 6th international conference on water resources and environment research, ICWRER (Vol. 6, No. 6, pp. 488-523).

Kour, R.; Patel, N.; Krishna, A.P. Climate and hydrological models to assess the impact of climate change on hydrological regime: A review. Arab. J. Geosci. 2016, 9, 1–31.

Kuma, H. G., Feyessa, F. F. & Demissie, T. A. 2021 Hydrologic responses to climate and land-use/land cover changes in the Bilate catchment, Southern Ethiopia. Journal of Water and Climate Change 12 (8), 3750–3769. https://doi.org/10.2166/wcc.2021.281.

Legesse, S., Tadele, K. & Mariam, B. G. 2015 Potential impacts of climate change on the hydrology and water resources availability of Didessa catchment, Blue Nile River Basin, Ethiopia. 04 (01), 1–7. https://doi.org/10.4172/2329-6755.1000193.

Leng, M., Yu, Y., Wang, S., & Zhang, Z. (2020). Simulating the hydrological processes of a meso-scale watershed on the Loess Plateau, China. Water, 12(3), 878.

Lennard, C & Nikulin, G.(2015). The 2nd CORDEX Africa Analysis Campaign; Phase 2, CORDEX Africa Analysis Workshop, November 2015, Cape Town.

Liemohn, M. W., Shane, A. D., Azari, A. R., Petersen, A. K., Swiger, B. M., & Mukhopadhyay, A. (2021). RMSE is not enough: Guidelines to robust data-model comparisons for magnetospheric physics. Journal of Atmospheric and SolarTerrestrial Physics, 218, 105624.

Liersch, S., Tecklenburg, J., Rust, H., Dobler, A., Fischer, M., Kruschke, T., Koch, H., Hattermann, F.F., 2018. Are we using the right fuel to drive hydrological models? A climate impact study in the Upper Blue Nile. Hydrol. Earth Syst. Sci. 22, 2163–2185.

Lindner, M., Maroschek, M., Netherer, S., Kremer, A., Barbati, A., Garcia-Gonzalo, J., ... & Marchetti, M. (2010). Climate change impacts, adaptive capacity, and vulnerability of European forest ecosystems. Forest ecology and management, 259(4), 698-709.

LIU, F.; Xu, C.; Long, Y.; Yin, G.; Wang, H. Assessment of CMIP6 Model Performance for Air Temperature in the Arid Region of Northwest China and Subregions. Atmosphere 2022, 13, 454.

Lopez, M. G., Wennerström, H., Nordén, L.-Å. & Seibert, J. 2015 Location and density of rain gauges for the estimation of spatial varying. Source: Geografiska Annaler. Series A 97 (1).

Lukas, P.; Melesse, A.M.; Kenea, T.T. Prediction of Future Land Use/Land Cover Changes Using a Coupled CA ANN Model in the Upper Omo–Gibe River Basin, Ethiopia. Remote Sens. 2023, 15, 1148.

Luo, K., Tao, F., Moiwo, J. P. & Xiao, D. 2016 Attribution of hydrological change in Heihe River Basin to climate and land use change in the past three decades. Scientific Reports 6, 33704. https://doi.org/10.1038/srep33704.

Makar, R.S.; Shahin, S.A.; El-Nazer, M.; Wheida, A.; Abd El-Hady, M. (2022). Evaluating the Impacts of Climate Change on Irrigation Water Requirements. Sustainabilit 2022, 14, 14833. https://doi.org/10.3390/su142214833

Masson-Delmotte, V. et al. 2018 Special report 1.5 —Summary for policymakers. In: An IPCC Special Report on the impacts of global warming of 1.5 o C above pre-industrial levels.

Mengistu, D., Bewket, W., Dosio, A., & Panitz, H. J. (2021). Climate change impacts on water resources in the upper blue nile (Abay) river basin, ethiopia. Journal of Hydrology, 592, 125614.

Mollel, G. R., Mulungu, D. M., Nobert, J., & Alexander, A. C. (2023). Assessment of climate change impacts on hydrological processes in the Usangu catchment of Tanzania under CMIP6 scenarios. Journal of Water and Climate Change, 14(11), 4162-4182.

Monteith, J. L. (1965). Evaporation and environment. In Symposia of the society for experimental biology (Vol. 19, pp. 205-234). Cambridge University Press (CUP) Cambridge.

MoWIE, Ministry of Water Resource, Irrigation and Electricity. 2018. The Ethiopian Government Water Resources Planning and Management, Department of Water Resources and Energy, Section; GIS, Addis Ababa: Ethiopia.

Mugo, J. W., Opijah, F. J., Ngaina, J., Karanja, F., & Mburu, M. W. (2020). Rainfall variability under present and future climate scenarios using the Rossby center Bias-corrected regional climate model.

Negewo, T. F., & Sarma, A. K. (2021). Spatial and temporal variability evaluation of sediment yield and sub basins/hydrologic response units prioritization on Genale Basin, Ethiopia. Journal of Hydrology, 603, 127190.

Negewo, T. F., & Sarma, A. K. (2022). Estimation of Water Yield under Baseline and Future Climate Change Scenarios in Genale Watershed, Genale Dawa River Basin, Ethiopia, Using SWAT Model. Journal of Hydrologic Engineering, 26(3), 05020051."

Neitsch SL, Arnold JG, Kiniry JR, Srinivasan R, Williams JR (2005) Soil and Water Assessment Tool Theoretical Documentation, Version 2005. Temple: Grassland, Soil and Water Research Laboratory, Agricultural Research Service.Nikulin et al. 2012.

Neway, K.G, Zewdie, M.B. 2020. Dam Breach Analysis And Downstream Damage Assessment using HEC-RAS and HEC-FIA: A Case Study of Gerhu-Sirnay Dam, Northern Ethiopia. MSc. Thesis, Hawassa University, Hawassa, Ethiopia.

Niang, A., Becker, M., Ewert, F., Dieng, I., Gaiser, T., Tanaka, A.,& Saito, K. (2014). Variability and determinants of yields in rice production systems of West Africa. Field Crops Research, 207,1-12.

Nigatu, Z. M., Rientjes, T. & Haile, A. T. 2016 Hydrological impact assessment of climate change on Lake Tana's water balance, Ethiopia. American Journal of Climate Change 05 (01), 27–37.

Nikulin, G., Jones, C., Giorgi, F., Asrar, G., Büchner, M., Cerezo-Mota, R., ... & Sushama, L. (2012). Precipitation climatology in an ensemble of CORDEX-Africa regional climate simulations. Journal of Climate, 25(18), 6057-6078.

NMA, National Meteorological Agency. 2018. The Ethiopian meteorological agency, Department of meteorology, Addis Ababa: Ethiopia

Noreika, N., Winterová, J., Li, T., Krása, J., & Dostál, T. (2021). The small water cycle in the Czech

landscape: How has it been affected by land management changes over time?. Sustainability, 13(24), 13757.

Osima, S., Indasi, V.S., Zaroug, M., Endris, H.S., Gudoshava, M., Misiani, H.O., Nimusiima, A., Anyah, R.O., Otieno, G., Ogwang, B.A., 2018. Projected climate over the Greater Horn of Africa under 1.5 C and 2 C global warming. Environ. Res. Lett. 13, 065004.

Panja, A., Garai, S., Zade, S. S., & Sahani, S. (2023). Climate Data Extraction for Social Science Research: A Step by Step Process. Social Science Dimensions of Climate Resilient Agriculture.

Pelletier, J. D. et al. (2015), Forecasting the response of Earth's surface to future climatic and land use changes: A review of methods and research needs, Earth's Future, 3, 220–251, doi:10.1002/2014EF000290.

Petpongpan, C., Ekkawatpanit, C., & Kositgittiwong, D. (2020). Climate change impact on surface water and groundwater recharge in Northern Thailand. Water, 12(4), 1029.

Piao, S., Ciais, P., Huang, Y., Shen, Z., Peng, S., Li, J., ... & Fang, J. (2010). The impacts of climate change on water resources and agriculture in China. Nature, 467(7311), 43-51.

Priestley, C. H. B., & Taylor, R. J. (1972). On the assessment of surface heat flux and evaporation using large-scale parameters. Monthly weather review, 100(2), 81-92.

Rahvareh, M., Motamedvaziri, B., Moghaddamnia, A., & Moridi, A. (2023). Modeling runoff management strategies under climate change scenarios using hydrological simulation in the Zarrineh River Basin, Iran. Journal of Water and Climate Change.

Saade, J.; Atieh, M.; Ghanimeh, S.; Golmohammadi, G. Modeling Impact of Climate Change on Surface Water Availability Using SWAT Model in a Semi-Arid Basin: Case of El Kalb River, Lebanon. Hydrology 2021, 8, 134. https:// doi.org/10.3390/hydrology8030134.

Sahu, M., Lahari, S., Gosain, A. K., & Ohri, A. (2016). Hydrological modeling of Mahi basin using SWAT. Journal of Water Resource and Hydraulic Engineering, 5, 68-79.

Shanka, A. S. (2017). Evaluation of climate change impacts on run-off in the Gidabo River Basin: Southern Ethiopia. Environment Pollution and Climate Change, 1(03), 1-6.

Shigute, M., Alamirew, T., Abebe, A., Ndehedehe, C. E., & Kassahun, H. T. (2022). Understanding hydrological processes under land use land cover change in the upper Genale River Basin, Ethiopia. Water, 14(23), 3881.

Stella C. Rotich, Deogratias M. M. Mulungu (2017). Adaptation to climate change impacts on crop water requirements in Kikafu catchment, Tanzania. Journal of Water and Climate Change 1 June 2017; 8 (2): 274–292. https://doi.org/10.2166/wcc.2017.058.

Strahler A. (1957). Quantitative Analysis of Watershed geomorphology. Transactions of American Geo physical Union 38:913-920.

Takele, G. S., Gebrie, G. S., Gebremariam, A. G., & Engida, A. N. (2022). Future climate change and impacts on water resources in the Upper Blue Nile basin. Journal of Water and Climate Change, 13(2), 908-925.

Tamoffo, A. T., Moufouma-Okia, W., Dosio, A., James, R., Pokam, W. M., Vondou, D. A., ... & Nouayou, R. (2019). Process-oriented assessment of RCA4 regional climate model projections over the Congo Basin under 1.5 ∘ C 1.5∘ C and 2 ∘ C 2∘ C global warming levels: influence of regional moisture fluxes. Climate Dynamics, 53, 1911-1935.

Taye, M.; Dyer, E.; Hirpa, F.; Charles, K. Climate change impact on water resources in the Awash basin, Ethiopia. Water 2018, 10, 1560. [CrossRef

Taylor, K. E. 2001 Summarizing multiple aspects of model performance in a single diagram. Journal of Geophysical Research Atmospheres, 106(D7), 7183–7192. https://doi.org/10.1029/2000JD900719.

Tessema, N., Kebede, A., & Yadeta, D. (2020). Modelling the effects of climate change on streamflow using climate and hydrological models: the case of the Kesem sub-basin of the Awash River basin, Ethiopia. International Journal of River Basin Management, 19(4), 469-480.

Teutschbein, C. & Seibert, J. 2012 Bias correction of regional climate model simulations for hydrological

climate-change impact studies: review and evaluation of different methods. Journal of Hydrology 456–457, 12–29. https://doi.org/10.1016/j.jhydrol.2012.05.052.

Tibangayuka, N., Mulungu, D. M., & Izdori, F. (2022). Assessing the potential impacts of climate change on streamflow in the data-scarce Upper Ruvu River watershed, Tanzania. *Journal of Water and Climate Change*, *13*(9), 3496-3513.

Tilahun ZA, Bizuneh YK, Mekonnen AG (2023) The impacts of climate change on hydrological processes of Gilgel Gibe catchment, southwest Ethiopia. PLoS ONE 18(6): e0287314. https://doi.org/10.1371/journal.pone.0287314.

Tufa, F. G., & Sime, C. H. (2020). Stream flow modeling using SWAT model and the model performance evaluation in Toba sub-watershed, Ethiopia. Modeling Earth Systems and Environment, 7(4), 2653-2665.

Tumsa, Chelkeba, B. (2022). Statistical and SWAT Model-Based Performance Evaluation of RCMs in Modeling Streamflow and Sediment Yield at Upper Awash Sub-Basin, Ethiopia. Applied & Environmental Soil Science.

Ukumo, T. Y., Edamo, M. L., Abdi, D. M., & Derebe, M. A. (2022). Evaluating water availability under changing climate scenarios in the Woybo catchment, Ethiopia. Journal of Water and Climate Change, 13(11), 4130-4149.

Wang Z, Ficklin DL, Zhang Y, Zhang M (2012) Impact of climate change on streamflow in the arid Shiyang River Basin of northwest China. Hydrol Proces 26(18):2733–2744. doi:10.1002/hyp.8378.

Wang, M., Shao, Y., Jiang, Q. O., Xiao, L., Yan, H., Gao, X., Wang, L. & Liu, P. 2014 Impacts of climate change and human activity on the runoff changes in the Guishui River Basin. Land 9 (9), 291. https://doi.org/10.3390/land9090291.

Wijesekera and Perera, T. a. 2012 Study on Key Issues of Data and Data Checking for Hydrological Analyses (case study of Attanagalu Oya Basin of Sri Lanka). xxxxv: p2.

Woldemeskel, F. M., Sivakumar, B., & Sharma, A. 2013 Merging gauge and satellite rainfall with specification of associated uncertainty across Australia. Journal of Hydrology, 499, 167-176.

World Food Programme. Status of Drought across the Eastern Horn; World Food Programme: Rome, Italy, 2022.

Worqlul, A. W., Dile, Y. T., Ayana, E. K., Jeong, J., Adem, A. A., & Gerik, T. (2018). Impact of climate change on streamflow hydrology in headwater catchments of the Upper Blue Nile Basin, Ethiopia. Water, 10(2), 120.

Xu, Hou, Z., Han, Y., & Guo, W. 2016 A diagram for evaluating multiple aspects of model performance in simulating vector fields. Geoscientific Model Development, 9(12), 4365–4380. https://doi.org/10.5194/gmd-9-4365-2016.

Xu, J., Ma, Z., Tang, G., Ji, Q., Min, X., Wan, W., & Shi, Z. 2019a Quantitative evaluations and error source analysis of fengyun-2-based and gpm-based precipitation products over mainland China in summer, 2018. Remote Sensing, 11(24). https://doi.org/10.3390/rs11242992.

Xu, J., Ma, Z., Tang, G., Ji, Q., Min, X., Wan, W., & Shi, Z. 2019b Quantitative evaluations and error source analysis of fengyun-2-based and gpm-based precipitation products over mainland China in summer, 2018. Remote Sensing, 11(24). https://doi.org/10.3390/rs11242992.

Yesuf, H., Assen, M., Alamirew, T. & Melesse, A. 2015 Modeling of sediment yield in Maybar gauged watershed using SWAT, northeast Ethiopia. CATENA 127. https://doi.org/10.1016/j.catena.2014.12.032.

Zhang H, Wang B, Liu D L, Zhang M X, Leslie L M, Yu Q (2018). Using an improved SWAT model to simulate hydrological responses to land use change: a case study of a catchment in tropical Australia. J Hydrol (Amst), 585:

Zhao, F., Wu, Y., Qiu, L., Sun, Y., Sun, L., Li, Q., Niu, J. & Wang, G. 2018 Parameter uncertainty analysis of the SWAT model in a mountain loess transitional watershed on the Chinese Loess Plateau. Water (Switzerland), 10 (6), 1–16.

Zhou, Q., Chen, D., Hu, Z., & Chen, X. 2021 Decompositions of Taylor diagram and DISO performance criteria. International Journal of Climatology, 41(12), 5726–5732. https://doi.org/10.1002/joc.7149.https://doi.org/10.3390/w10060690.

APPENDIXES

Appendix I: Daily maximum of each and across stations, and annual maximum precipitation of all stations

Year	Daily max rainfall (mm) each station			Daily max rainfall (mm) across stations	Annual rainfall (mm)
	May-dingur	Enticho	Gerhu-Sirnay		
1990	67.8	78.4	51.5	78.4	616.5
1991	56.5	126.5	61.2	126.5	837.1
1992	76	38.3	61.5	76	854.8
1993	39.7	42.7	48.3	48.3	642.7
1994	54.6	53.6	30.5	54.6	805.9
1995	40.9	42	36.2	42	446.4
1996	54.1	37.5	22.6	54.1	703.9
1997	35.2	45.4	70.7	70.7	662.7
1998	84.4	169	15.1	169	872.1
1999	80.6	45.1	38.4	80.6	665.6
2000	52.5	25.3	43.275	52.5	726.2
2001	150.5	56	43.9	150.5	910.6
2002	28.7	75.6	60.3	75.6	589.0
2003	40.8	54.5	69	69	716.1
2004	45.7	93	85.4	93	629.5
2005	34.7	26	72.325	72.325	747.3
2006	84.9	48	61	84.9	657.7
2007	68.2	55	74.0625	74.0625	923.2
2008	37.6	30.1	59.6	59.6	642.3
2009	44.5	96.5	100.74	100.74	594.9
2010	72.6	43.2	73.1	73.1	596.1
2011	41.8	38	70.15	70.15	730.7
2012	61.2	45	30.5	61.2	623.2
2013	71	50	68.03	71	551.8
2014	55.5	35.2	43.43	55.5	569.9
2015	30	45	56.3	56.3	391.0
2016	55	60.3	24.2	60.3	525.7

2017	56	35.2	55.6	56	887.3
2018	58.4	58.4	54.9	58.4	557.0

Appendix II: Constant Number Kn, for a Function of Precipitation Series Size, n

Sample Size, n	Kn	Sample Size, n	Kn	Sample Size, n	Kn	Sample Size, n	Kn	Sample Size, n	Kn
10	2.036	21	2.408	32	2.591	43	2.71	70	2.893
11	2.088	22	2.429	33	2.604	44	2.719	75	2.917
12	2.134	23	2.448	34	2.616	45	2.727	80	2.94
13	2.175	24	2.467	35	2.628	46	2.736	85	2.961
14	2.213	25	2.486	36	2.639	47	2.744	90	2.981
15	2.247	26	2.502	37	2.65	48	2.753	95	3
16	2.279	27	2.519	38	2.661	49	2.76	100	3.017
17	2.309	28	2.534	39	2.671	50	2.768	110	3.049
18	2.335	29	2.549	40	2.682	55	2.804	120	3.078
19	2.361	30	2.563	41	2.692	60	2.837	130	3.104
20	2.385	31	2.577	42	2.7	65	2.866	140	3.129

Appendix-III; Rainfall (mm) datasets of the observed areal and 7CORDEX-RCA4 model

Maximum-reference (Areal-Observed)	**NorESM1-M**	**MPI-M-MPI-ESM-LR**	**MIROC-MIROC5**	**ICHEC-EC-EARTH**	**GFDL-ESM2M**	**CNRM-CERFACS-CM5**	**CCCma-CanESM2**
14.28	1.96	4.08	2.79	2.8	2.7	3.16	2.92
2.8	2.95	1.62	3.42	1.84	4.06	1.29	1.44
14.77	2.43	2.12	5.11	4.95	2.06	3.98	0.03
13.3	2.83	5.16	7.59	5.56	4.54	1.95	1.24
21.1	2.96	3.65	0	6.95	4.36	10.05	3.37
39.4	0	7.19	6.94	10.94	6.97	0	5.6
170.5	5.75	8.03	20.29	12.44	7.98	12.88	26.62
403.7	0	5.03	15.86	21.33	5.3	6.79	18.75
135.3	0	10.89	8.64	5.7	10.8	4.88	1.04

23.7	2.45	6.27	1.37	2.53	4.01	0.97	0.99
57.3	2.78	7.23	3.49	3.4	2.56	5.1	2.8
3.9	1.55	3.3	3.13	0.92	1.09	0.56	3.45
0	2.55	2.11	3.77	1.94	1.4	2.71	1.92
3.2	0	1.82	0.95	2.3	0	5.44	2
0	1.02	3.39	3.3	6.62	2.04	6.75	0
8.4	0	2.45	2.28	4.37	1.11	2.46	0.6
23.3	0	0	0	4.42	8.27	7.24	1.85
166.6	8.87	9.71	4.71	11.47	10.96	0	0
204.6	19.66	13.85	9.38	22.4	23.19	14.43	10.91
261.7	23.98	6.6	17.19	17.91	12.69	22.98	10.53
33.1	5.34	15.44	2.4	7.27	6.31	13.28	0.62
2.4	5.79	6.85	4.15	0.79	1.08	1.94	1.98
0	1.65	1.93	1.48	4.62	2.95	3.77	5.06
0	1.49	1.73	2.85	0.94	2.75	3.2	1.48
0	0.99	2.44	1.56	1.75	1.44	1.68	3.22
61.67	0	1.56	3.55	1.04	1.69	3.64	4.12
16.53	0	0.69	2.07	5.56	2.11	6.72	0.79
22.6	11.2	7.13	5.19	4.6	9.03	2.79	0
64	12.94	6.56	0	13.17	2	9.69	3.97
26.5	10.19	9.15	0	8.32	6.49	5	7.91
208.6	23.39	11.65	23.41	15.89	19.5	19.21	16.68
313.1	8.64	24.64	0	19.61	25.17	9.99	0
150.4	0	10.54	2.17	6.62	0.91	16.8	0
10.9	2.44	2.85	2.06	3.13	0.53	1.29	2.01
16.7	3.37	1.68	2.15	3.77	1.71	1.71	5.33
3.5	2.69	1.44	1.74	2.67	2.8	0.98	3.06
3.4	3.06	2.71	1.27	2.89	3.19	2.62	0
2.7	0	2.46	2.29	2.92	0	2.61	0
42	3.19	0	1.7	1.23	6.05	3.26	0.79
68.1	7.46	3.54	6.89	5.04	0	4.04	0
61.2	3.23	2.35	1.74	5.38	3.82	0.91	0.47
42.2	5.27	5.7	1.67	9.39	4.39	3.7	8.86
199.2	4.22	15.65	9.17	12.91	15.79	17.59	14.45
176	8.99	2.18	0	9.04	16.98	12.88	0
130.3	3.25	8.55	1.38	13.61	5.73	10.56	1.11
32	2.68	4.33	2.38	1.09	4.89	1.13	1.39
0	3.48	3.41	3.58	2.26	0.47	3.32	2.86
0	2.03	1.95	2.41	2.53	3.94	1.33	3.03
0	1.57	1.98	1.36	3	3.02	2.82	0.96
6	0	2.36	4	1.58	1.24	3.53	0

0	9.12	2.71	3.28	1.16	0.69	5.05	0.75
17	1.65	4.71	1.49	1.51	1.47	5.04	1.82
44.4	0	5.28	5.91	6.9	5.67	6.47	1.29
122.8	7.37	7.13	6.82	0.29	5.53	2.59	5.06
200	13.28	9.06	14.81	16.99	22.4	16.25	8.23
369.8	10.72	13.4	16.41	13.46	13.25	15.36	10.42
132.8	1.38	11.53	3.27	9.68	5.19	9.52	1.83
0	1.46	4	3.82	3.56	1.13	5.23	1.39
17.8	2.08	2.83	2.08	3.59	0.33	1.15	2.56
1	1.22	2.06	1.87	3.08	3.19	1.49	0
0	3.9	2.28	0.94	1.48	2.44	1.4	0
0	0	1.28	3.83	2.99	0.81	1.1	0
30.7	0	2.93	7.81	10.19	8.93	4.53	0
31.8	3.7	0	1.9	8.59	4.6	0.8	0.6
79.5	0	4.12	7.8	3.89	9.4	6.35	1.66
39.6	10.65	10.47	11.47	9.77	3.16	6.36	5.67
213.3	22.62	18.9	17.55	4.37	4.04	13.04	7.95
233.7	0	17.93	15.14	26.21	8.63	16.07	0
174.2	1.75	7.67	2.03	5.45	2.81	5.37	0.32
8.5	2.38	4.36	2.39	2.8	1.93	2.9	0
0	2.06	1.61	0	3.06	4.58	1.1	0
11.2	2.85	2.19	2.4	1.09	2.53	2.71	1.95
13.2	0	1.99	1.29	1.65	1.24	2.01	1.97
0	3.78	2.31	2.02	3.43	0	2.54	0.13
110	2.64	1.81	6.12	4.7	6.63	2.02	1.24
62.6	9.22	5.1	1.4	10.35	14.9	0.67	1.82
97	0	3.92	4.86	13.41	5.62	4.6	0
151.9	4.75	9.14	11.07	4.48	10.91	3.52	1.01
182.8	13.17	30.16	16.04	11.58	23.77	10.78	20.69
243.2	15.08	15.86	6.86	10.91	10.63	12.82	6.28
128.3	1	15.19	4.08	14.11	1.62	10.42	0.17
0	2.66	5	0	1.31	4.98	1.86	2.24
45	1.28	2.56	3.59	1.52	2.83	2.55	3.92
1.6	3.13	2.08	4.21	2.12	1.78	0.35	2.38
0	1.46	2.46	4.16	2.46	2.42	1.17	1.14
0	0	1	1.67	3.33	3.09	2.6	0
32.75	0.06	6.42	13.43	9.08	7.75	7.82	0.12
0	2.43	8.72	0	5.1	2.53	3.37	2.53
76.6	0	7.36	2.49	7.04	3.5	5.23	0.33
88	0.79	6.71	0	8.95	2.47	8.74	2.54
186	21.06	16.33	8.06	0	9.45	12.48	21.6

152.4	19.73	11.75	6.71	12.3	8.55	16.32	6.35
73.73	0.93	12.61	1.17	15.53	10	3.97	0
149.3	2.98	1.22	0	2.34	0	4.99	1.72
30.3	1.98	1.29	0.97	3.55	1.05	1.44	2.49
0	0	1.82	1.72	2.51	2.89	2.61	3.51
0.8	2.4	2.45	2.77	2.33	1.61	2.51	1.42
0	0	2.65	0	3.08	3.24	1.63	0
13.5	1.89	10.9	6.56	6	2.06	6.03	0
3.1	4.49	2.73	0	3.49	5.76	3.68	0.26
46.2	1.53	8	0.48	3.05	7.83	1.61	1.51
104	0	5.51	13.25	13.3	6.03	11.85	19.56
386.7	19.64	15.17	19.63	27.31	19.69	15.54	22.33
360.8	0	6.71	11.98	10.01	18.53	26.51	19.01
121.5	0	10.98	2.92	6.02	2.9	8.39	1.32
17.5	2.01	1.04	5.22	1.63	5.69	0	0
0	3.68	5.64	2.85	3.25	1.85	1.38	1.62
0	2.72	2.34	2.93	3.69	2.63	1.83	3.58
41.9	4.82	2.35	1.8	2.1	1.4	2.3	3.45
0	2.04	1.58	1.13	2.1	2.58	1.24	1
11.9	3.18	7.15	2.78	2.19	3.36	0.67	0
8.6	8.94	2.65	4.23	0.35	4.63	1.79	0
24.9	0	12.29	0	2.08	1.2	0.94	0.45
61.2	2.22	6.92	13.99	0	1.21	8.36	0
274.6	10.84	7.91	8.33	6.17	12.72	27.98	9.99
327.9	5.24	20.59	18.75	18.75	17.75	13.37	6.12
123.3	2.5	7.64	6.87	10.19	3.84	5.3	8.54
43.47	1.36	0.94	1.76	0.44	4.25	4.66	4.86
0	3.76	0.91	4.23	1.9	0.72	0.78	2.6
25.8	1.57	1.82	1.88	2.12	2.73	2.3	1.54
0	1.28	3.03	1.56	2.3	3.21	3.14	1
0	0.75	1.63	2.37	1.37	0	1.83	3.01
1.7	3.33	2.61	0.99	6.96	7.53	3.75	0
91.3	3.97	0	3.4	1.32	8.96	3.02	0
29.5	5.03	2.2	3.19	5.29	6.2	9.25	0.32
33.1	10.06	8.32	1.7	2.88	3.42	0	13.82
183	17.23	16.88	17.93	11.26	19.96	16.73	23.73
215.9	1.58	16.82	20.01	21.31	7.06	16.52	15.19
114.3	0	4.4	5.15	5.23	2.36	9.29	0.82
86.1	2.27	2.42	1.77	0.58	1.03	1.92	0
22.3	2.38	1.75	2.71	3.91	0.81	1.06	3.58
9.5	2.54	0.5	2.99	2.26	1.7	0.92	3.35

0	4.29	1.84	1.34	3.32	1.82	1.43	3.39
0	0	0.91	0	4.68	0	1.98	0
14.9	0.07	5.84	5	1.84	3.88	11.49	0
2.9	0	3.66	2.42	5.21	7.96	2.67	0.44
9.8	0	2.95	1.69	3.3	5.12	7.64	1.9
81.7	3.57	6.3	12.15	6.46	9.08	0.49	21.83
264.6	14.38	9.63	14.41	15.92	6.1	3.56	9.73
430.7	5.52	14.96	17.68	19.18	3.06	11.16	11.27
39.5	0	9.47	8.2	6.42	3.92	6.76	1.18
16.5	1.41	1.59	1.69	4.95	3.06	2.37	3.37
0	3.28	1.87	4.39	4.07	0.69	1.99	3.43
0	2.28	2.95	2.8	2.12	4.03	1.48	3.41

Appendix-IV; Codes applied to draw Taylor diagram in R

```
library(chron)
library(lattice)
library(ggplot2)
library(plotrix)
library(graphics)
ref <-as.numeric(Maximumreference[[1]])
CCCma_CanESM2 <-as.numeric(CCCma_CanESM2[[1]])
CNRM_CERFACS_CM5 <-as.numeric(CNRM_CERFACS_CM5[[1]])
GFDL_ESM2M<-as.numeric(GFDL_ESM2M[[1]])
ICHEC_EC_EARTH <-as.numeric(ICHEC_EC_EARTH[[1]])
NorESM1_M <-as.numeric(NorESM1_M[[1]])
MPI_M_MPI_ESM_LR <-as.numeric(MPI_M_MPI_ESM_LR[[1]])
MIROC_MIROC5 <-as.numeric(MIROC_MIROC5[[1]])
taylor.diagram(ref, CCCma_CanESM2,add=FALSE,col="blue",pch=7,pos.cor=TRUE,
xlab="",ylab="Normalized Standard Deviation",main="Taylor Diagram",
show.gamma=TRUE,ngamma=6,gamma.col=5,sd.arcs=8,
ref.sd=TRUE,sd.method="population",grad.corr.lines=c(0.1,0.2,0.3,0.4,0.5,0.6,0.7,0.8,0.9,0.9
5,0.99,1), pcex=1.8,cex.axis=1,normalize=FALSE,mar=c(4,8,2,8),)
taylor.diagram(ref,CNRM_CERFACS_CM5,add=TRUE,col="black",pch=22,pcex=1.9)
taylor.diagram(ref,GFDL_ESM2M,add=TRUE,col="blue",pch=13,pcex=1.5)
taylor.diagram(ref,ICHEC_EC_EARTH,add=TRUE,col="blue",pch=17,pcex=1.5)
taylor.diagram(ref,NorESM1_M,add=TRUE,col=" black",pch=16,pcex=1.5)
taylor.diagram(ref,MPI_M_MPI_ESM_LR,add=TRUE,col="black",pch=17,pcex=1.5)
taylor.diagram(ref,MIROC_MIROC5,add=TRUE,col=" blue ",pch=16,pcex=1.5)
legend(180,200,cex=0.6,pt.cex=1,legend=c("CCCma_CanESM2","
CNRM_CERFACS_CM5"," GFDL_ESM2M"," ICHEC_EC_EARTH"," NorESM1_M","
MPI_M_MPI_ESM_LR"," MIROC_MIROC5"),pch=c(7,22,13
,17,16,17,16),col=c(4,1,4,4,1,1,4))
```

Appendix-V; Flow data(m^3/s) for the calibration and validation periods

Calibration (1992-1999)			Validation (2000-2003)		
Seasons	Observed	Best Simulation	Date	Observed	Best Simulation
Winter-92	0.3	0.276	Winter-00	0.24	0.1496
Autumn-92	0.5	0.4376	Autumn-00	4.3	2.89578
Summer-92	2.93	3.2798	Summer-00	12.93	11.5096
Spring-92	0.88	0.5559	Spring-00	0.28	0.0691
Winter-93	0.38	0.3533	Winter-01	0.28	0.2347
Autumn-93	0.44	0.5551	Autumn-01	0.76	0.6997
Summer-93	2.74	2.2837	Summer-01	2.39	3.2257
Spring-93	0.9	0.8639	Spring-01	0.32	0.0997
Winter-94	0.29	0.3162	Winter-02	0.12	0.0166
Autumn-94	0.6	0.8262	Autumn-02	0.64	0.7893
Summer-94	3.91	3.9283	Summer-02	1.09	0.72564
Spring-94	1.16	0.886	Spring-02	0.34	0.05
Winter-95	0.44	0.3606	Winter-03	0.15	0.1359
Autumn-95	1.35	0.96046	Autumn-03	1.21	1.4387
Summer-95	7.33	6.5539	Summer-03	2.85	3.43278
Spring-95	0.6	0.4115	Spring-03	0.26	0.0513
Winter-96	0.79	0.7966			
Autumn-96	0.7	1.0233			
Summer-96	4.74	4.9061			
Spring-96	0.58	0.4096			
Winter-97	0.97	0.614			
Autumn-97	1.01	0.6688			
Summer-97	8.44	6.6458			
Spring-97	0.25	0.31654			
Winter-98	0.76	0.8947			
Autumn-98	1.95	1.1987			
Summer-98	7.45	7.4219			
Spring-98	0.12	0.0426			
Winter-99	0.92	0.8319			
Autumn-99	1.95	1.26685			
Summer-99	10.91	8.7935			
Spring-99	0.21	0.19022			